

UNIVERSITY OF MINNESOTA
ST. ANTHONY FALLS LABORATORY
Engineering, Environmental and Geophysical Fluid Dynamics

Project Report 383

**Climate Change Effects on Water
Temperature and Dissolved Oxygen in
Five North Carolina Lakes**

by

A. H. Rasmussen and H. G. Stefan

Prepared for

ENVIRONMENTAL RESEARCH LABORATORY
U. S. Environmental Protection Agency
Duluth Minnesota

In cooperation with

NATIONAL AGRICULTURAL WATER QUALITY LABORATORY
Agricultural Research Service
U.S. Department of Agriculture
Durant, Oklahoma

July 1996
Minneapolis, Minnesota

Prepared for: USEPA, Environmental Research Laboratory - Duluth
ARS, National Agricultural Water Quality Lab

Date Submitted: March 1996

Last Revised: July 2, 1996

Disk Location: c:\WP51\docs\Chap1-5.doc and Chap6on.doc
(Disk #197)

The University of Minnesota is committed to the policy that all persons shall have equal access to its programs, facilities, and employment without regard to race, religion, color, sex, national origin, handicap, age or veteran status.

ABSTRACT

A deterministic, year-round, one-dimensional water quality model, MINLAKE95, was used to investigate climate change effects on water temperatures and dissolved oxygen (DO) in five North Carolina lakes. The model was applied in daily timesteps over periods of several years. Past (recorded) weather conditions and a projected climate scenario under a doubling of atmospheric carbon dioxide were used as model inputs. Many of the lakes in the southeastern United States are man-made reservoirs. Three such reservoirs and two shallow natural lakes were modeled. The reservoirs are in the Piedmont and Mountain regions of North Carolina and are from 20 m to 65 m deep. The natural lakes are in the Coastal Plain and less than 4 m deep. All five lakes are major water bodies with long hydraulic residence times and surface areas ranging from 11 to 58 km². Standard errors of simulation relative to point measurements were 2.0°C for water temperature and 1.4 mg L⁻¹ for dissolved oxygen. Measurements were available as profiles against depth at a single station in each lake. Each lake was modeled under past 1xCO₂ climate conditions (1961-79) and under a projected 2xCO₂ climate scenario. To illustrate the climate change effect, plots of isotherms and DO-isopleths in a depth versus time coordinate system were prepared. Mean annual and extreme year values were plotted. To quantify the climate change effect further, extreme values of temperature and DO values in the surface layer and the bottom layer of each lake were tabulated, as well as periods of anoxia, lake volumes affected by anoxia, and periods and lake volumes with DO < 2 mg/l or DO < 3 mg/l. The climate change effects were most apparent in maximum surface temperature increases of 2.8 to 3°C, maximum bottom temperature increases of 1.6 to 2.9°C, and a 20% increase in evaporation in all five lakes. Low DO levels in the three reservoir hypolimnia were projected to be extended by up to 48 days in the 2xCO₂ climate scenario. Implications for fish habitat are that only the most temperature tolerant of the warm-water fishes would find suitable habitat in the natural lakes under the 2xCO₂ climate scenario. Cool-water fishes might survive at the intermediate (thermocline) depths of reservoirs where DO levels are sufficient and maximum temperatures tolerable. Cold-water fishes would not find suitable habitat, except in refugia, e.g. due to groundwater inflows.

ACKNOWLEDGEMENTS

This study was initiated under a grant from the United States Environmental Protection Agency, Environmental Research Laboratory, Duluth, MN, and completed with support from the U. S. Department of Agriculture, Agricultural Research Service, Durant, OK. John G. Eaton (EPA) and Frank R. Schiebe (DOA) were project officers. They and J. Howard McCormick of the USEPA/MED made valuable suggestions during presentations of this material. John Eaton and Howard McCormick also reviewed this report and suggested numerous improvements. We thank them for their support and input.

TABLE OF CONTENTS

		<u>Page No.</u>
Abstract		i
Acknowledgements		ii
List of Figures		v
List of Tables		xii
Chapter 1	Introduction	1
1.1	Background and previous modeling efforts	1
1.2	Objective of study	2
Chapter 2	Lake characteristics in the southeast region of the United States	4
2.1	Physiographic regions of the study area	4
2.2	Lake characteristics by state	4
2.3	Lake classification	10
Chapter 3	Weather conditions in the southeast region of the United States	13
3.1	Past weather conditions	13
3.2	Projected climate change under 2xCO ₂ conditions	23
Chapter 4	Methodology of temperature and dissolved oxygen modeling for lakes of the southeast region of the United States	28
4.1	Review of MINLAKE95	28
4.2	Applicability of MINLAKE95 to the southeast region	32
4.3	Lake classification problems	37
Chapter 5	Case studies	38
5.1	Reservoir and lake selection	38
5.2	In-lake measurements used for calibration/validation	38
5.3	Input information for MINLAKE95	46
5.4	B. Everett Jordan Reservoir	49
5.5	Lake James	72
5.6	Santeetlah Lake	77
5.7	Lake Phelps	77
5.8	Lake Waccamaw	83
5.9	Discussion of simulation results	91

Chapter 6	Simulations for extended time periods under two climate scenarios	92
6.1	Methodology for simulations with 1xCO ₂ and 2xCO ₂ climate scenarios	92
6.2	Simulated selective lake characteristics	93
6.3	Simulations for 1xCO ₂ climate scenario	94
6.4	Simulations for 2xCO ₂ climate scenario	117
6.5	Projected effects of climate change from 1xCO ₂ to 2xCO ₂ climate scenarios	140
Chapter 7	Implication for fish habitat and growth	144
Chapter 8	Summary and conclusions	148
References	151
Appendix	Sensitivity of simulation results for Lakes Phelps and Waccamaw to local hydrology, geology, and meteorology	155

LIST OF FIGURES

Chapter 1

Fig. 1.1 Southeastern United States.

Chapter 2

Fig. 2.1 Physiographic regions in the southeastern States (after Yount, 1966).

Fig. 2.2 Lake surface area frequency distribution in Georgia, North and South Carolina, Virginia, and Minnesota. Georgia lakes are less than 2.02 km² (500 acres). S. Carolina lakes are greater than 0.16 km² (40 acres).

Fig. 2.3 Maximum depth frequency distribution in Carolina and Minnesota lakes. North Carolina lakes are additionally divided into reservoirs (res.) and natural lakes (lakes).

Fig. 2.4 Secchi depth frequency distributions in Carolina and Minnesota lakes. North Carolina lakes are additionally divided into reservoirs (res.) and natural lakes (lakes).

Fig. 2.5 Various lake shapes in the southeastern US: (a) Chatuge Lake (reservoir), NC; (b) four natural Carolina Bay lakes, NC; (c) Smith Mountain Lake (reservoir), VA.

Chapter 3

Fig. 3.1 Selected weather stations in the southeast U.S.

Fig. 3.2a Average (1961-1979) daily values \pm standard deviations (σ) of air temperature, dew point temperature, wind speed, and solar radiation at Asheville, North Carolina.

Fig. 3.2b Average (1961-1979) daily values \pm standard deviations (σ) of air temperature, dew point temperature, wind speed, and solar radiation at Raleigh, North Carolina.

- Fig. 3.2c Average (1961-1979) daily values \pm standard deviations (σ) of air temperature, dew point temperature, wind speed, and solar radiation at Wilmington, North Carolina.
- Fig. 3.3 Average (1961-1979) daily values \pm standard deviations (σ) of air temperature, dew point temperature, wind speed, and solar radiation at Minneapolis/St. Paul, Minnesota.
- Fig. 3.4 Monthly average weather parameters (1961-1979) for Asheville, Raleigh, and Wilmington, North Carolina.
- Fig. 3.5 Monthly average weather parameters (1961-1979) for Minneapolis/St. Paul, Minnesota.
- Fig. 3.6 Means of the predicted changes of air temperature in the continental United States for the months of July, August, and September from the CCC GCM.

Chapter 4

- Fig. 4.1 A schematic representation of physical processes represented in MINLAKE95.
- Fig. 4.2 MINLAKE95 schematic flowchart.
- Fig. 4.3 Total attenuation coefficient vs. (Secchi depth)⁻¹ for lakes and reservoirs in South Carolina.
- Fig. 4.4 Previously modeled Minnesota lakes: (a) Orchard Lake, (b) Lake George, (c) Cedar Lake, (d) Fish Lake (Stefan et al., 1994).
- Fig. 4.5 Three distinct zones resulting from gradients in reservoirs (Thornton et al., 1990).

Chapter 5

- Fig. 5.1 Locations of selected water bodies and associated weather stations.
- Fig. 5.2a Temperature and dissolved oxygen profiles from simulation and measurements at several field stations in Jordan Reservoir on September 7, 1983.
- Fig. 5.2b Temperature and dissolved oxygen profiles from simulation and measurements at several field stations in Lake James on July 17, 1984.

- Fig. 5.2c Temperature and dissolved oxygen profiles from simulation and measurements at three field stations in Santeetlah Lake on June 10, 1982.
- Fig. 5.2d Temperature and dissolved oxygen profiles from simulation and measurements at two field stations in Lake Phelps on August 22, 1989.
- Fig. 5.2e Temperature and dissolved oxygen profiles from simulation and measurements at two field stations in Lake Waccamaw on September 11, 1986.
- Fig. 5.3 Approximate temperature ($^{\circ}\text{C}$) of groundwater in the United States (from Todd, 1980, after Collins, 1925).
- Fig. 5.4 B. Everett Jordan Reservoir with sampling stations. Data from stations B4030000 and B3995000 were used to check simulation results.
- Fig. 5.5 Water temperature time series for Jordan Reservoir (1983-87), using chl-a measurements. Field data are from station B3995000 (run #10).
- Fig. 5.6 Dissolved oxygen time series for Jordan Reservoir (1983-87), using chl-a measurements. Field data are from station B3995000 (run #10).
- Fig. 5.7 Simulated versus measured temperature and dissolved oxygen in Jordan Reservoir (simulation #10, station B3995000).
- Fig. 5.8 Water temperature time series for Jordan Reservoir (1983-85), using chl-a measurements. Field data are from station B4030000 (run #12).
- Fig. 5.9 Dissolved oxygen time series for Jordan Reservoir (1983-85), using chl-a measurements. Field data are from station B4030000 (run #12).
- Fig. 5.10 Simulated versus measured temperature and dissolved oxygen in Jordan Reservoir (simulation #12, station B4030000).
- Fig. 5.11 Isotherms ($^{\circ}\text{C}$) in Jordan Res. (1983-84) from simulation (top), field data at station B4030000 (middle) and B3995000 (bottom).
- Fig. 5.12 Dissolved oxygen isopleths (mg L^{-1}) in Jordan Res. (1983-84) from simulation (top), field data at station B4030000 (middle) and B3995000 (bottom).
- Fig. 5.13 Daily wind speeds at Raleigh, North Carolina (1982-85).

- Fig. 5.14 Chlorophyll-a vs. average wind speed for 3 days, 1 week, and 2 weeks prior to measurement at Jordan Reservoir. Wind speeds were measured at Raleigh, NC.
- Fig. 5.15 Chlorophyll-a measurements during several years at field stations B3959000, B3995000, and B4030000 in Jordan Reservoir.
- Fig. 5.16 Water temperature time series for Jordan Reservoir (1983-87), using chl-a cycle. Field data are from station B3995000 (run #11).
- Fig. 5.17 Dissolved oxygen time series for Jordan Reservoir (1983-87), using chl-a cycle. Field data are from station B3995000 (run #11).
- Fig. 5.18 Simulated versus measured temperature and dissolved oxygen in Jordan Reservoir (simulation #11, station B3995000).
- Fig. 5.19 Water temperature time series for Jordan Reservoir (1987-90), using chl-a cycle. Field data are from station B3995000 (run #7).
- Fig. 5.20 Dissolved oxygen time series for Jordan Reservoir (1987-90), using chl-a cycle. Field data are from station B3995000 (run #7).
- Fig. 5.21 Simulated versus measured temperature and dissolved oxygen in Jordan Reservoir (simulation #7, station B3995000).
- Fig. 5.22 Lake James with sampling stations. Data from station C0730000 were used to check simulation results.
- Fig. 5.23 Water temperature time series for Lake James (1981-89).
- Fig. 5.24 Dissolved oxygen time series for Lake James (1981-89).
- Fig. 5.25 Simulated versus measured temperatures and dissolved oxygen in Lake James.
- Fig. 5.26 Santeetlah Lake with sampling stations. Data from station G9840000 were used to check simulation results.
- Fig. 5.27 Water temperature time series for Santeetlah Lake (1981-90).
- Fig. 5.28 Dissolved oxygen time series for Santeetlah Lake (1981-90).
- Fig. 5.29 Simulated versus measured temperature and dissolved oxygen in Santeetlah Lake.

- Fig. 5.30 Lake Phelps with sampling stations. Data from station M6270000 were used to check simulation results.
- Fig. 5.31 Water temperature time series for Lake Phelps (1981-89).
- Fig. 5.32 Dissolved oxygen time series for Lake Phelps (1981-89).
- Fig. 5.33 Simulated versus measured temperature and dissolved oxygen in Lake Phelps.
- Fig. 5.34 Lake Waccamaw with sampling stations. Data from station I7710000 were used to check simulation results.
- Fig. 5.35 Water temperature time series for Lake Waccamaw (1983-90).
- Fig. 5.36 Dissolved oxygen time series for Lake Waccamaw (1983-90).
- Fig. 5.37 Simulated versus measured temperature and dissolved oxygen in Lake Waccamaw.

Chapter 6

- Fig. 6.1 Isotherms ($^{\circ}\text{C}$) in Jordan Reservoir for an average year under the $1\times\text{CO}_2$ climate scenario (top) with isopleths of standard deviations (σ) and isotherms for extreme ($\text{mean} \pm 2\sigma$) events.
- Fig. 6.2 DO isopleths (mg L^{-1}) in Jordan Reservoir for an average year under the $1\times\text{CO}_2$ climate scenario (top) with isopleths of standard deviations (σ) and of DO for extreme ($\text{mean} \pm 2\sigma$) events.
- Fig. 6.3 Isotherms ($^{\circ}\text{C}$) in Lake James for an average year under the $1\times\text{CO}_2$ climate scenario (top) with isopleths of standard deviations (σ) and isotherms for extreme ($\text{mean} \pm 2\sigma$) events.
- Fig. 6.4 DO isopleths (mg L^{-1}) in Lake James for an average year under the $1\times\text{CO}_2$ climate scenario (top) with isopleths of standard deviations (σ) and of DO for extreme ($\text{mean} \pm 2\sigma$) events.
- Fig. 6.5 Isotherms ($^{\circ}\text{C}$) in Santeetlah Lake for an average year under the $1\times\text{CO}_2$ climate scenario (top) with isopleths of standard deviations (σ) and isotherms for extreme ($\text{mean} \pm 2\sigma$) events.

- Table 6.10 Selected characteristics from simulation of Lake Phelps under the CCC 2xCO₂ climate scenario. Each is an extreme value for a particular year (except EVAP, which is cumulative).
- Table 6.11 Selected characteristics from simulation of Lake Waccamaw under the CCC 2xCO₂ climate scenario. Each is an extreme value for a particular year (except EVAP, which is cumulative).
- Table 6.12 Results of simulation under the 2xCO₂ climate scenario showing averages and standard deviations of selected characteristics for each lake.
- Table 6.13 Results of student's *t*-test analysis between the 1xCO₂ and 2xCO₂ mean values for each lake. The *t*-test was two-tailed with a level of significance of 0.05.
- Table 6.14 Projected change (2xCO₂-1xCO₂) in those lake characteristics found by *t*-test to be different.

Chapter 7

- Table 7.1 Thermal and dissolved oxygen habitat criteria for fish.
- Table 7.2 Lake characteristics related to fish habitat.
- Table 7.3 Fish habitat limitations.

Appendix

- Table A.1 Standard errors (S.E.) of water temperature and DO simulations with varying values of wind coefficient (W_{coef}).
- Table A.2 Standard errors (S.E.) of water temperature and DO simulations with varying values of wind sheltering coefficient (W_{st}).
- Table A.3 Standard errors (S.E.) of water temperature and DO simulations with varying inputs from groundwater. $Q_{gw}=0$ represents the current MINLAKE95 method.
- Table A.4 Thermal diffusivities of various materials.

CHAPTER 1

INTRODUCTION

1.1 Background and previous modeling efforts

An increase in global air temperatures is expected to have a direct effect on the temperatures, dissolved oxygen content, and stratification dynamics of lakes, which are key water quality determinants of aquatic ecosystems. Being able to project water quality changes under projected climate change is of value, because many regions derive much economic and recreational benefit from their lakes. Water quality modeling has been the focus of considerable research in recent years. Such modeling enhances our understanding of how lakes function and allows us to project the effects of naturally or artificially induced changes.

Lake water quality models are typically developed for particular lakes. MINLAKE is a deterministic, one-dimensional water quality model which simulates vertical profiles of temperature, dissolved oxygen, and other parameters in lakes with a wide variety of morphometries and trophic states using a daily time step. It was developed by Riley and Stefan (1987) and is calibrated to each lake under study. Using the MINLAKE framework, Hondzo and Stefan (1992) and Fang and Stefan (1994) with algorithms from Gu and Stefan (1990) have developed a regional, deterministic, year-round, one-dimensional, daily model named "MINLAKE95" (Stefan et al., 1994). Hondzo and Stefan (1992) developed the temperature simulation component capable of dealing with a variety of morphometric, trophic, and meteorological conditions. Fang and Stefan (1994) built upon the temperature model by adding a DO simulation algorithm. Both models were at first developed for the open water season (approximately April through October in Minnesota). For multi-year simulations, conditions were reinitialized at the end of the winter ice cover period of each year. Subsequently, Stefan et al. (1994) incorporated a winter ice cover simulation (Gu and Stefan, 1990) into the model in order to provide a continuous year-round simulation, without the need for reinitialization. This version was developed to investigate the effects of projected global climate change on water temperature, dissolved oxygen, and fish habitat in Minnesota lakes.

The goal of these modeling efforts has been to simulate water temperature to within 1 °C and DO to within 1 mg L⁻¹ standard error. Hondzo and Stefan (1992), using nine Minnesota lakes for model validation, simulated lake temperatures to within 1.1 °C on average during the open water season. The standard error for the simulated DO (Fang and Stefan, 1994) in five Minnesota lakes was 1.9 mg L⁻¹ for the open water season. For

the year-round model (Stefan and Fang, 1995), 5,976 data pairs of water temperature and DO, measured in nine Minnesota lakes, were available for model validation. Standard errors between measurements and simulations were 1.4 °C and 1.9 mg L⁻¹ for temperature and DO, respectively.

While MINLAKE95 simulates only one lake at a time, the regionality of the analysis arises from the application of the model to various lake classes within a given region without recalibration for individual lakes. Minnesota lakes were divided into 27 lake classes using three parameters (surface area, maximum depth, and trophic state) with three ranges within each parameter (Hondzo and Stefan, 1992, Fang and Stefan, 1994). Surface area and maximum depth were chosen because they have a direct relationship to stratification dynamics, and trophic state because it affects radiation attenuation and oxygen production and consumption. Secchi disk transparency was used as a surrogate for trophic state. Ranges and representative values of each lake class in Minnesota are given by Stefan et al. (1993).

1.2 Objective of study

An interest in studying the potential impact of projected climate change on aquatic ecosystems of the southeastern United States has been expressed by the U.S. Environmental Protection Agency.

The purpose of this study is to explore the utility of the MINLAKE95 model to determine long-term trends for water temperature and DO in southeastern U.S. lakes under projected climate scenarios. Four States were included in the study (Fig. 1.1): Virginia, North and South Carolina, and Georgia. The first step in this attempt was to characterize lakes in the southeast region according to surface area, maximum depth, and trophic state. Information on water residence time was also needed, since most of the lakes in this region are reservoirs and since the regional MINLAKE95 model neglects inflows and outflows. Ultimately, five lakes in North Carolina were chosen for investigation because lakes in the other States lack sufficient data. MINLAKE95 was then calibrated for these lakes using available in-lake measurements and past weather conditions. However, differences between lakes in Minnesota and North Carolina did not allow an extension of the modeling effort into a full regional analysis. Lakes in the southeastern U.S. are more diverse in shape and often more influenced by watershed runoff and withdrawal, as indicated by shorter hydraulic residence times. Secchi depth, as a measure of lake turbidity is not as directly linked to phytoplankton standing crop as in Minnesota because of inorganic and detrital suspended sediment inflow from the watershed. A lake classification based on only three parameters (surface area, maximum depth, and Secchi depth), which worked reasonably well in Minnesota, was therefore not attempted in the Southeast. Climate change responses were thus investigated only on the five North Carolina lakes.

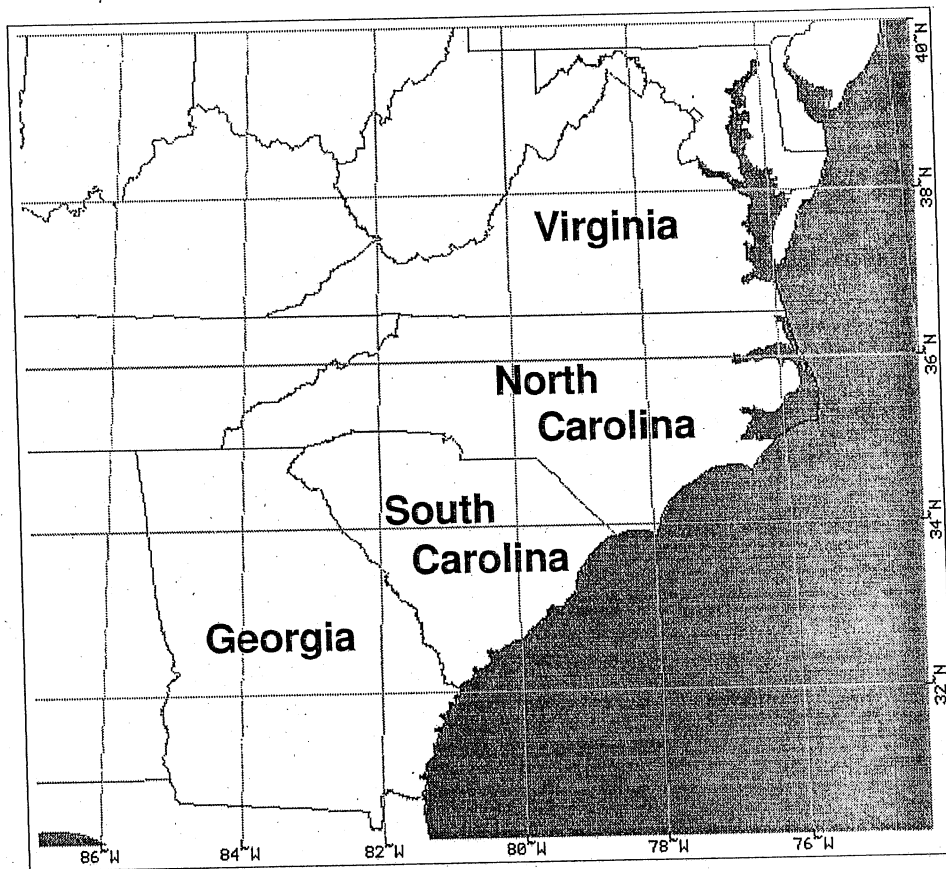


Fig. 1.1. Southeastern United States study area.

CHAPTER 2

LAKE CHARACTERISTICS IN THE SOUTHEAST REGION OF THE UNITED STATES

2.1 Physiographic regions of the study area

The States of the study area are divided into three main physiographic regions: Mountain, Piedmont, and Coastal Plain (Fig. 2.1). The Mountain zone is a narrow strip along the western edges of the states in the Appalachian Mountains. Elevations range from about 490 m to 2037 m above sea level. Virtually all lakes in this region are artificial impoundments, with one significant exception, Smith Mountain Lake, Virginia, which was formed by a landslide into a stream valley. Waters are rather oligotrophic here. The Piedmont region lies to the southeast of the Mountain zone and ranges in elevation from about 75 m to 490 m. As in the Mountain zone, lakes in the Piedmont are mostly artificial. Waters in this region are generally turbid due to runoff from agricultural lands. The Coastal Plain extends from the Piedmont region to the Atlantic coast and contains many natural lakes called "Carolina Bays." These bays, not connected to the ocean, are generally elliptical in shape and are oriented in a northwest-southeast direction. They are rather shallow with maximum depths of about six meters (Reid and Wood, 1976) and have peat or sandy bottoms. The water has low suspended particulates but is colored from extensive marsh and swamp drainage. These bay lakes are of unknown origin, and the reader is referred to Yount (1966) and Reid and Wood (1976) for an overview of present theories of the origins of the Carolina Bays.

2.2 Lake characteristics by state

Characterization of a region's lakes with respect to key parameters is important, because lakes exhibit a wide range of water temperature and dissolved oxygen responses given equal meteorological inputs. Accurate temperature and dissolved oxygen prediction requires accurate modeling of stratification dynamics. Stratification is heavily influenced by surface area and maximum depth (Gorham and Boyce, 1989). Trophic state, which can be correlated to Secchi disk transparency, is important for the oxygen balance. Cumulative frequency distributions of surface areas, maximum depths, and Secchi disk transparencies (Figs. 2.2 to 2.4, respectively) were determined from information on lakes in Virginia, North and South Carolina, and Georgia, mostly obtained from Water Quality Assessment (305(b)) reports required by the U.S. Environmental Protection Agency.

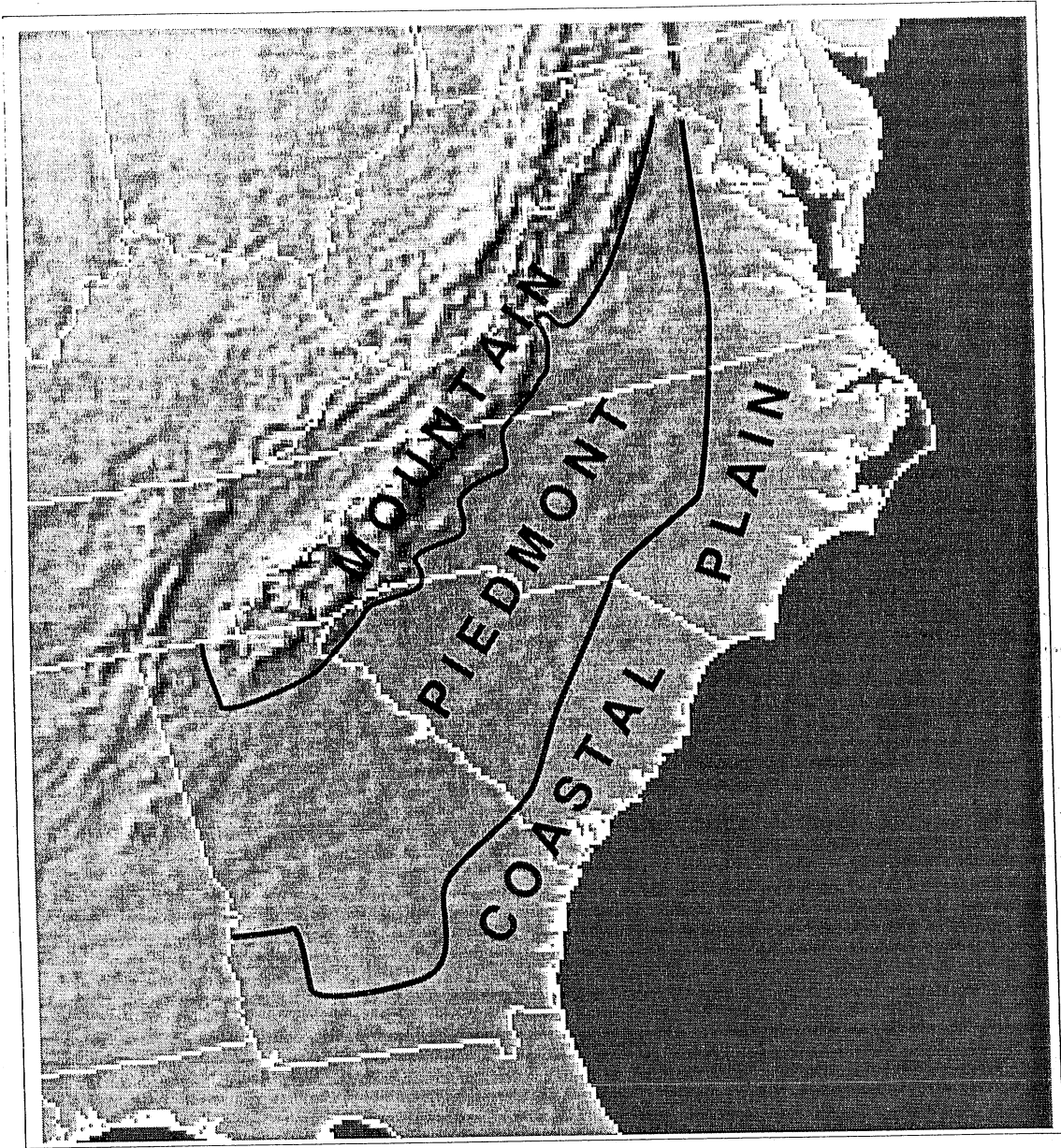


Fig. 2.1. Physiographic regions in the southeastern States (after Yount, 1966).

For **Virginia**, surface area information was available for 247 publicly-owned lakes (Virginia DEQ, 1994). Most of these 247 lakes are smaller than the 3002 Minnesota lakes in the Minnesota Department of Natural Resources database (Fig. 2.2). Three very large reservoirs account for about two-thirds of the total surface area of publicly-owned lakes. There was no information available stating maximum depths, Secchi depths, or whether the lakes are reservoirs or natural lakes. Trophic state was reported by the DEQ using Carlson's Trophic State Index.

North Carolina has 1800 lakes larger than 0.04 km² (10 acres), most of which are impoundments (reservoirs or millponds). Natural lakes occur in the coastal plains and are generally shallow. A sample of over 100 (North Carolina DEHNR, 1992) showed that lakes in this state are generally larger in surface area and deeper than Minnesota lakes (Figs. 2.2 and 2.3). Cumulative frequencies of Secchi depths are shown in Fig. 2.4 and reveal that water clarity is generally less than that found in Minnesota. Trophic state was determined using the North Carolina Trophic State Index, developed specifically for North Carolina; it uses a combination of organic nitrogen, phosphorus, Secchi depth, and chlorophyll-a measures to calculate the index value.

There are 1617 lakes with surface area larger than 0.04 km² (10 acres) in **South Carolina** (South Carolina WRC, 1991). A summary of lakes in this State (Stecker and Crocker, 1991) provides information about 40 lakes which offer public access and have surface areas greater than 0.16 km² (40 acres). These 40 lakes are larger and deeper than lakes in Minnesota (Figs. 2.2 and 2.3). All of the lakes in South Carolina are impoundments (South Carolina WRC, 1991). Trophic state was quantified using a multi-parameter percentile index developed for South Carolina. Water clarity is overall lower than in Minnesota (Fig. 2.4).

There are 11,813 lakes in **Georgia** (Georgia DNR, 1993). Only 48 are larger than 2.02 km² (500 acres). Fig. 2.2 shows the distribution of surface area of 224 publicly owned lakes smaller than 2.02 km² (500 acres). Individual measures of Carlson's Trophic State Index (Secchi depth, phosphorus, and chlorophyll-a) were summed to yield a single new trophic state index for Georgia.

Lakes in the southeastern United States vary widely in shape. Natural coastal lakes tend to be elliptical, while reservoirs can be very dendritic. Examples are shown in Fig. 2.5.

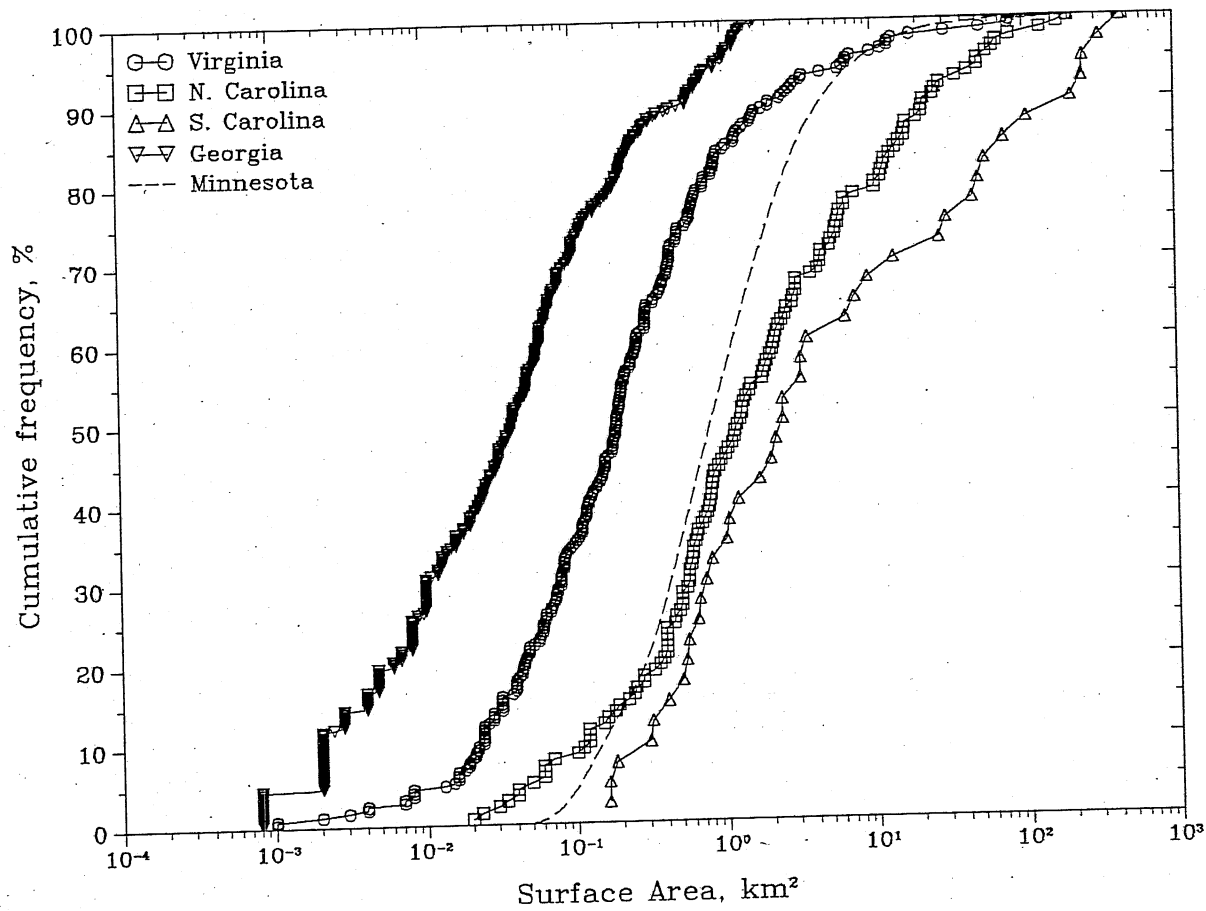


Fig. 2.2. Lake surface area frequency distribution in Georgia, North and South Carolina, Virginia, and Minnesota. Georgia lakes are less than 2.02 km² (500 acres). S. Carolina lakes are greater than 0.16 km² (40 acres).

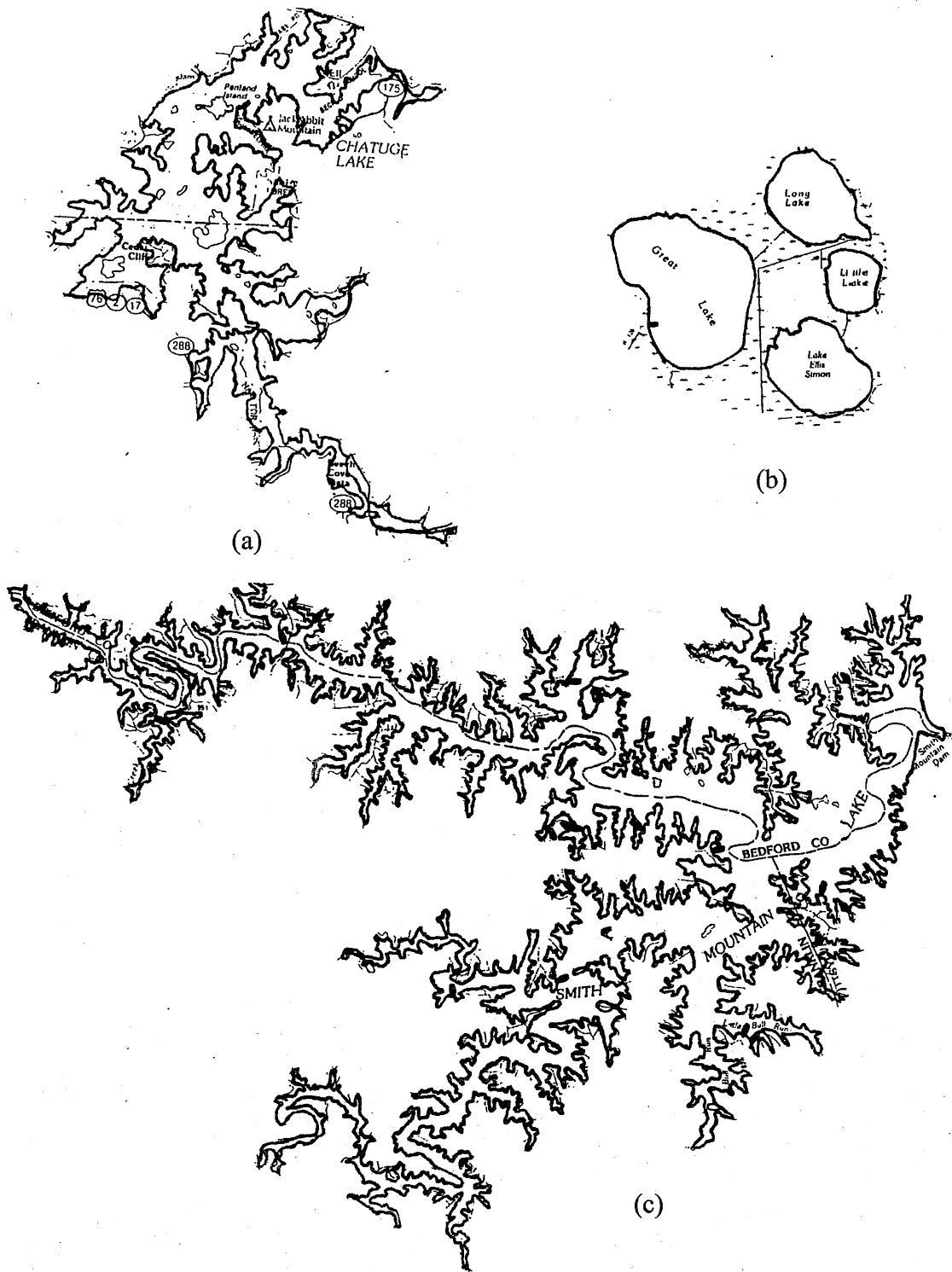


Fig. 2.5. Various lakes shapes in the southeastern U.S.: (a) Chatuge Lake (reservoir), NC; (b) four natural Carolina Bay lakes, NC; (c) Smith Mountain Lake (reservoir), VA.

Chapter 3

Weather Conditions in the Southeast Region of the United States

One of the most important factors influencing water temperatures in a lake is meteorological forcing. Thus, an overview of a region's weather gives an insight into the behavior of lakes in that region. In addition to looking at the past climate ($1\times\text{CO}_2$), projected climate conditions under a doubling of atmospheric CO_2 ($2\times\text{CO}_2$) are discussed in the following sections.

3.1 Past weather conditions

The weather in the Southeast is largely determined by its proximity to the Atlantic Ocean (and the Gulf of Mexico for Georgia), its latitude, and its topography (NOAA, 1974). Summers are hot and humid while winters are mild to moderately cold. The area is generally broken into three physiographic regions: Mountain, Piedmont, and Coastal Plain (Fig. 2.1). Average temperatures in the Mountain zone can vary by more than 10°C from those of the Coastal Plain at a given latitude. While freezing temperatures do occur in all regions, mean maximum temperatures in January in the coldest mountain areas of Virginia still rise above 5°C ; thus, no significant ice formation can be expected for lakes in the Southeast.

Weather data used as model input were obtained from the Solar and Meteorological Surface Observation Network for the years 1961-1990, compiled by the National Climatic Data Center (Asheville, North Carolina); it contains data taken at major cities in the Southeast. The past ($1\times\text{CO}_2$) climate condition was taken to be the 19-year period 1961-1979. The year 1979 was taken as the last year of the $1\times\text{CO}_2$ scenario, which is in line with previous studies (Hondzo and Stefan, 1992; Fang and Stefan, 1994; Stefan and Fang, 1995).

Meteorological data from three weather stations in the southeastern U.S. (Fig. 3.1) were investigated in detail: Asheville, Raleigh, and Wilmington, North Carolina. Asheville is located in the Mountain zone, Raleigh in the Piedmont region, and Wilmington in the Coastal Plain. These stations were chosen because of their proximity to the lakes modeled in this study (see Chapter 5).

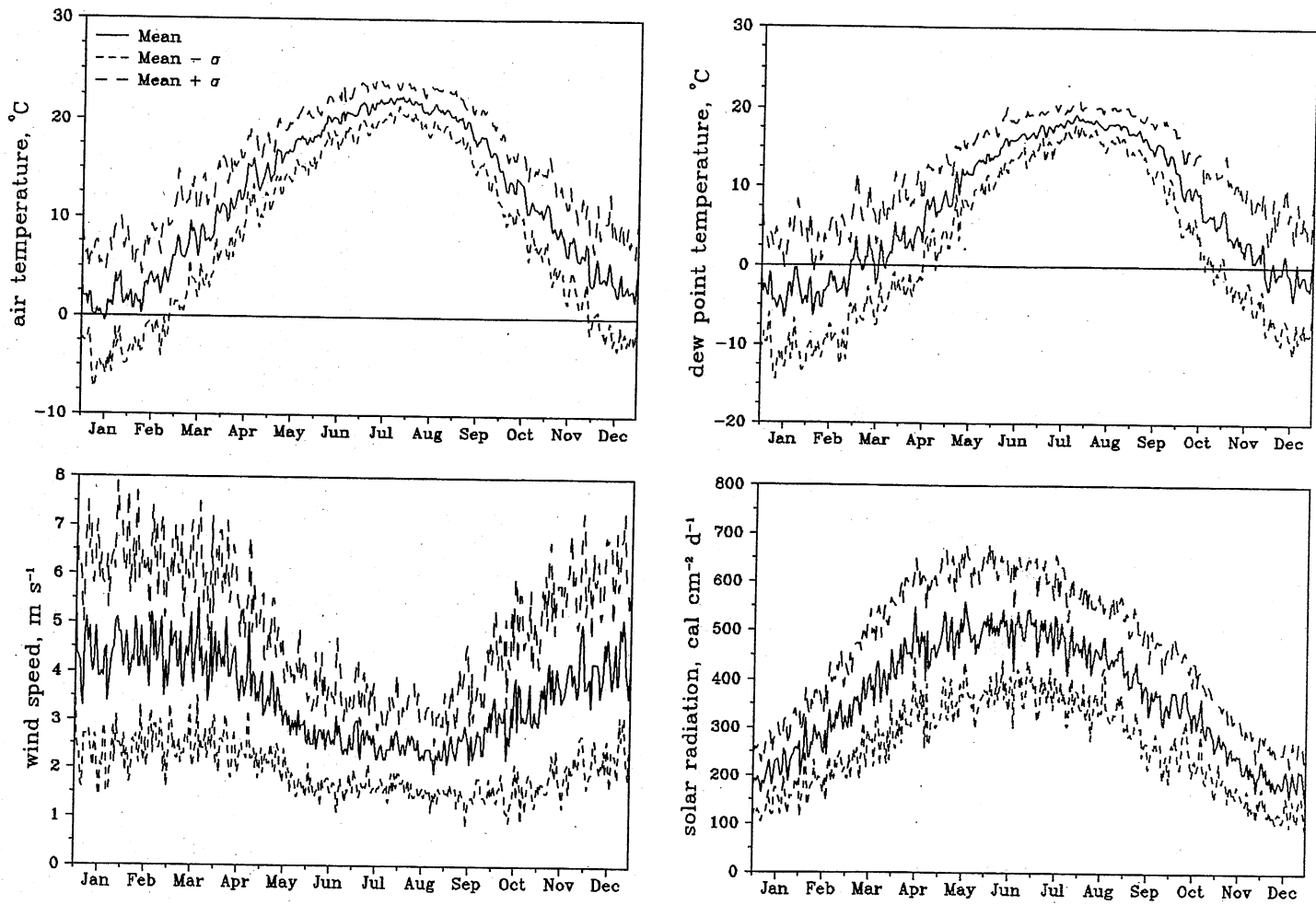


Fig. 3.2a. Average (1961-1979) daily values \pm standard deviations (σ) of air temperature, dew point temperature, wind speed, and solar radiation at Asheville, North Carolina.

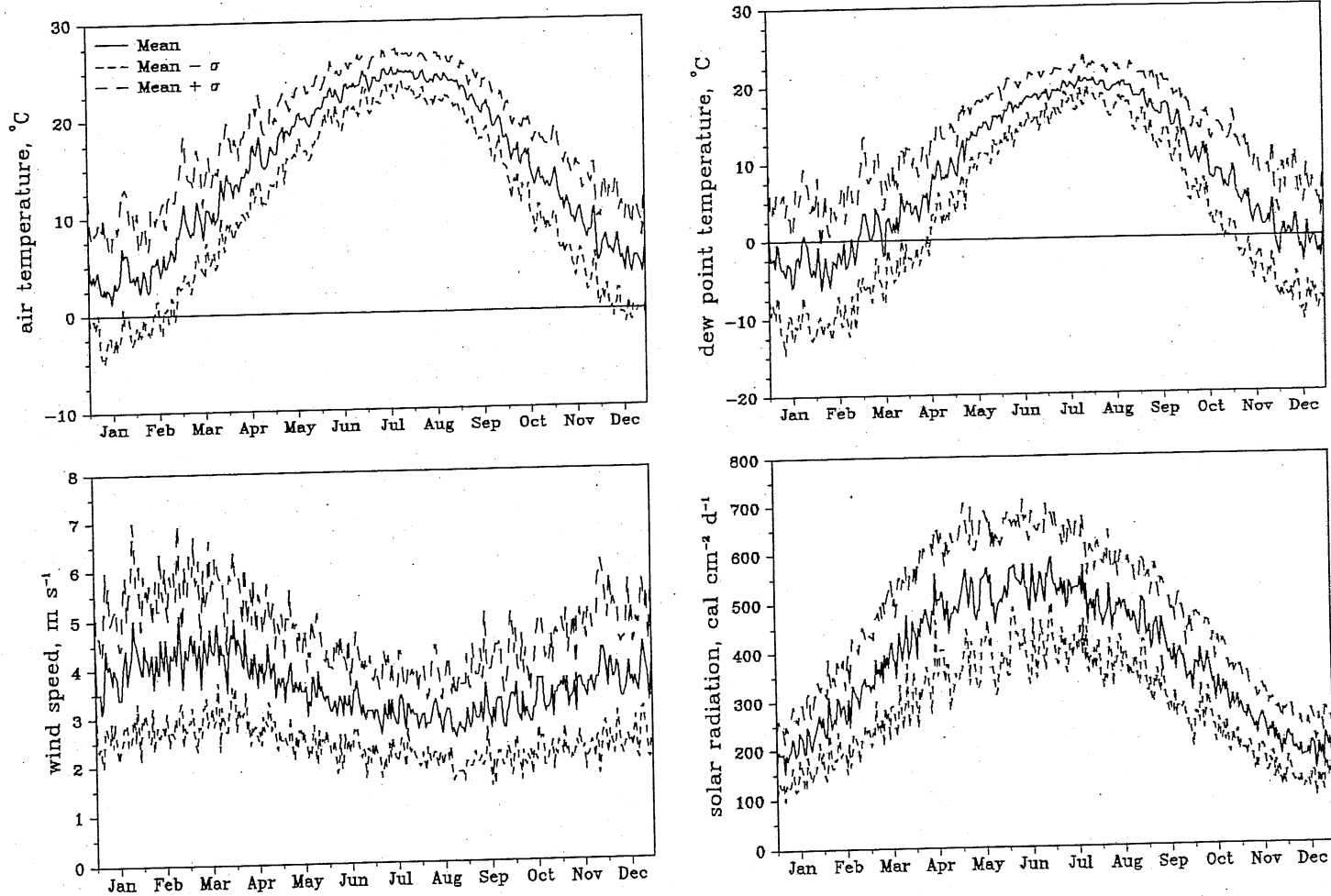


Fig. 3.2b. Average (1961-1979) daily values \pm standard deviations (σ) of air temperature, dew point temperature, wind speed, and solar radiation at Raleigh, North Carolina.

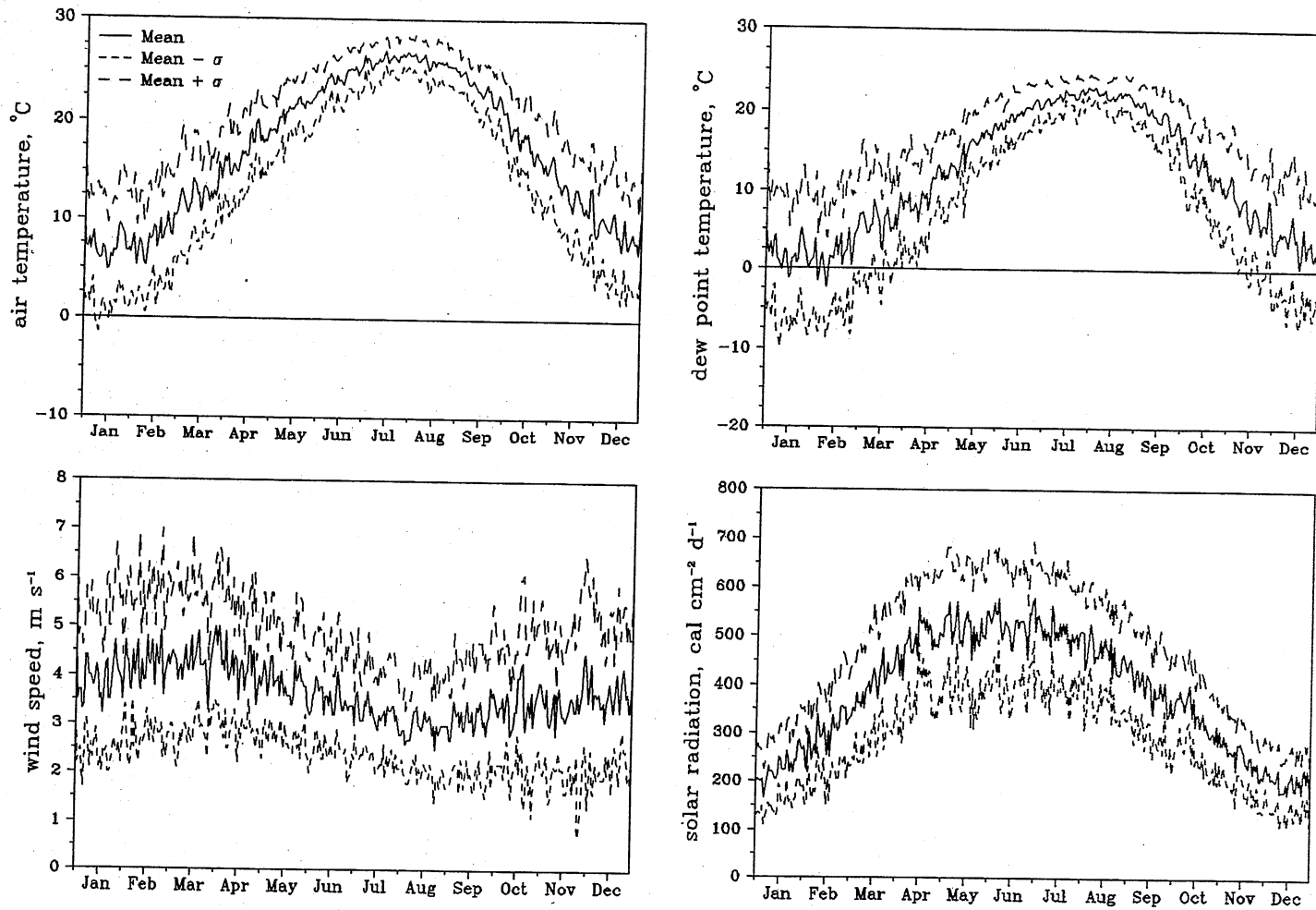


Fig. 3.2c. Average (1961-1979) daily values \pm standard deviations (σ) of air temperature, dew point temperature, wind speed, and solar radiation at Wilmington, North Carolina.

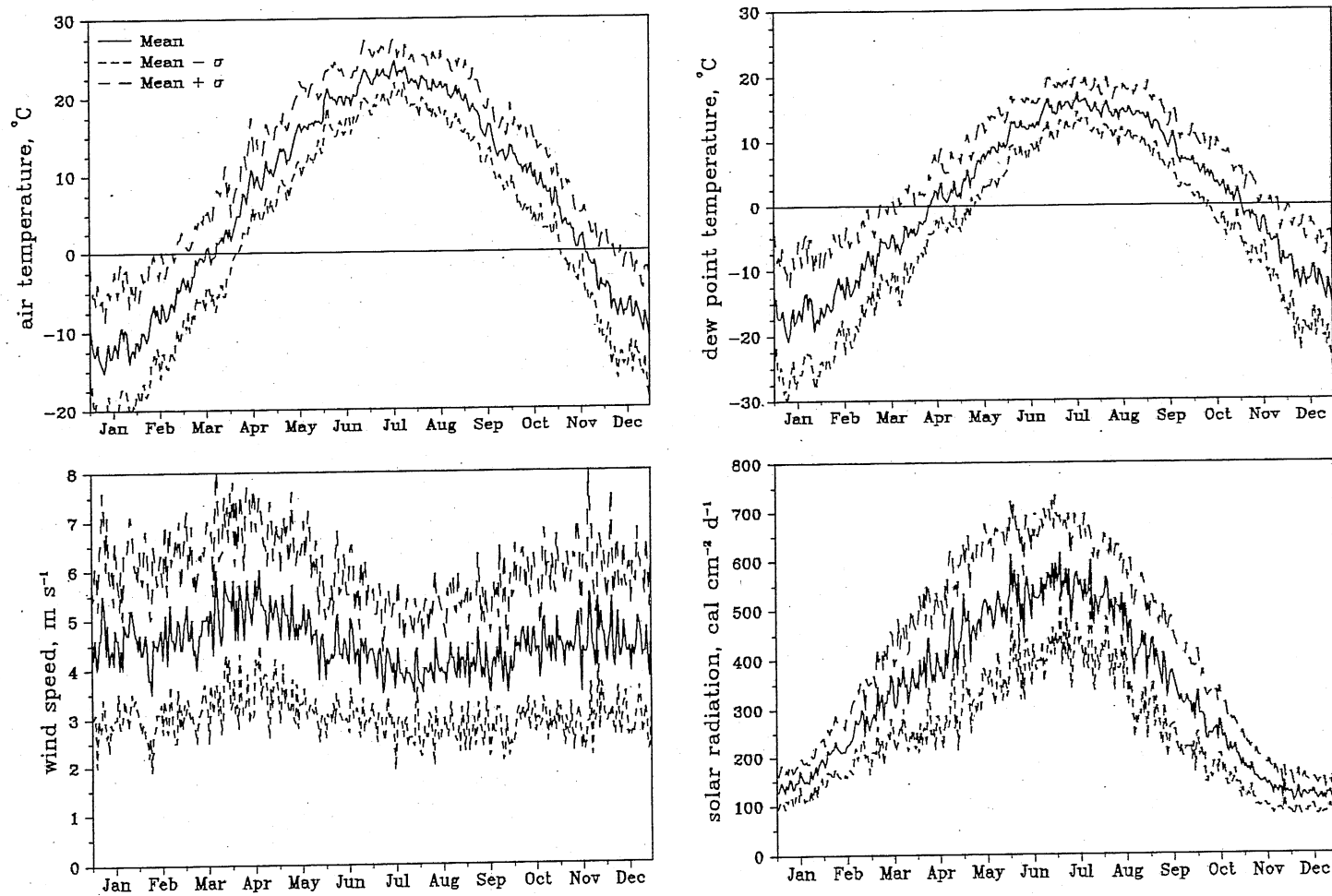


Fig. 3.3. Average (1961-1979) daily values \pm standard deviations (σ) of air temperature, dew point temperature, wind speed, and solar radiation at Minneapolis/St. Paul, Minnesota.

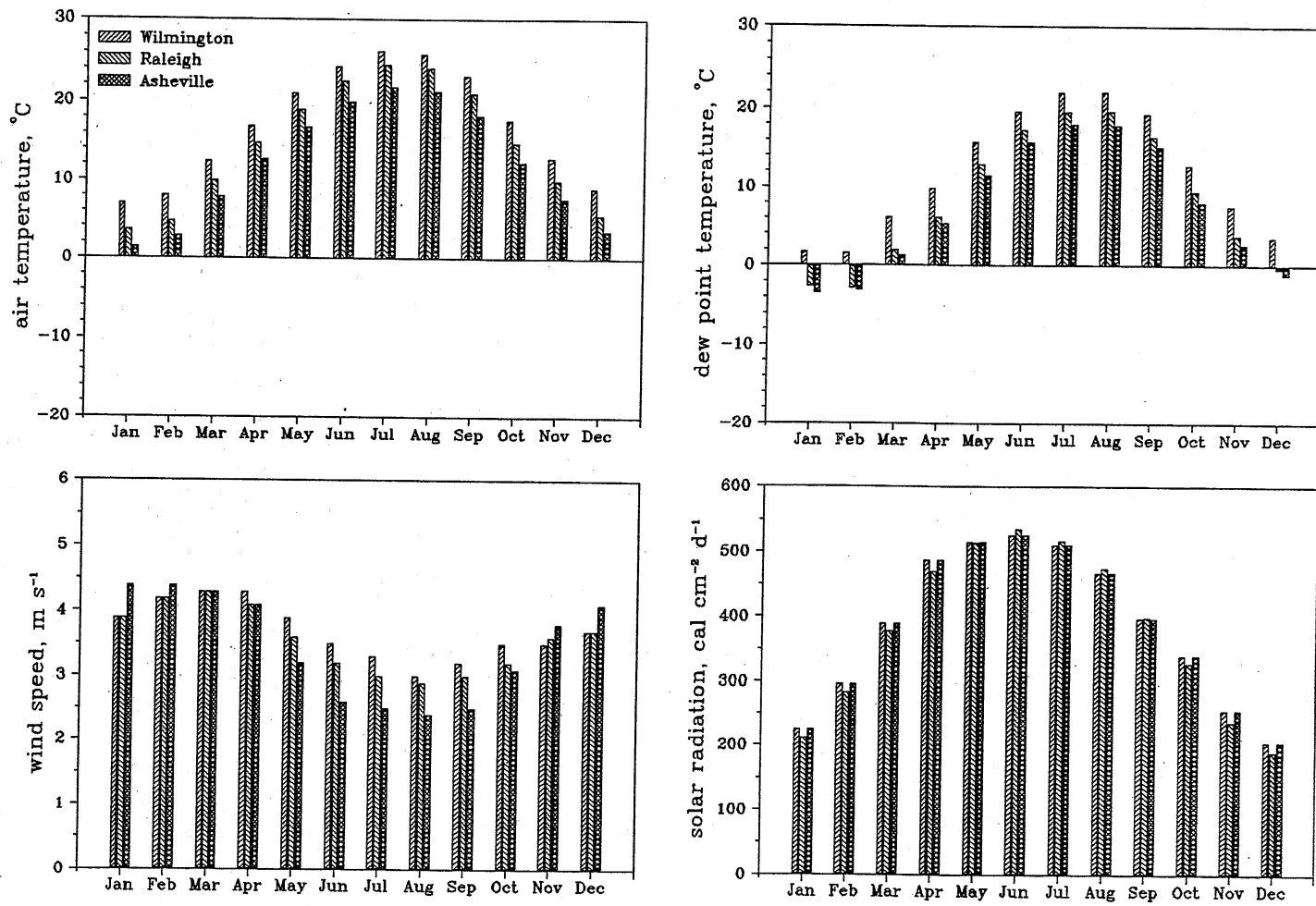


Fig. 3.4. Monthly average weather parameters (1961-1979) for Asheville, Raleigh, and Wilmington, North Carolina.

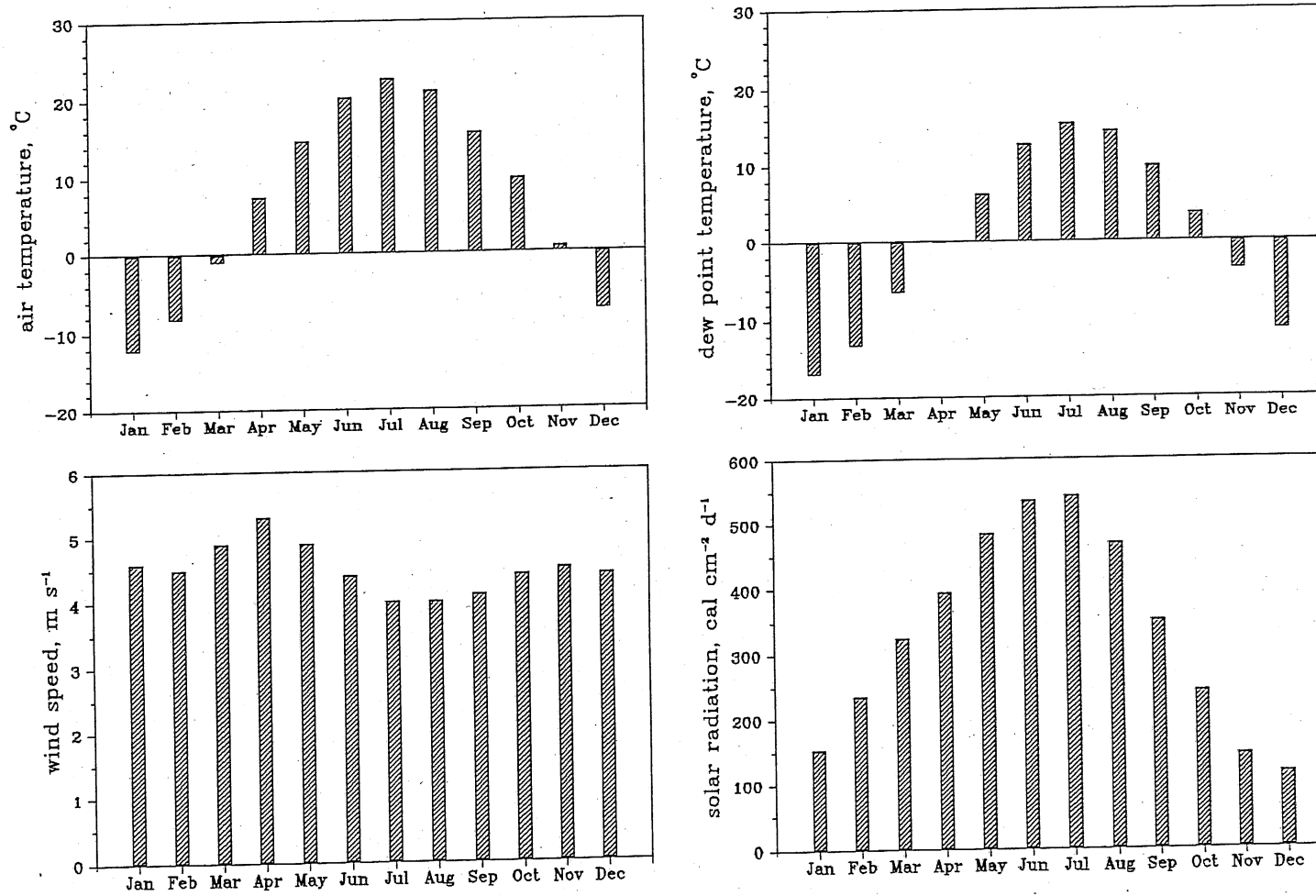


Fig. 3.5. Monthly average weather parameters (1961-1979) for Minneapolis/St. Paul, Minnesota.

Table 3.2. Monthly weather averages at Raleigh, North Carolina (1961-1979).

Month	Air temp. °C	Dew pt. temp., °C	Wind speed m s ⁻¹	Solar radiation cal cm ⁻² d ⁻¹
Jan	3.7	-2.7	3.9	212
Feb	4.7	-2.9	4.2	285
Mar	10.0	2.0	4.3	379
Apr	14.8	6.2	4.1	472
May	19.0	13.0	3.6	515
Jun	22.6	17.4	3.2	536
Jul	24.5	19.6	3.0	518
Aug	24.1	19.7	2.9	476
Sep	21.0	16.5	3.0	400
Oct	14.9	9.5	3.2	328
Nov	10.0	3.8	3.6	237
Dec	5.5	-0.4	3.7	191

Table 3.3. Monthly weather averages at Wilmington, North Carolina (1961-1979).

Month	Air temp. °C	Dew pt. temp., °C	Wind speed m s ⁻¹	Solar radiation cal cm ⁻² d ⁻¹
Jan	7.1	1.8	3.9	226
Feb	8.0	1.6	4.2	297
Mar	12.5	6.2	4.3	391
Apr	17.0	9.9	4.3	489
May	21.1	15.8	3.9	516
Jun	24.3	19.7	3.5	527
Jul	26.2	22.0	3.3	512
Aug	25.8	22.1	3.0	469
Sep	23.2	19.4	3.2	398
Oct	17.7	12.9	3.5	340
Nov	12.9	7.6	3.5	256
Dec	9.0	3.6	3.7	206

Table 3.4. Monthly weather averages at Minneapolis/St. Paul, Minnesota (1961-1979).

Month	Air temp. °C	Dew pt. temp., °C	Wind speed m s ⁻¹	Solar radiation cal cm ⁻² d ⁻¹
Jan	-12.2	-16.9	4.6	154
Feb	-8.3	-13.3	4.5	235
Mar	-1.0	-6.5	4.9	324
Apr	7.5	-0.1	5.3	395
May	14.7	6.3	4.9	484
Jun	20.3	12.7	4.4	535
Jul	22.8	15.4	4.0	542
Aug	21.2	14.4	4.0	470
Sep	15.7	9.9	4.1	351
Oct	9.8	3.7	4.4	243
Nov	0.8	-3.8	4.5	145
Dec	-7.4	-11.5	4.4	117

3.2 Projected climate change under 2xCO₂ conditions

The projected climate changes under a doubling of atmospheric carbon dioxide (2xCO₂) were obtained from the Canadian Climate Centre General Circulation Model (CCC-GCM) (Canadian Climate Centre, 4905 Dufferin Street, Downsview, Ontario; discussed by Boer et al., 1992, and McFarlane et al., 1992). The meteorological changes at the three weather stations (Asheville, Raleigh, and Wilmington) were taken to be equal to the output from the CCC-GCM grid point closest to each particular weather station. The changes in mean summer air temperatures predicted for the continental U.S. are shown in Fig. 3.6. The CCC-GCM model has a global spacial resolution of 3.75° by 3.75°. Raleigh and Wilmington both have the same climate corrections. Monthly averaged changes in air temperature, dew point temperature, wind speed, and solar radiation are given in Tables 3.5 to 3.7 for Asheville, Raleigh, and Wilmington, respectively.

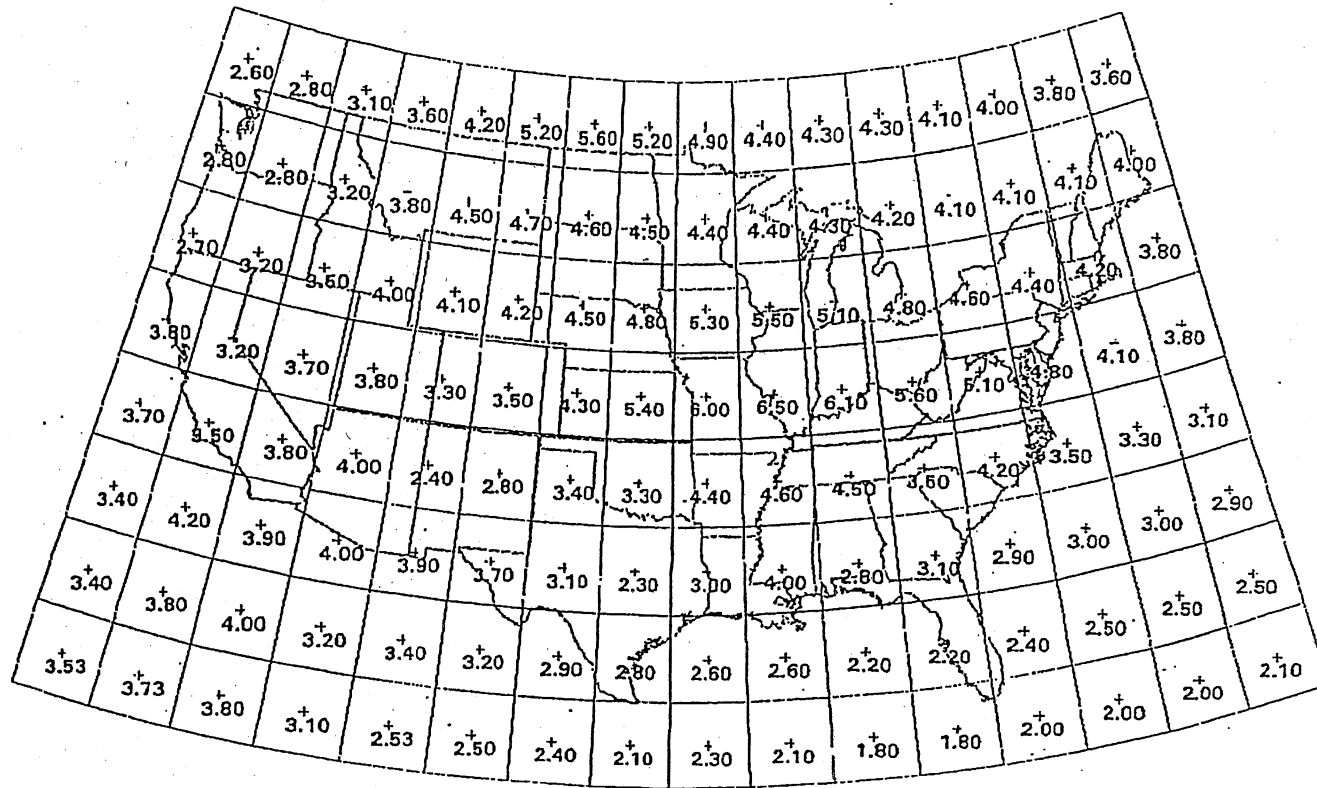


Fig. 3.6. Means of the predicted changes of air temperature in the continental United States for the months of July, August, and September from the CCC GCM 2xCO₂ scenario.

Table 3.5. CCC-GCM 2xCO₂ climate scenario for Asheville, North Carolina.

Month	Air temp. difference ¹ °C	Dew pt. temp. difference °C	Wind speed ratio ²	Solar radiation ratio
Jan	3.70	1.21	0.83	1.06
Feb	6.83	1.59	0.99	1.01
Mar	4.31	1.24	0.93	1.02
Apr	4.43	1.35	0.95	0.93
May	4.53	1.33	0.97	0.98
Jun	3.71	1.24	0.83	0.96
Jul	2.84	1.14	0.80	1.05
Aug	3.45	1.14	0.72	1.11
Sep	4.18	1.18	0.69	0.97
Oct	4.42	1.29	0.87	0.92
Nov	3.59	1.25	0.83	0.97
Dec	1.64	1.10	0.83	1.02

¹Difference = 2xCO₂ - 1xCO₂

²Ratio = 2xCO₂/1xCO₂

Table 3.6. CCC-GCM 2xCO₂ climate scenario for Raleigh, North Carolina.

Month	Air temp. difference ¹ °C	Dew pt. temp. difference °C	Wind speed ratio ²	Solar radiation ratio
Jan	2.66	1.20	0.88	1.05
Feb	5.23	1.47	0.95	1.02
Mar	2.95	1.22	0.85	1.01
Apr	4.04	1.30	0.95	0.93
May	4.17	1.30	0.97	0.96
Jun	3.41	1.24	0.86	0.91
Jul	3.20	1.19	0.86	1.10
Aug	4.49	1.19	0.88	1.15
Sep	4.87	1.22	0.89	0.96
Oct	4.08	1.28	0.97	0.91
Nov	3.86	1.28	0.96	0.97
Dec	2.12	1.14	0.97	1.00

¹Difference = 2xCO₂ - 1xCO₂

²Ratio = 2xCO₂/1xCO₂

Table 3.7. CCC-GCM 2xCO₂ climate scenario for Wilmington, North Carolina.

Month	Air temp. difference ¹ °C	Dew pt. temp. difference °C	Wind speed ratio ²	Solar radiation ratio
Jan	2.66	1.20	0.88	1.05
Feb	5.23	1.47	0.95	1.02
Mar	2.95	1.22	0.85	1.01
Apr	4.04	1.30	0.95	0.93
May	4.17	1.30	0.97	0.96
Jun	3.41	1.24	0.86	0.91
Jul	3.20	1.19	0.86	1.10
Aug	4.49	1.19	0.88	1.15
Sep	4.87	1.22	0.89	0.96
Oct	4.08	1.28	0.97	0.91
Nov	3.86	1.28	0.96	0.97
Dec	2.12	1.14	0.97	1.00

¹Difference = 2xCO₂ - 1xCO₂

²Ratio = 2xCO₂/1xCO₂

CHAPTER 4

METHODOLOGY OF TEMPERATURE AND DISSOLVED OXYGEN MODELING FOR LAKES OF THE SOUTHEAST REGION OF THE UNITED STATES

4.1 Review of MINLAKE95

MINLAKE95 is a one-dimensional, year-round water quality model which simulates vertical temperature and dissolved oxygen profiles in lakes (Stefan et al., 1994). Its intended use is to determine long-term trends for lakes on a regional basis under different climate scenarios.

The model is deterministic in nature and accounts for, among others, all the processes shown in Fig. 4.1. The mechanisms used in the modeling of temperature are wind mixing, surface heat exchange, vertical dispersion in the water, heat absorption from solar radiation, and sediment-water heat exchange. The processes used for the modeling of dissolved oxygen are air-water oxygen exchange, vertical dispersion in the water, photosynthesis, biochemical oxygen demand (BOD), respiration, and sediment oxygen demand (SOD). Lakes are divided into a series of discrete horizontal layers and a daily time step is used. A simplified flowchart of the model is given in Fig. 4.2.

MINLAKE95 was originally developed to simulate lakes in the State of Minnesota. Thus, lakes within that region were used to establish a number of the model coefficients. Testing of the applicability of these coefficients to areas outside Minnesota was not within the scope of this exploratory study. However, a comparison of simulations with measurements in lakes of the southeastern U.S. was made to establish new error limits for individual lakes. A general discussion pertaining to this issue is given in section 4.2.

As with any model, MINLAKE95 has embedded in it a number of underlying assumptions, among which are the following:

1. Transport is unsteady and one-dimensional with depth; each discretized horizontal layer of the lake is well-mixed.
2. Only temperature and dissolved oxygen are modeled; thus, the chlorophyll-a and BOD concentrations have to be specified depending on trophic status. BOD remains constant during the year while a seasonal cycle is superimposed on the specified mean chlorophyll-a concentration. Total dissolved solids and total suspended solids are not modeled.

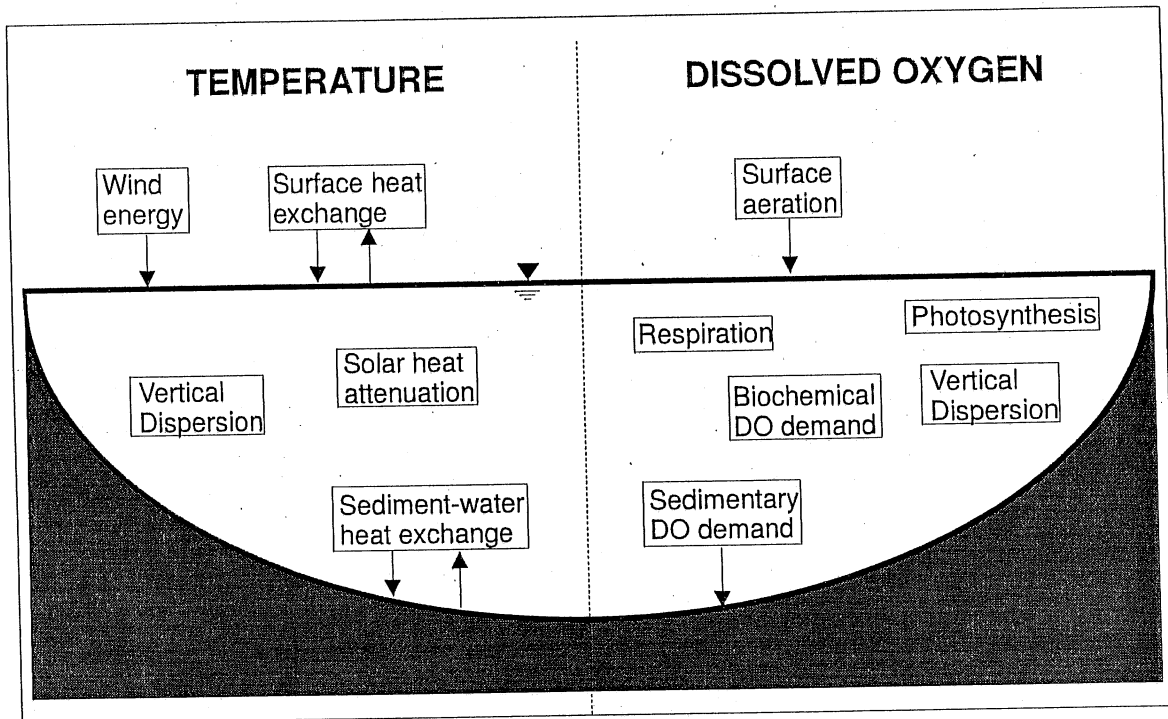


Fig. 4.1. A schematic representation of physical processes represented in MINLAKE95.

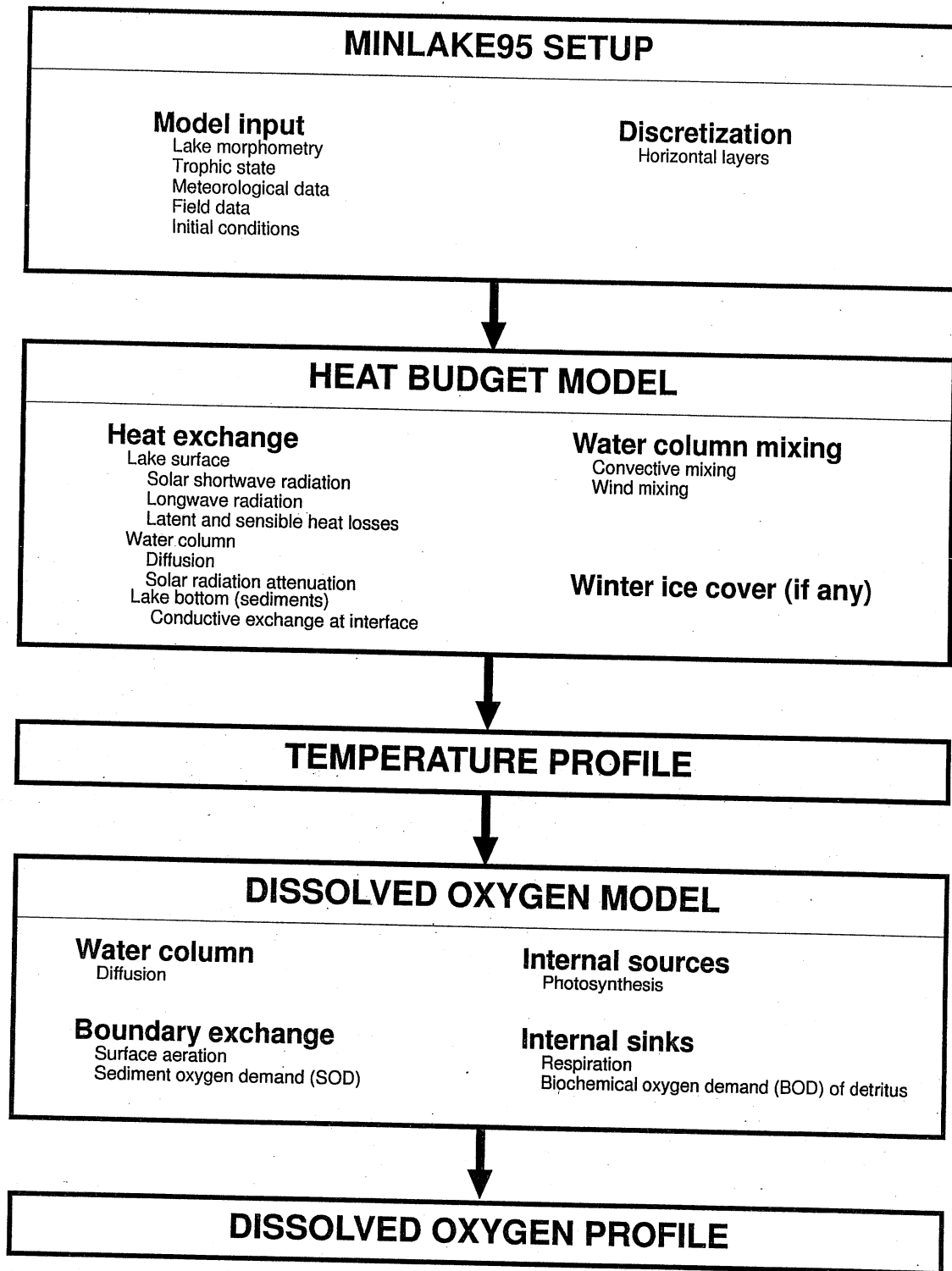


Fig. 4.2. MINLAKE95 schematic flowchart.

3. There are no inflows or outflows; hence, advection in the transport equation is neglected. The stage of a lake remains constant.

The general one-dimensional, unsteady transport equation used for temperature and dissolved oxygen (DO) in MINLAKE95 is

$$\frac{\partial \Phi}{\partial t} = \frac{1}{A} \frac{\partial}{\partial z} \left[AK_z \frac{\partial \Phi}{\partial z} \right] \pm S_1 \Phi \pm S_2 \quad (4.1)$$

where $\Phi(z,t)$ is the temperature ($^{\circ}\text{C}$) or DO concentration (mg L^{-1}) as a function of depth z in meters below the water surface and time t in days, $A(z)$ is the horizontal lake area (m^2), $K_z(z,t)$ is the vertical eddy diffusion coefficient ($\text{m}^2 \text{d}^{-1}$), and S_1 and S_2 are the first- and zero-order source/sink terms, respectively. The reader is referred to Hondzo and Stefan (1992), Fang and Stefan (1994), and Stefan et al. (1994) for further details about the individual source and sink terms. The first term on the right-hand side of equation (4.1) represents the net vertical diffusive flux per unit volume. The discretized form of the transport equation is

$$\begin{aligned} \frac{\Phi_{i,j+1} - \Phi_{i,j}}{\Delta t} = & \frac{1}{A_i \Delta z} \left[A_{i+1/2} K_{i+1/2} \left[\frac{\Phi_{i+1,j+1} - \Phi_{i,j+1}}{\frac{1}{2}(\Delta z_i + \Delta z_{i+1})} \right] \right. \\ & \left. - A_{i-1/2} K_{i-1/2} \left[\frac{\Phi_{i,j+1} - \Phi_{i-1,j+1}}{\frac{1}{2}(\Delta z_i + \Delta z_{i-1})} \right] \right] \pm S_1(\Phi_{i,j+1}) \pm S_2 \end{aligned} \quad (4.2)$$

where i is a node and j is a time step (i.e. $\Phi_{i,j}$ is the temperature or DO concentration in layer i at time step j). Rearranging and combining like terms gives an equation of the form

$$B_1 \Phi_{i-1,j+1} + B_2 \Phi_{i,j+1} + B_3 \Phi_{i+1,j+1} = B_4 \quad (4.3)$$

This formulation yields n equations with n unknowns, where n is the number of layers. These equations can be put into matrix form (see Riley and Stefan, 1987) which is then solved by Gaussian elimination with the appropriate boundary and initial conditions.

MINLAKE95 requires the following information as input: lake morphometry,

trophic state, meteorological data, and initial conditions. Various coefficients also must be specified.

4.2 Applicability of MINLAKE95 to the southeast region

A number of conditions and assumptions imposed in the development of MINLAKE95 pose potential applicability problems in the southeastern study area. These issues include inflows to and outflows from lakes, hydraulic residence times, suspended solids concentrations, lake shape, horizontal variations in water quality, and changes in lake stage.

As stated in the previous section, the MINLAKE95 model does not incorporate inflows or outflows, which presents a problem when modeling reservoirs, in which advection can play a major role in the transport equation (eq. 4.1). This is especially important in reservoirs with short hydraulic residence times, which are prevalent in the southeastern U.S. Incorporating advection, influent plunging flows, and outflows into MINLAKE95 was not within the scope of this study. It was therefore decided to model only lakes with long water residence times (greater than 150 days) and with in-lake water quality measurements available for model validation.

Inorganic suspended solids, such as clay particles, are not explicitly modeled by MINLAKE95. Non-phytoplanktonic suspended solids can make an important contribution to light attenuation with depth. Extinction of light with depth in water is given by

$$\frac{I_z}{I_0} = e^{-kz} \quad (4.4)$$

where I_z and I_0 are the light intensities (e.g. kcal m⁻² d⁻¹) at depth z and at the surface, respectively, and k is the overall light attenuation coefficient (m⁻¹). The attenuation coefficient can be given as (Bannister, 1974; Megard et al., 1979)

$$k = k_w + k_{ss}SS + k_c Chl-a \quad (4.5)$$

where k_w is the attenuation due to water (m⁻¹), k_{ss} is the attenuation due to suspended solids (L mg⁻¹ m⁻¹), SS is the non-phytoplanktonic suspended solids concentration (mg L⁻¹), k_c is the attenuation due to phytoplankton (L mg⁻¹ m⁻¹), and $Chl-a$ is the phytoplankton concentration as measured by chlorophyll-a (mg L⁻¹).

Since inorganic suspended solids were not routinely measured in the lakes of the study area and since they are not included in MINLAKE95, an alternative determination of the extinction coefficient was used:

$$k = \frac{c}{Z_s} \quad (4.6)$$

where c is a constant and Z_s is the Secchi depth (m). A regression on data from South Carolina (Fig. 4.3) showed the value of the constant c to be 1.64, which is comparable with values presented by other researchers (Poole and Atkins, 1929; Idso and Gilbert, 1974; Koenings and Edmundson, 1991; Hondzo and Stefan, 1992). This value was used in MINLAKE95 for application to the southeastern US.

The shape of a lake has a noticeable effect on wind fetch, which is used in calculating wind mixing energy and surface reaeration. MINLAKE95 models the surface of each lake as circular, and, therefore, the fetch is simply the diameter of the lake, irrespective of wind direction. This has worked well with lakes in Minnesota (Stefan et al., 1994), even with those of less-than-circular shapes (Fig. 4.4). The dendritic shapes (Fig. 2.4) of the reservoirs in the southeastern U.S. have, however, vastly different fetches, depending on wind direction.

Horizontal variations of temperature and DO do exist in any lake for a variety of reasons, such as differential heating, inflow, and mixing (Ford, 1990). The assumption of well-mixed layers works well for modeling of natural lakes of moderate size but not for dendritic reservoirs with sheltered coves, especially if they are many kilometers in length. Fig. 4.5 from Thornton et al. (1990) gives a schematic of a reservoir, showing how the water quality in the headwaters or in one of the arms can be different from that near the dam.

Due to changes in water storage, water surface elevations (stages) in reservoirs can vary significantly and with them surface area, maximum fetch and depth. These stage changes can have significant impacts on water quality. Under stratified conditions, layers of water are removed selectively so that the effect of withdrawal is analogous to removing cards from a stack of cards. Hypolimnetic withdrawal has the effect of lowering the thermocline and raising the average water temperature in the reservoir. Surface withdrawal also causes the thermocline to drop since the thinned epilimnion will readjust to atmospheric conditions. Overall temperatures, however, may not increase, for the warmest water from the surface mixed layer has been removed. Because MINLAKE95 keeps the lake stage constant, effects of major inflow and outflow changes are not taken into account.

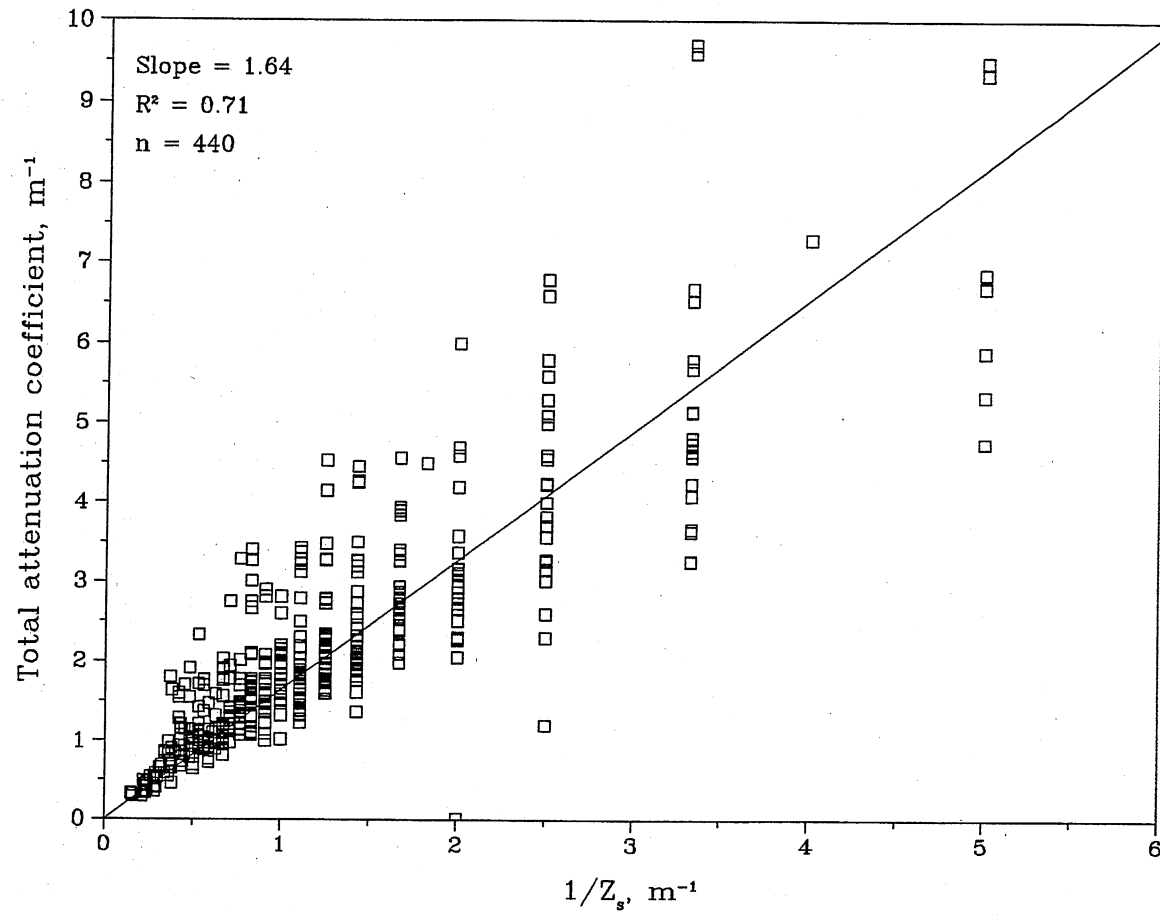
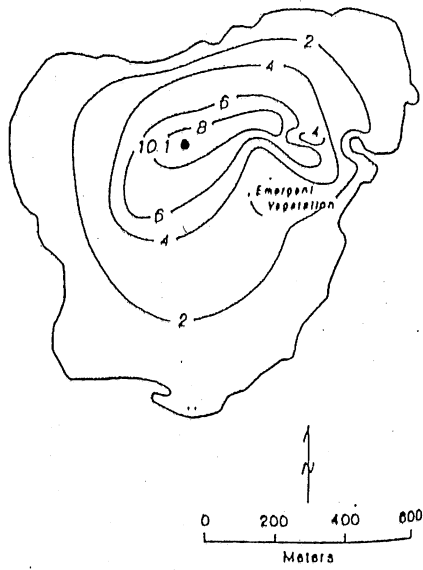
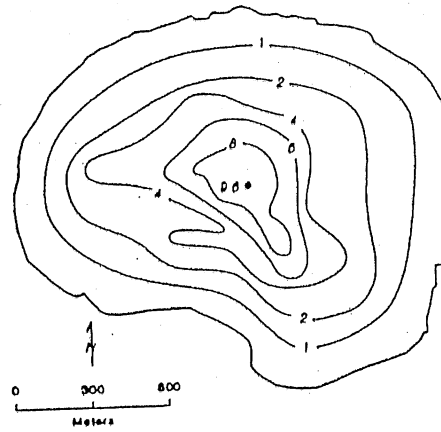


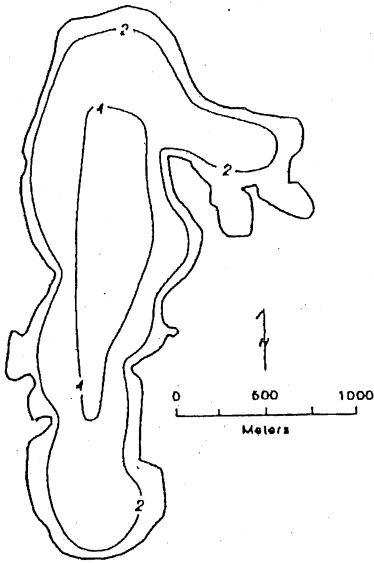
Fig. 4.3. Total attenuation coefficient vs. $(\text{Secchi depth})^{-1}$ for lakes and reservoirs in South Carolina.



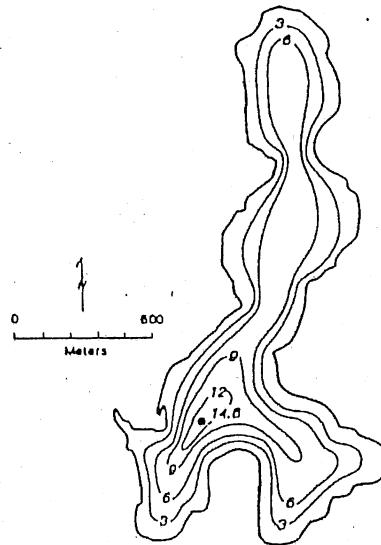
(a)



(b)



(c)



(d)

Fig. 4.4. Previously modeled Minnesota lakes: (a) Orchard Lake, (b) Lake George, (c) Cedar Lake, (d) Fish Lake (Stefan et al., 1994).

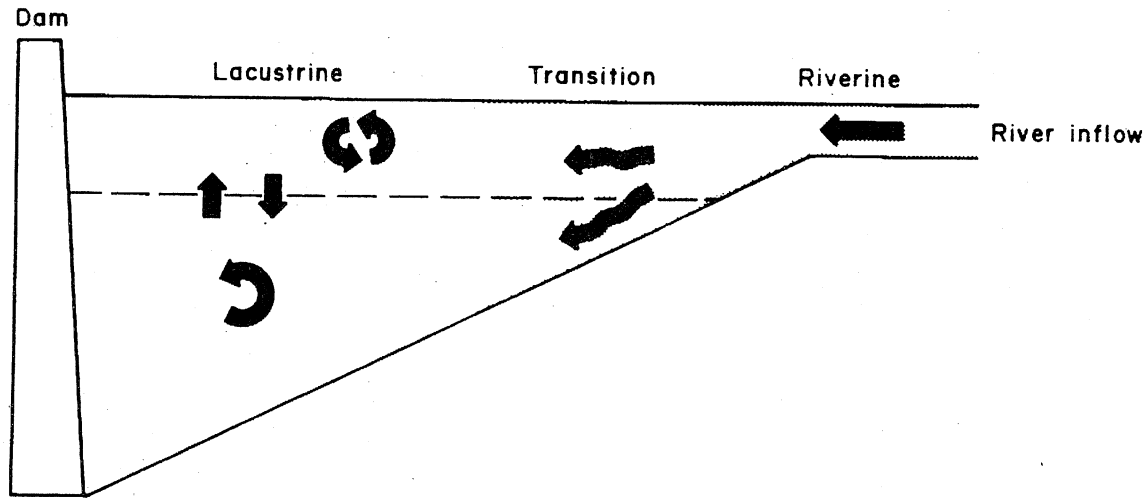


Fig. 4.5. Three distinct zones resulting from gradients in reservoirs (Thornton et al., 1990).

4.3 Lake classification problems

Hondzo and Stefan (1992) devised a classification scheme for Minnesota based on a sample of 3002 Minnesota lakes. The scheme divides lakes into 27 classes based on surface area, maximum depth, and trophic state as mentioned earlier. The groupings were given in Table 2.1.

For Minnesota, the classification with respect to trophic status was based on Secchi disk transparency (Hondzo and Stefan, 1992). Secchi depth can be related to trophic status using Carlson's Trophic State Index (Carlson, 1977). This scheme works reasonably well in Minnesota lakes, which are generally natural, have long residence times, are mostly phosphorus limited, and contain particulate matter consisting mainly of phytoplankton.

The majority of the lakes in the southeastern U.S. are reservoirs. For a number of reasons, reservoirs are difficult to classify by a simple empirical trophic state index (Kimmel et al., 1990; Higgins et al., 1980; Hannan et al., 1980). Many reservoirs can have a trophic state in the riverine reach different from that in the lacustrine reach (Fig. 4.5) (Hannan et al., 1980). Inorganic suspended sediment particles often contribute heavily to light attenuation in these lakes. The classification scheme which works reasonably well for Minnesota cannot be applied to the reservoirs found in the southeastern U.S., where parameters that affect productivity (e.g. inflows, inorganic suspended solids, exchange flows with sidearms)--heretofore assumed as insignificant--become significant. Additional parameters, e.g. hydraulic residence time, elevation of outlet, and turbidity measures would have to be considered in the classification. With more than three or four independent variables to consider, any classification becomes cumbersome.

For these reasons, the study was directed to specific reservoirs and lakes for which in-lake water quality measurements were available for model calibration and validation. The results are given in the next section.

CHAPTER 5

CASE STUDIES

5.1 Reservoir and lake selection

Lakes were selected on the basis of hydraulic residence time (see section 4.2) and availability of water quality data. Table 5.1 lists residence times in addition to other morphometric parameters for 44 lakes in North and South Carolina. At first, only lakes with hydraulic residence times of one year or longer were considered, but lack of water quality field data necessitated lowering that limit. Finally, lakes with hydraulic residence times between 1161 and 161 days were selected. They are highlighted in Table 5.1. Case studies of three reservoirs (B. Everett Jordan Reservoir, Lake James, Santeetlah Lake) and two natural Carolina Bay lakes (Lake Phelps, Lake Waccamaw) were conducted. The locations of the selected water bodies are shown in Fig. 5.1. Also shown in Fig. 5.1 are the weather stations from which meteorological data were obtained as input for the modeling of each lake. Significant parameter values are summarized in Table 5.2.

5.2 In-lake measurements used for calibration/validation

In-lake water quality measurements used to validate MINLAKE95 for the five lakes were obtained from the USEPA water quality database "STORET."

There are temporal and spacial limitations to using in-lake measurements for validation. Since MINLAKE95 uses a daily time step, simulated temperatures and DO concentrations are the average for any particular day. Actual measurements are made at a particular time of the day. As a one-dimensional model, MINLAKE95 assumes well-mixed horizontal layers, meaning that temperatures and DO concentrations are the same in any particular layer, regardless of the location in the lake (e.g. north end, east end, or center).

Many of the reservoirs in the southeastern US are quite dendritic in shape, and the water quality in the headwaters, in a sidearm, and near the dam can all be different. Figs. 5.2a-e show examples of the variations in temperature and DO profiles measured at several stations in the lakes used in this study. Locations of the sampling stations are shown in the figures for each lake, found in the following sections. The different maximum depths at which measurements were taken may reflect different depths to the lake bottom at the different station locations, but that is not known, since measurements

Table 5.1. Lakes and reservoirs in the southeast region with known hydraulic residence times. N = natural lake, R = reservoir.

Lake	State	Residence time days	Surface area km ²	Max. depth m	Volume 10 ⁶ m ³
High Rock (R)	NC	3.6-50.8	63.74	19	310
Parr (R)	SC	2.5	7.487	7.6	34.7
Saluda (R)	SC	3.1	2.023	12.2	4.9
Boyd (R)	SC	3.2	0.737	9.5	2.7
Yonah (R)	SC	4.9	0.809	20.4	7.9
Blewett Falls (R)	NC	7	10.4	12	8.3
Lookout Shoals (R)	NC	7	5.14	21	46.26
Fishing Creek (R)	SC	7.8	13.638	27.3	98.7
Mountain Island (R)	NC	12	13.09	16	71
Junaluska (R)	NC	13	0.81	7	4.5
Tillery (R)	NC	15	21.3	21	210
Rhodhiss (R)	NC	21	14.23	16	83.4
Adger (R)	NC	21	1.86	22	14.4
Wateree (R)	SC	25	55.484	19.5	382.4
Big Lake (R)	NC	25	0.25	5	0.5
Badin (R)	NC	28	21.65	53	340
Roxboro Lake (R)	NC	30	0.86	7	3.01
Wylie (R)	SC	32	50.405	28.4	347.7
Hickory (R)	NC	33	16.59	26	165.9
Wylie (R)	NC	39	50.39	21	352.73
Burlington (R)	NC	40	0.55	8	1.5
Moultrie (R)	SC	61	244.435	23	1493.8
Greenwood (R)	SC	69	46.135	21	320.7
Robinson, H. (R)	SC	69	9.106	9.4	38.2
Secession (R)	SC	70	3.561	28	23.9
Wheeler (R)	NC	72	2.23	9	0.0076
Little River (R)	NC	74	2.14	15	18
Summit (R)	NC	75	1.3	24	11.5
John H. Kerr (R)	NC	124	198.3	NA	450
Bowen (R)	SC	128	6.475	12.5	30.3
<i>Santee</i> (R)	NC	161	11.53	65	195
Fontana (R)	NC	179	43.18	134	1782
Hyco (R)	NC	180	15.18	15	99
<i>James</i> (R)	NC	208	26.35	36	368.9
Clarks Hill (R)	SC	214	317.685	43	3577.1
Norman (R)	NC	239	131.57	36	1315.7
White (N)	NC	292	4.25	3.2	9.45
Thorpe (R)	NC	294	5.92	NA	82.6
Marion (R)	SC	320	447.592	23.4	1726.9
Murray (R)	SC	378	206.394	57.8	2607.6
<i>B. Everett Jordan</i> (R)	NC	418	57.87	20	270
Hartwell (R)	SC	440	248.28	53.4	3503.1
<i>Phelps</i> (N)	NC	1161	67.18	3	100.77
Belews (R)	NC	1500	16.3	44	228

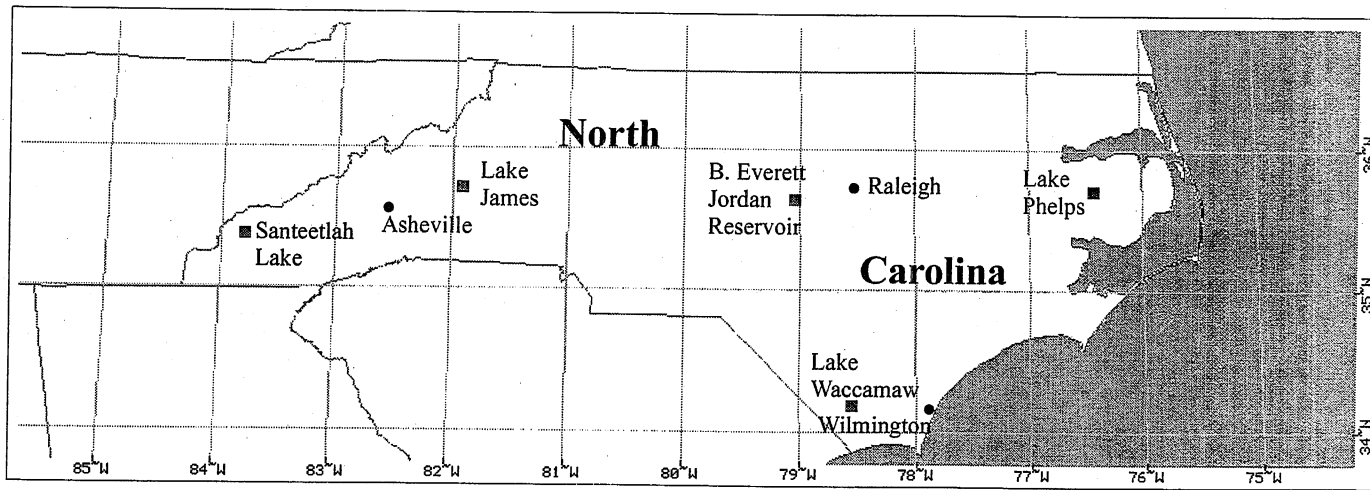


Fig. 5.1. Locations of selected water bodies and associated weather stations.

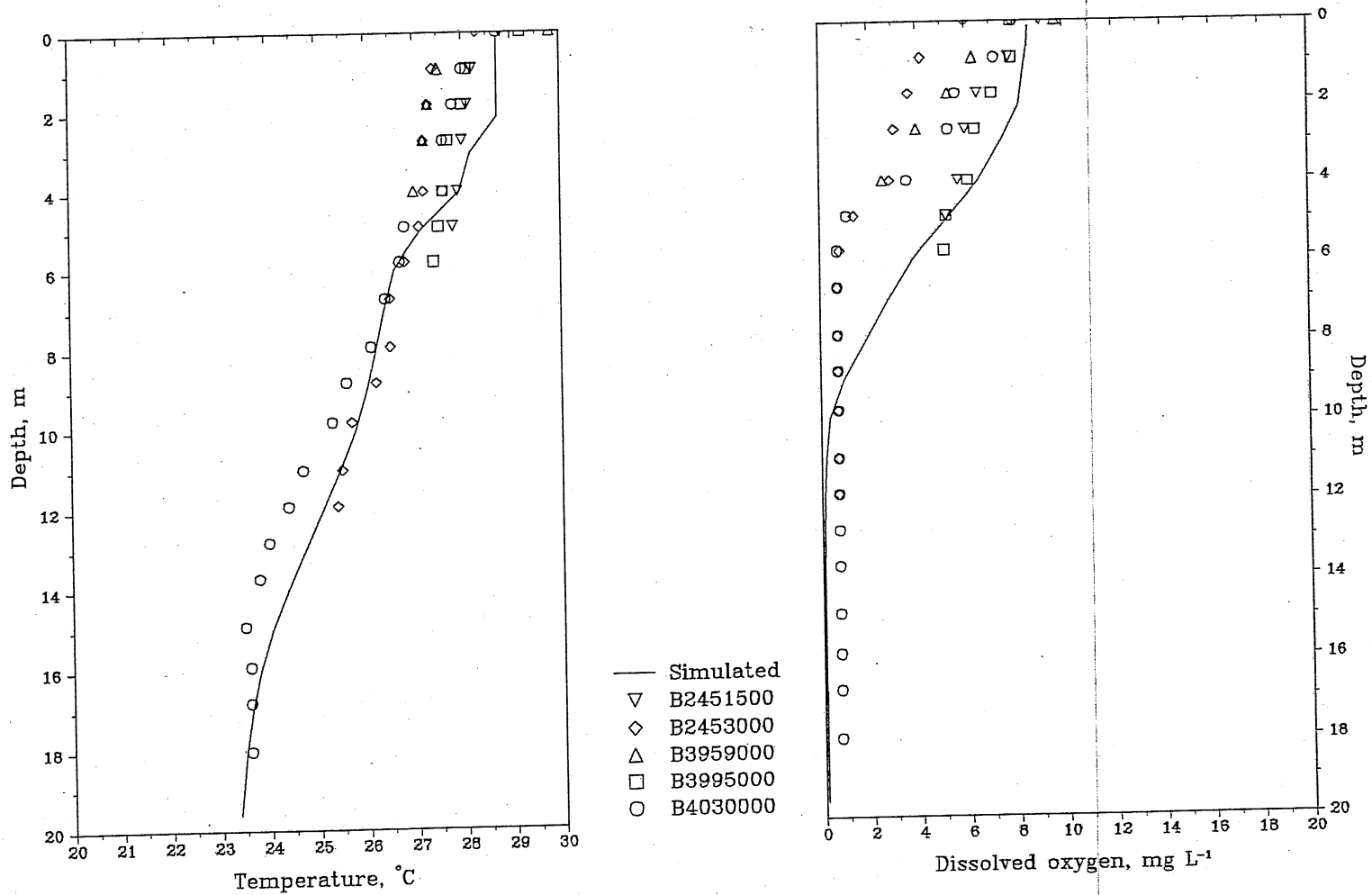


Fig. 5.2a. Temperature and dissolved oxygen profiles from simulation and measurements at several field stations in Jordan Reservoir on September 7, 1983.

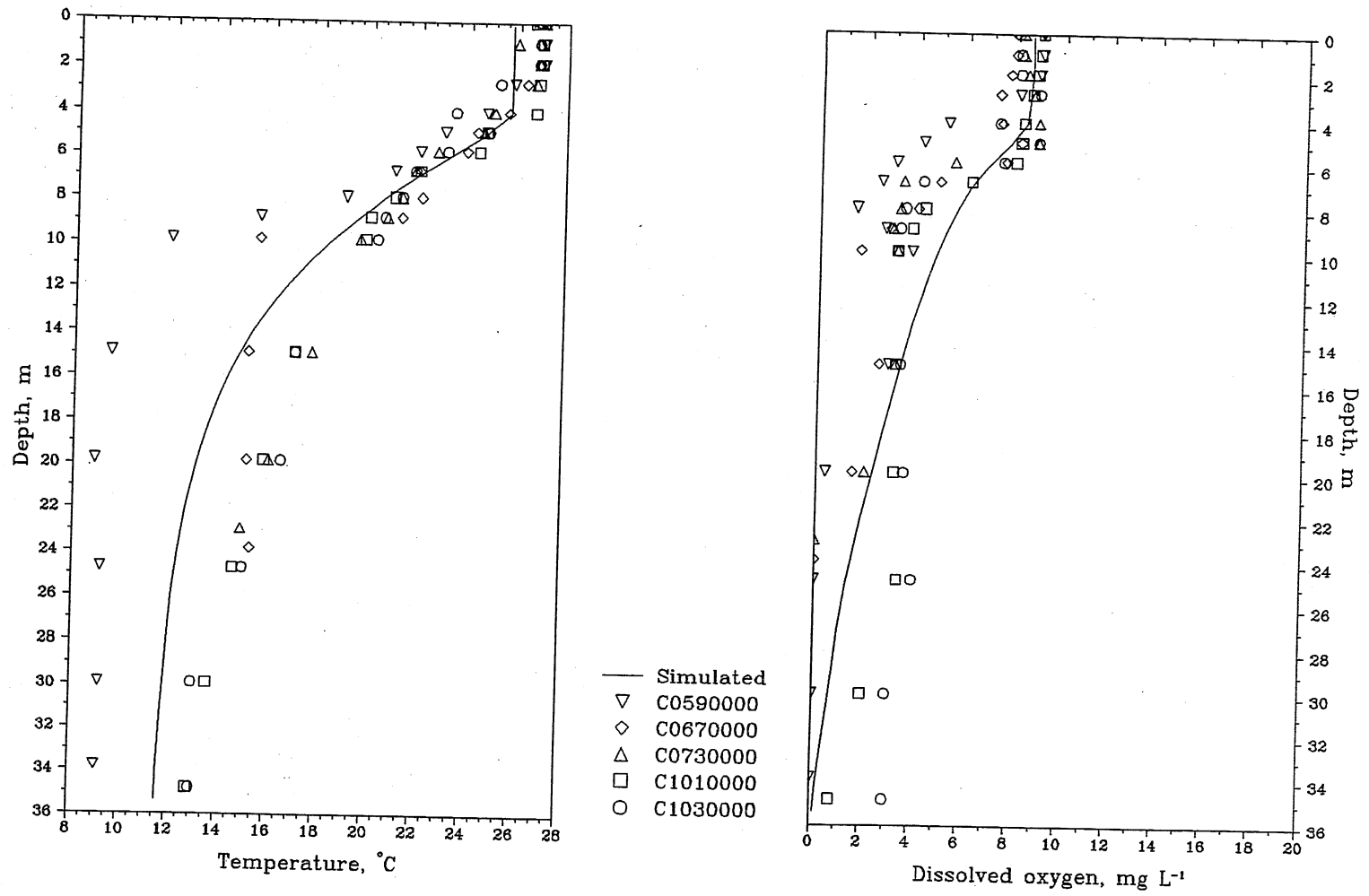


Fig. 5.2b. Temperature and dissolved oxygen profiles from simulation and measurements at several field stations in Lake James on July 17, 1984.

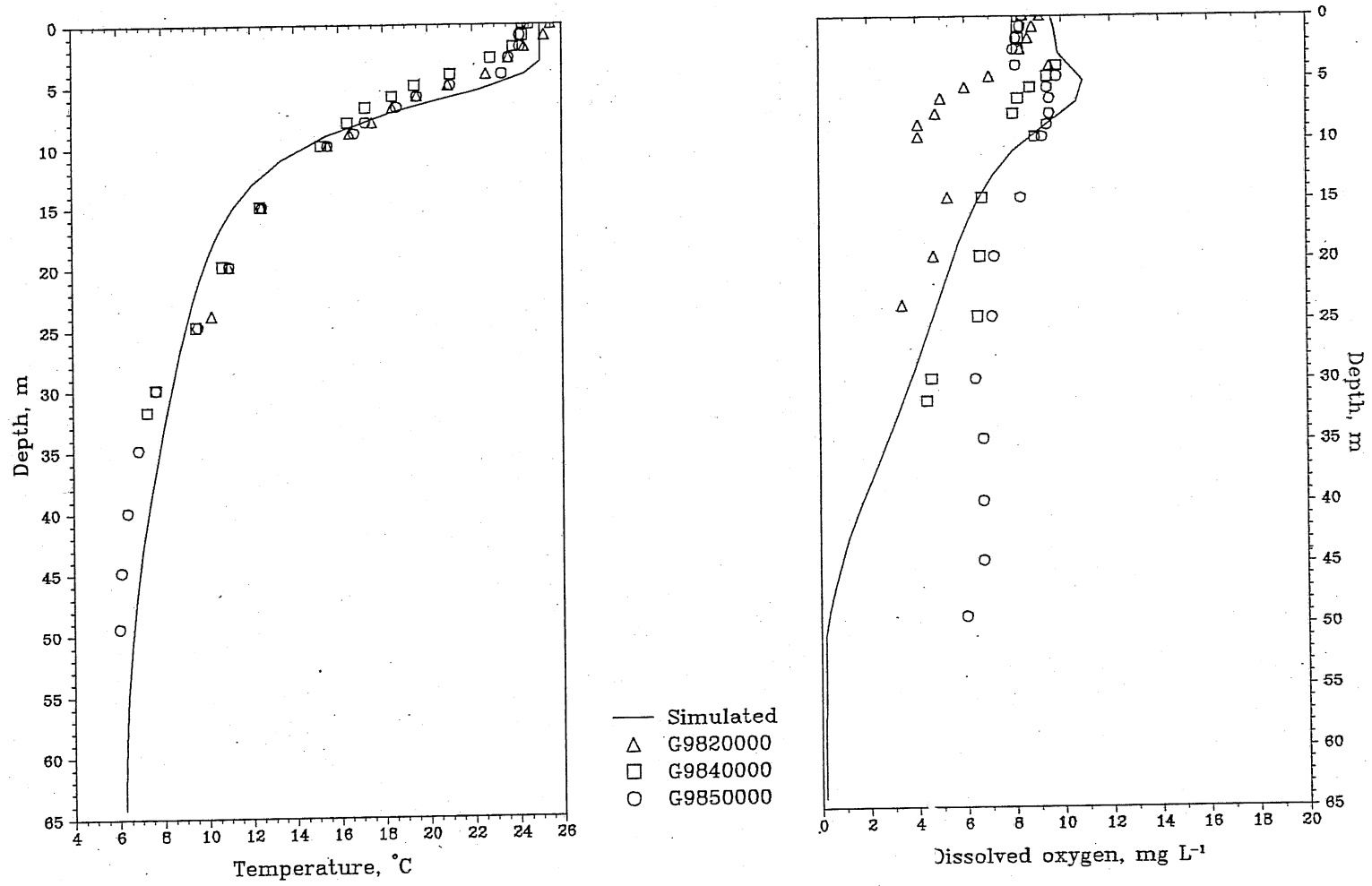


Fig. 5.2c. Temperature and dissolved oxygen profiles from simulation and measurements at three field stations in Santeetlah Lake on June 10, 1982.

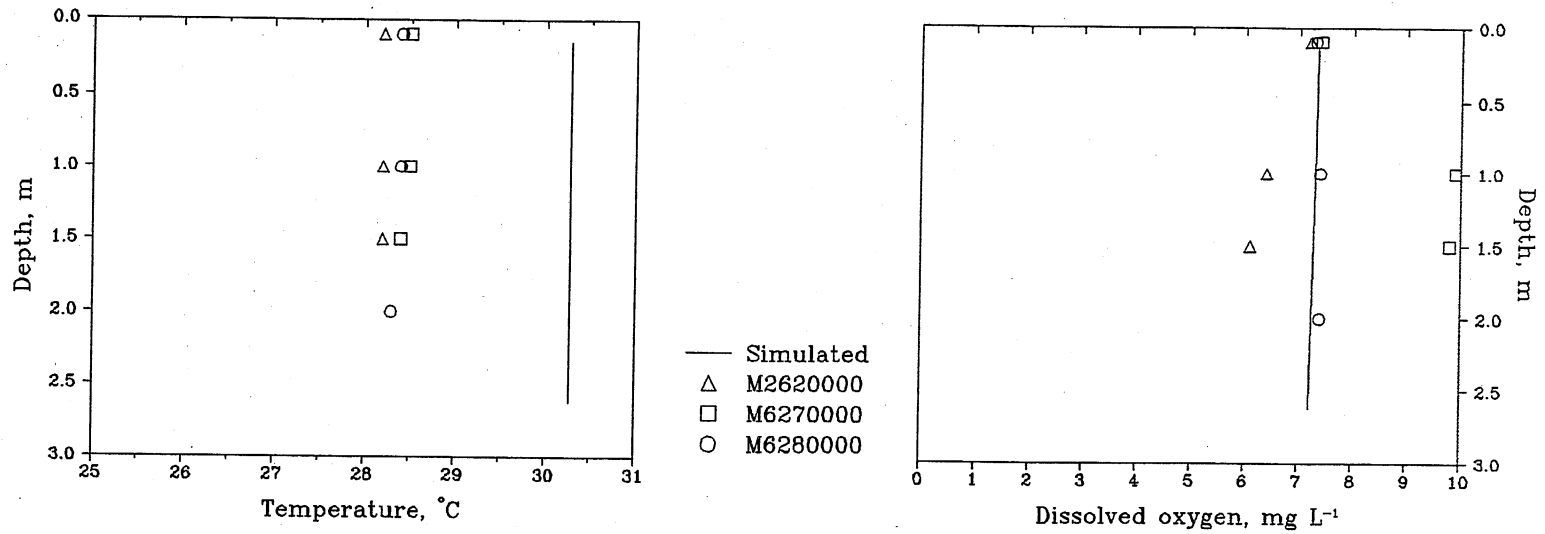
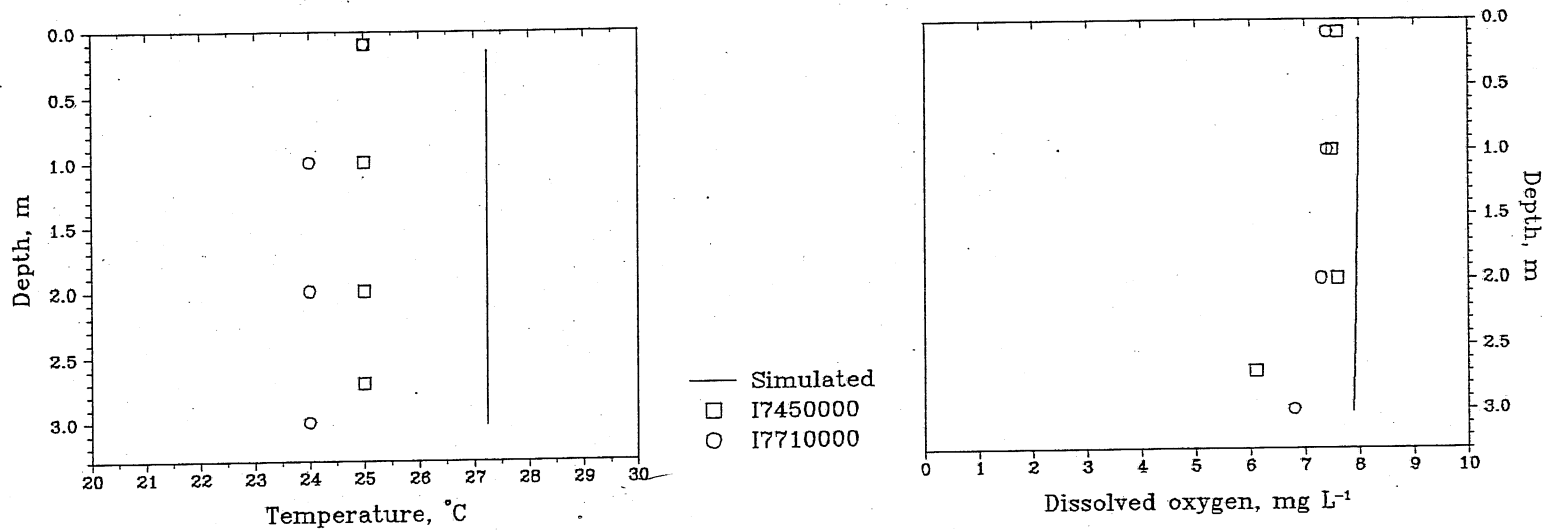


Fig. 5.2d. Temperature and dissolved oxygen profiles from simulation and measurements at two field stations in Lake Phelps on August 22, 1989.



45

Fig. 5.2e. Temperature and dissolved oxygen profiles from simulation and measurements at two field stations in Lake Waccamaw on September 11, 1986.

Table 5.2. Morphometric data summary of modeled lakes. N = natural lake, R = reservoir. Trophic state was determined based on nitrogen, phosphorus, chlorophyll-a, and Secchi depth measurements taken on a single day (from North Carolina DEHNR, 1992).

Lake	Surface Area km ²	Max. depth m	Res. time days	Trophic State ¹	Elev. m	Drainage area, km ²
Jordan (R)	57.87	20	418	E	66	4403
James (R)	26.35	36	208	O	365	984
Santeetlah (R)	11.53	65	161	O	609	450
Phelps (N)	67.18	3	1161	O	3	*
Waccamaw (N)	36.22	3.3	**	O	12	**

¹O=oligotrophic, E=eutrophic

*Lake Phelps has no known overland inflow, but is recharged primarily from precipitation with a small fraction coming from groundwater.

**These values are not available from the North Carolina DEHNR (1992) report.

were not always done to the same maximum depth at a given sampling station. It was decided to use measurements near the middle of each lake, since these measurements were thought to be most representative of the pelagic region of a lake. A more accurate method to model these types of lakes would be to use a two-dimensional model.

5.3 Input information for MINLAKE95

MINLAKE95 requires a variety of inputs. Of mentionable significance are some equation coefficients, lake morphometry, and sediment temperature.

For the initial simulations, coefficients (Table 5.3) were set to the values used by Stefan et al. (1994). When the simulation results proved satisfactory, these coefficient values were kept the same for the rest of the simulations, with a few exceptions. The exceptions are the following three variables: Wind function coefficient (W_{coef}), wind sheltering coefficient (W_{str}), and sediment oxygen demand rate coefficient (S_{b20}). The wind function coefficient is used in the determination of latent and sensible heat loss and has been specified in the past as a function of surface area (Hondzo and Stefan, 1992). The wind sheltering coefficient is used to determine the kinetic energy of the wind which is imparted onto a lake and has been determined in the past by calibration (Stefan et al., 1994). The sediment oxygen demand rate coefficient is the rate at 20 °C. Discussions of the values used for each lake can be found in the following sections.

Table 5.3. Coefficients and parameters used in MINLAKE95 (Stefan et al., 1994).

Coefficient	Units	Selected value	
Temperature model			
Radiation absorption for water	-	0.4	
Sediment specific heat	kcal kg ⁻¹ °C ⁻¹	0.28	
Sediment thermal conductivity	kcal °C ⁻¹ m ⁻¹ day ⁻¹	19.25	
Sediment density	kg m ⁻³	1970	
Dissolved oxygen model, independent of trophic state			
BOD decay rate	day ⁻¹	0.1	
Respiration rate	day ⁻¹	0.1	
BOD temperature adjustment	-	1.047	
Photosynthesis temperature adjustment	-	1.036	
Respiration temperature adjustment	-	1.047	
Sediment temperature adjustment	-	1.065	
Respiration ratio	mg O ₂ (mg Chl-a) ⁻¹	0.0083	
Dissolved oxygen model, dependent on trophic state			
Parameter	Units	Trophic state	Selected value
Biological oxygen demand (BOD)	mg L ⁻¹	eutrophic	1.0
		mesotrophic	0.5
		oligotrophic	0.2
Sedimentary oxygen demand (SOD) at 20°C	g m ⁻² day ⁻¹	eutrophic	1.0 (z _{max} =24m)
			1.5 (z _{max} =13m)
			2.0 (z _{max} =4m)
		mesotrophic	0.5 (z _{max} =24m)
			0.75 (z _{max} =13m)
			1.0 (z _{max} =4m)
		oligotrophic	0.2 (z _{max} =24m)
			0.4 (z _{max} =13m)
			0.5 (z _{max} =4m)

Table 5.4. Values of the lake-specific parameters used to estimate lake morphometry.

Lake	a	n
Jordan*	-	-
James	1.414×10^{-3}	1.273
Santeetlah	0.3192	0.7034
Phelps	1.403×10^{-7}	2
Waccamaw	4.361×10^{-6}	1.665

*Area and volume versus depth information was obtained from the U.S. Army Corps of Engineers.

Lake morphometry is specified in MINLAKE95 as a series of horizontal areas and volumes at various depths. Area and volume versus depth information was obtained for Jordan Reservoir from the U.S. Army Corps of Engineers. This information was not available for any of the other lakes. Since MINLAKE95 assumes that each lake is circular for fetch determination (see Section 4.2), a power function was used to estimate each lake's morphometry. It is of the form

$$A_z = \pi \left[\frac{z}{a} \right]^{2/n} \quad (5.1)$$

where A_z is the horizontal area (m^2) at depth z (m) and a and n are lake-specific parameters. The values a and n can be determined from a lake's total volume (m^3), surface area (m^2), and maximum depth (m). Table 5.4 shows the values of a and n for each of the lakes.

The calculation of sediment heat exchange at the sediment-water interface requires an adiabatic (constant temperature) boundary conditions to be specified at a certain depth (Sinokot and Stefan, 1992, Fang and Stefan, 1994), which is 10 m in MINLAKE95. From Fig. 5.3, this constant temperature was chosen to be 15 °C for all five lakes.

5.4 B. Everett Jordan Reservoir

B. Everett Jordan Reservoir (Fig. 5.4) is located in the center of North Carolina (Fig. 5.1), and was created by the U.S. Army Corps of Engineers in 1974, but its initial filling did not occur until 1981. It has a surface area of 58 km², maximum and mean depths of 20 m and 4.7 m, respectively, and a residence time of 418 days in the New Hope arm, which has about 90% of the total surface area. The Haw River arm has a retention time of only five days and accounts for 70-90% of the annual flow through the reservoir. The two arms are separated by a very narrow section. Jordan Reservoir is classified as eutrophic according to the North Carolina Trophic State Index (NCTSI) (see section 2.1 and North Carolina DEHNR, 1992). Meteorological data from Raleigh were used.

Jordan Reservoir has an abundance of field data, which made it the best candidate for modeling. Several simulations were done; some are not reported here because they are subsets of those discussed below. The simulations differ only by the years of simulation and the field data used to compare with the simulation results.

The reservoir was simulated for the years 1983-1987 (simulation #10). The values of W_{coef} and W_{str} were 1.0 and 0.6, respectively, and this gave satisfactory results. The value of S_{b20} was 1.5 g O₂ m⁻² d⁻¹ as suggested for a deep, eutrophic lake by Stefan et al. (1994). Simulated temperatures and DO profiles were compared with 51 days of field

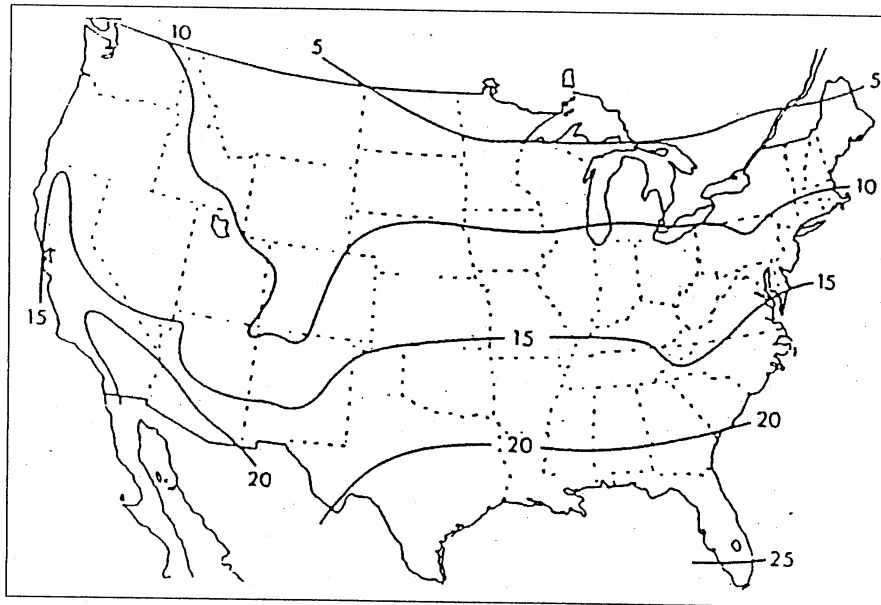


Fig. 5.3. Approximate temperature ($^{\circ}\text{C}$) of groundwater in the United States (from Todd, 1980, after Collins, 1925).

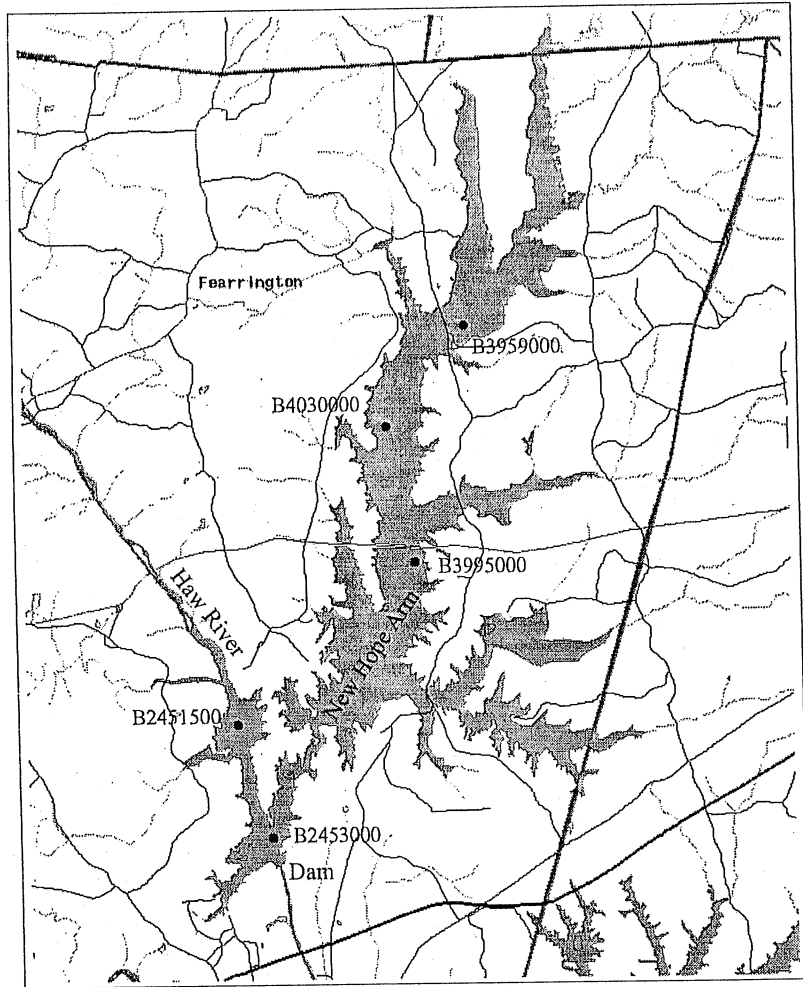


Fig. 5.4. B. Everett Jordan Reservoir with sampling stations. Data from stations B4030000 and B3995000 were used to check simulation results.

measurements from sampling station B3995000. The r^2 values for temperature and DO values (a total of 405 points) were 0.97 and 0.74, respectively. The standard errors were 1.32 °C and 1.67 mgL⁻¹, respectively. Field-measured water temperatures vary from about 4 °C during winter to about 30 °C in the summer months; these seasonal variations were simulated well, as shown in the temperature time series plots in Fig. 5.5. The model was also able to follow the seasonal trends of DO (Fig. 5.6), which varied from anoxic conditions in the hypolimnion during summer to about 12 mg L⁻¹ in spring. Fig. 5.7 shows that there was overall good agreement between measured and simulated water temperatures, while the model tended to overestimate DO concentrations, especially at low DO levels.

Another simulation (#12) was done for the years 1983-85 and checked against 29 days of field data from station B4030000, which is located to the north of station B3995000 but still within the open waters of Jordan Reservoir (Fig. 5.4). This was done because measurements at station B4030000 usually went deeper than those at station B3995000 and, thus, simulated values could be compared with field data at greater depths. Station B3995000 was still thought to be the most representative of Jordan Reservoir as a whole and hence was used for the calibration of the W_{cof} and W_{str} coefficients. The r^2 values for temperature and DO were 0.97 and 0.60, respectively. The standard errors were 1.25 °C and 2.36 mg L⁻¹, respectively. Time series plots are given in Figs. 5.8 and 5.9. As shown in Fig. 5.10, there was very good agreement between measured and simulated water temperatures but significant over- and underestimations of DO concentrations occurred.

Isotherms interpolated from simulated temperatures and field data from stations B3995000 and B4030000 are given in Fig. 5.11 for the years 1983-84. Figure 5.12 shows interpolated values for dissolved oxygen. There were 300 data points from station B403000, 182 from station B3995000, and 298 from the simulation. The isopleths were generated from these data points using Plot-IT, which uses a fifth-order interpolation scheme and can handle up to 300 original data points for a single contour plot. Field data were taken at approximately monthly intervals, though not at consistent maximum depths. The depth of the field data plots reflects at most the average maximum depth of Fig. 5.5 measurements for which the isopleths would be accurate. Data points from the simulation were taken from the middle of each month.

Jordan Reservoir is a monomictic lake, as can be seen in Fig. 5.11. Water temperatures during winter reach a minimum of about 4 °C. Maximum surface temperatures in summer reach 30 °C. Fig. 5.11 also demonstrates that the simulation was able to catch the onset of stratification and fall overturn at approximately the same time as is shown by the field data in both 1983 and 1984. As seen in Fig. 5.12, anoxia extends from the bottom up to a maximum of about 5 m below the water surface, and lasts from approximately May to September. The simulated DO values are a bit high in winter but low during summer stratification compared with the field data.

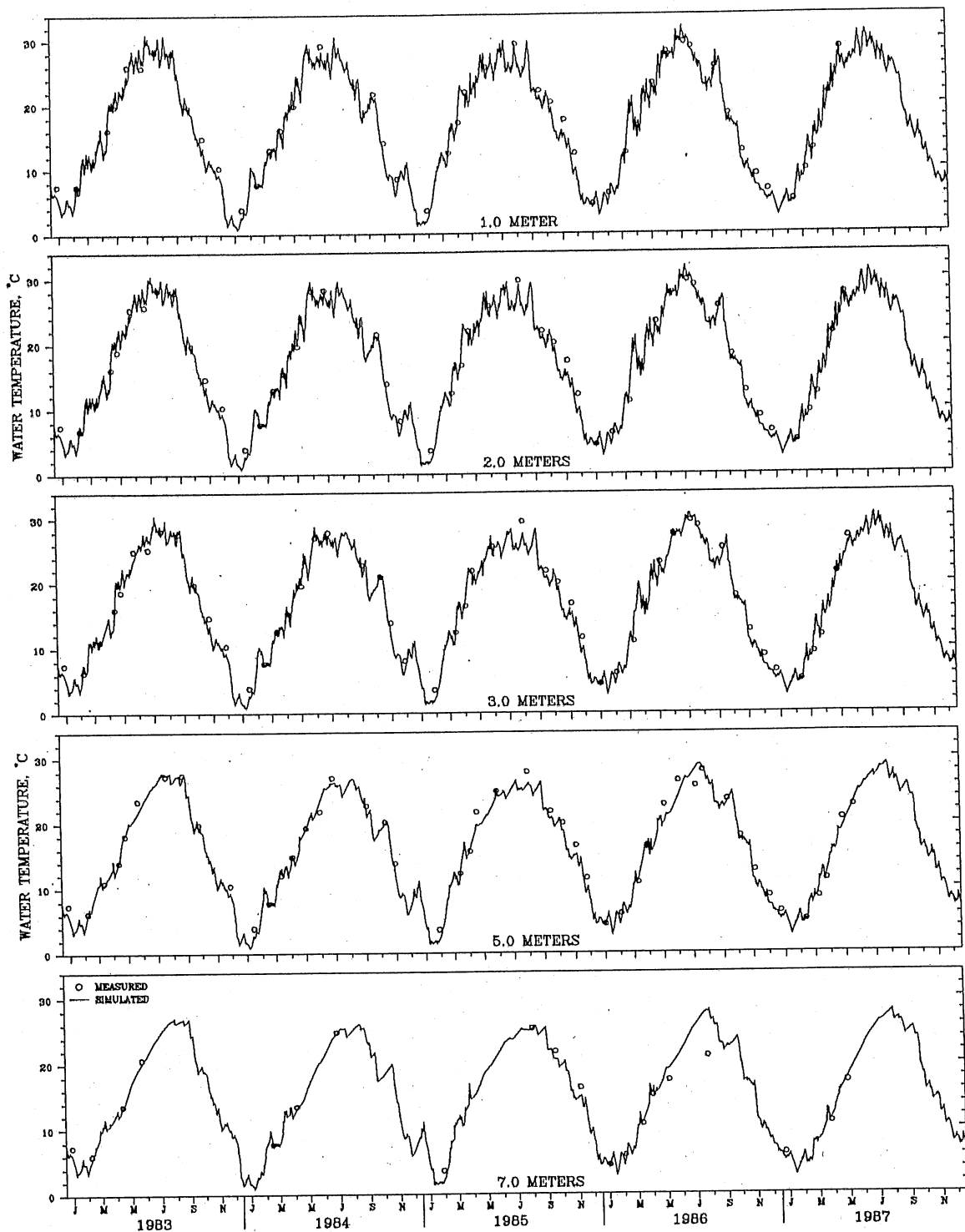


Fig. 5.5. Water temperature time series for Jordan Reservoir (1983-87), using chlorophyll-a (chl-a) measurements. Field data are from station B3995000 (simulation #10).

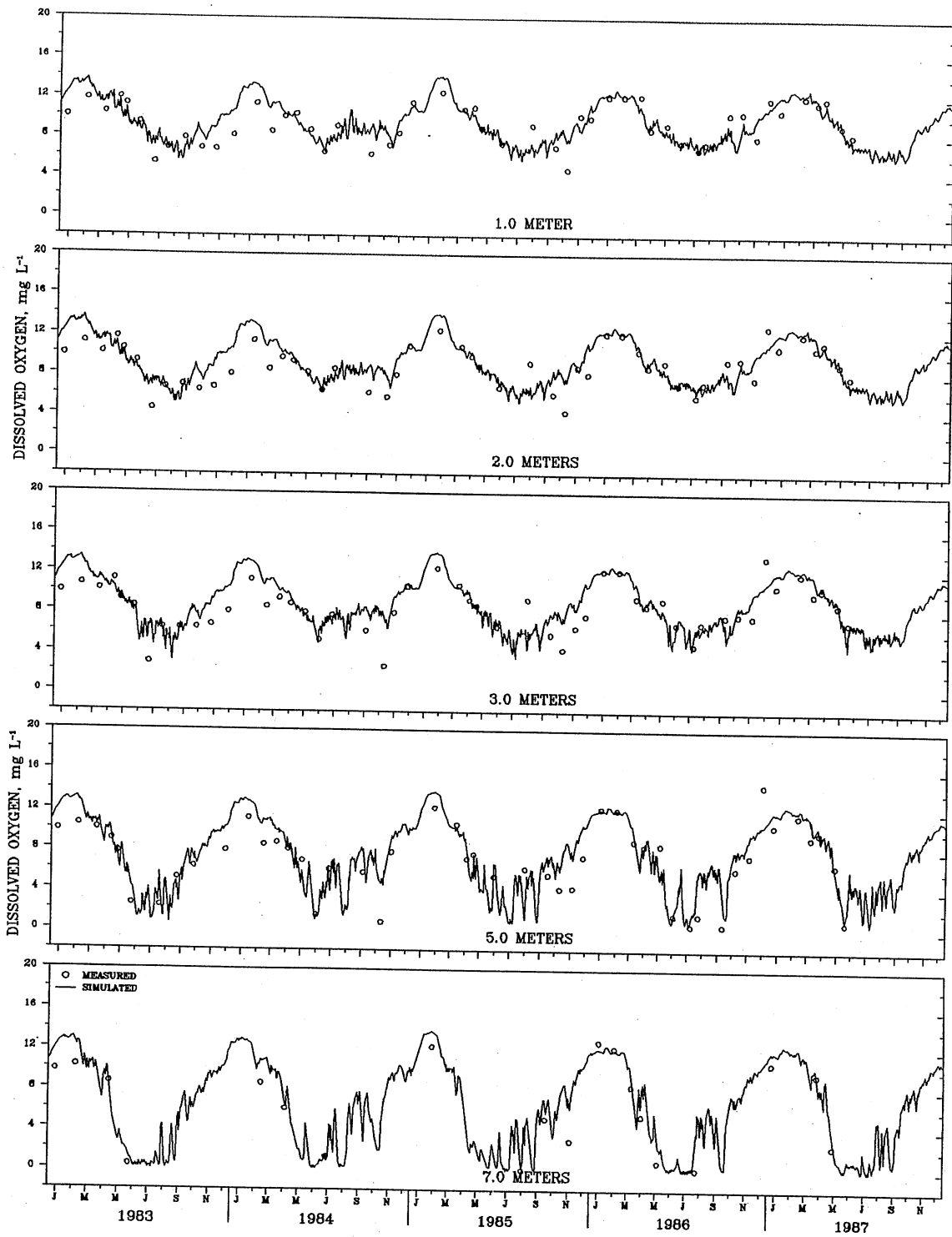


Fig. 5.6. Dissolved oxygen time series for Jordan Reservoir (1983-87), using chl-a measurements. Field data are from station B3995000 (simulation #10).

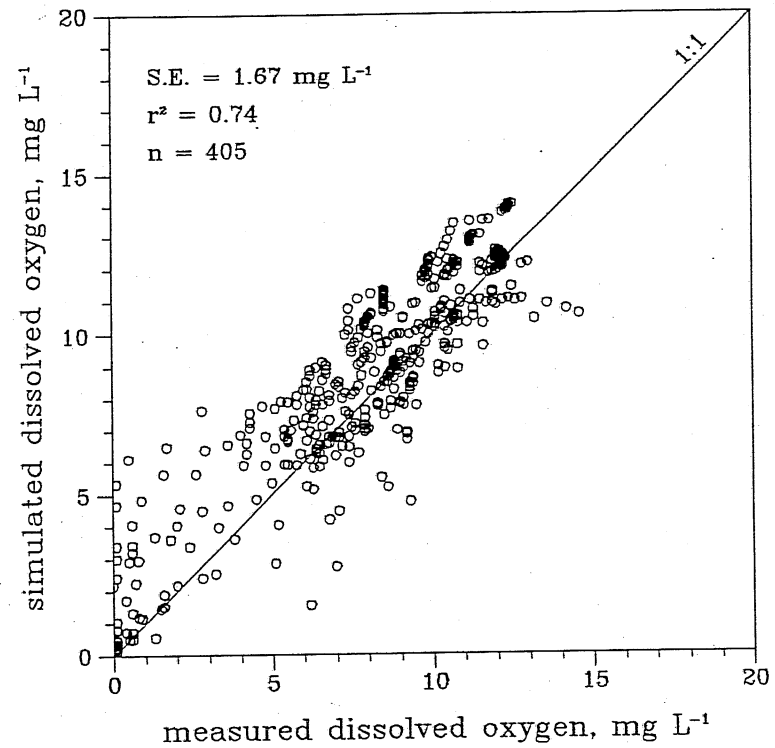
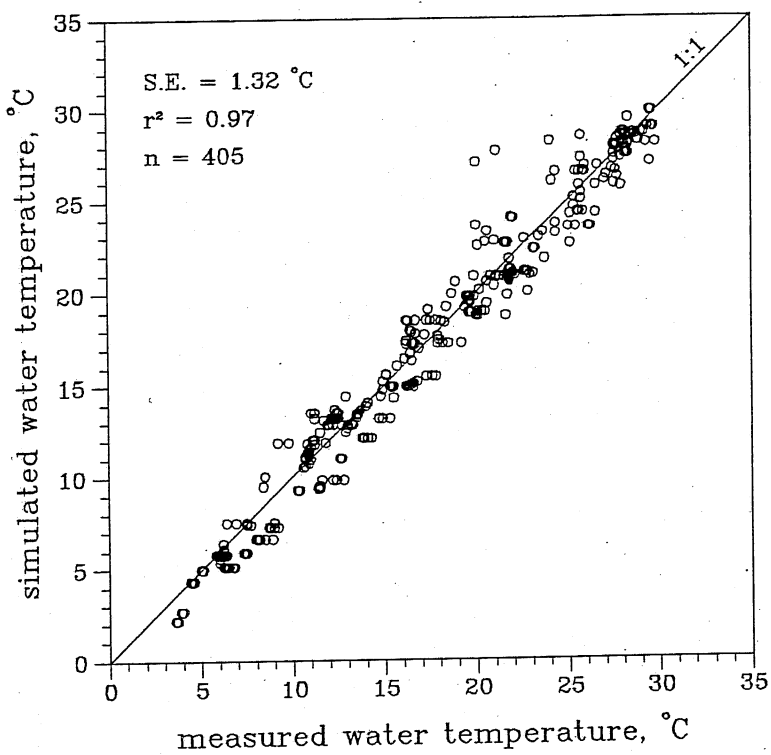


Fig. 5.7. Simulated versus measured temperature and dissolved oxygen in Jordan Reservoir (simulation #10, station B3995000).

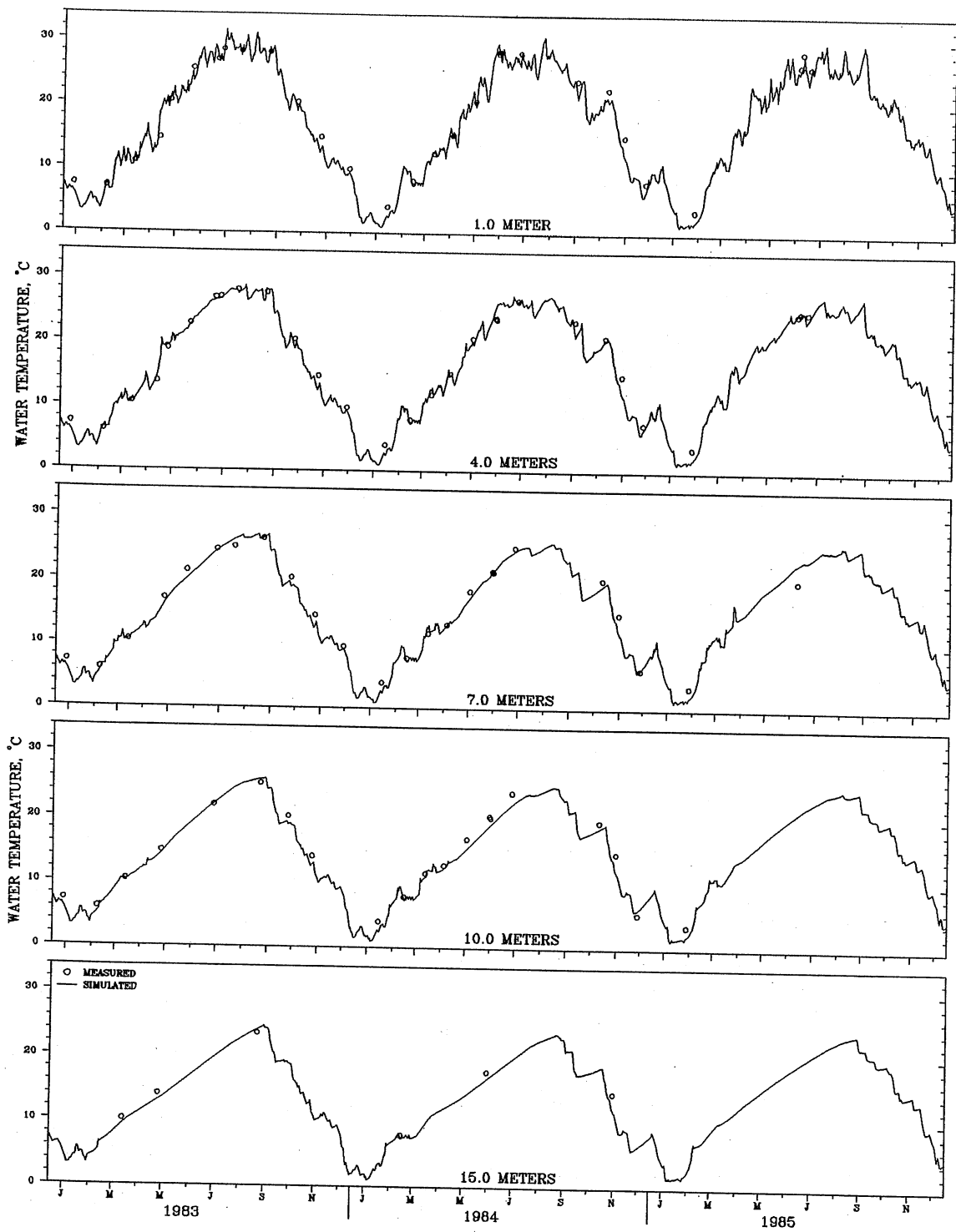


Fig. 5.8. Water temperature time series for Jordan Reservoir (1983-85), using chl-a measurements. Field data are from station B4030000 (simulation #12).

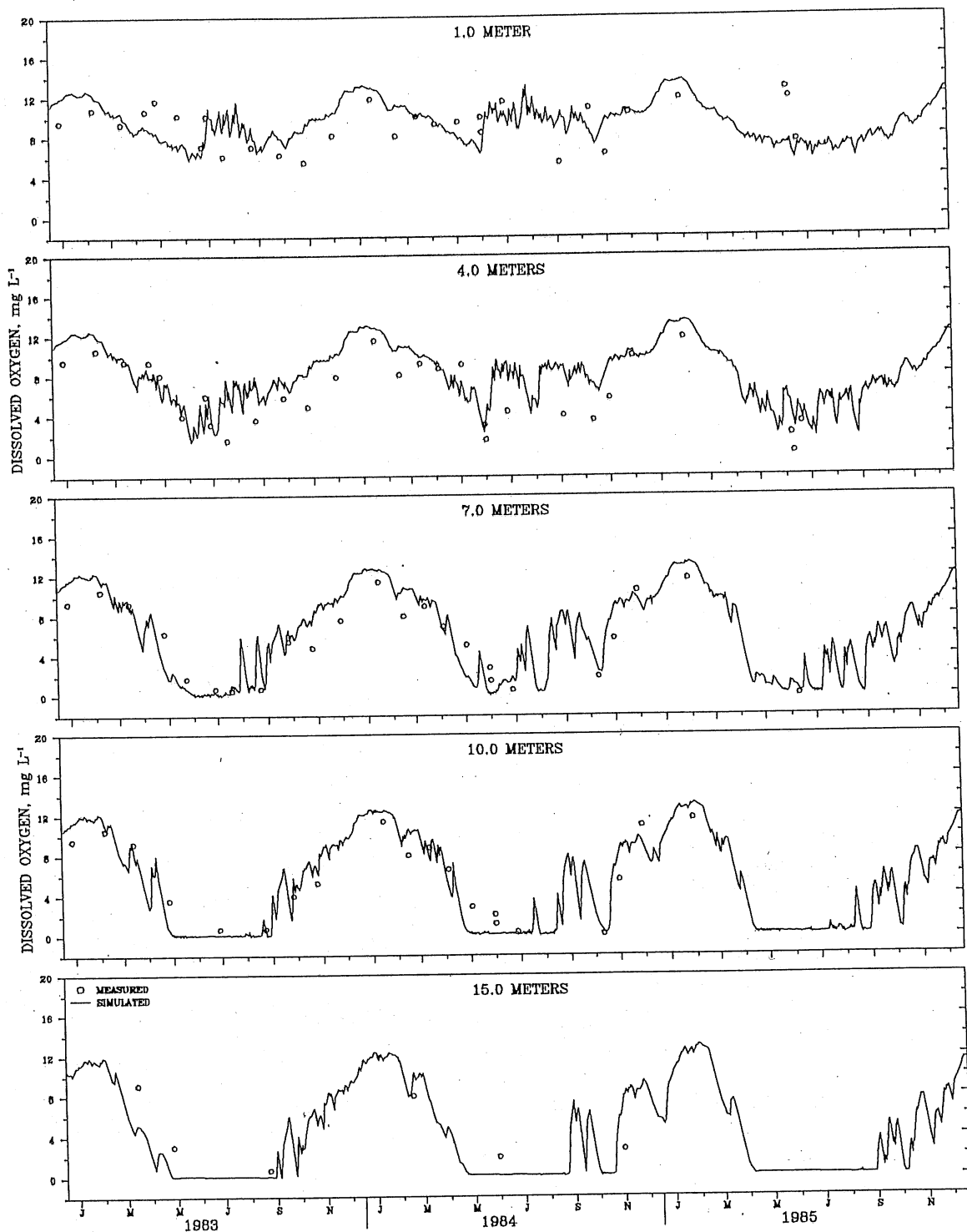


Fig. 5.9. Dissolved oxygen time series for Jordan Reservoir (1983-85), using chl-a measurements. Field data are from station B4030000 (simulation #12).

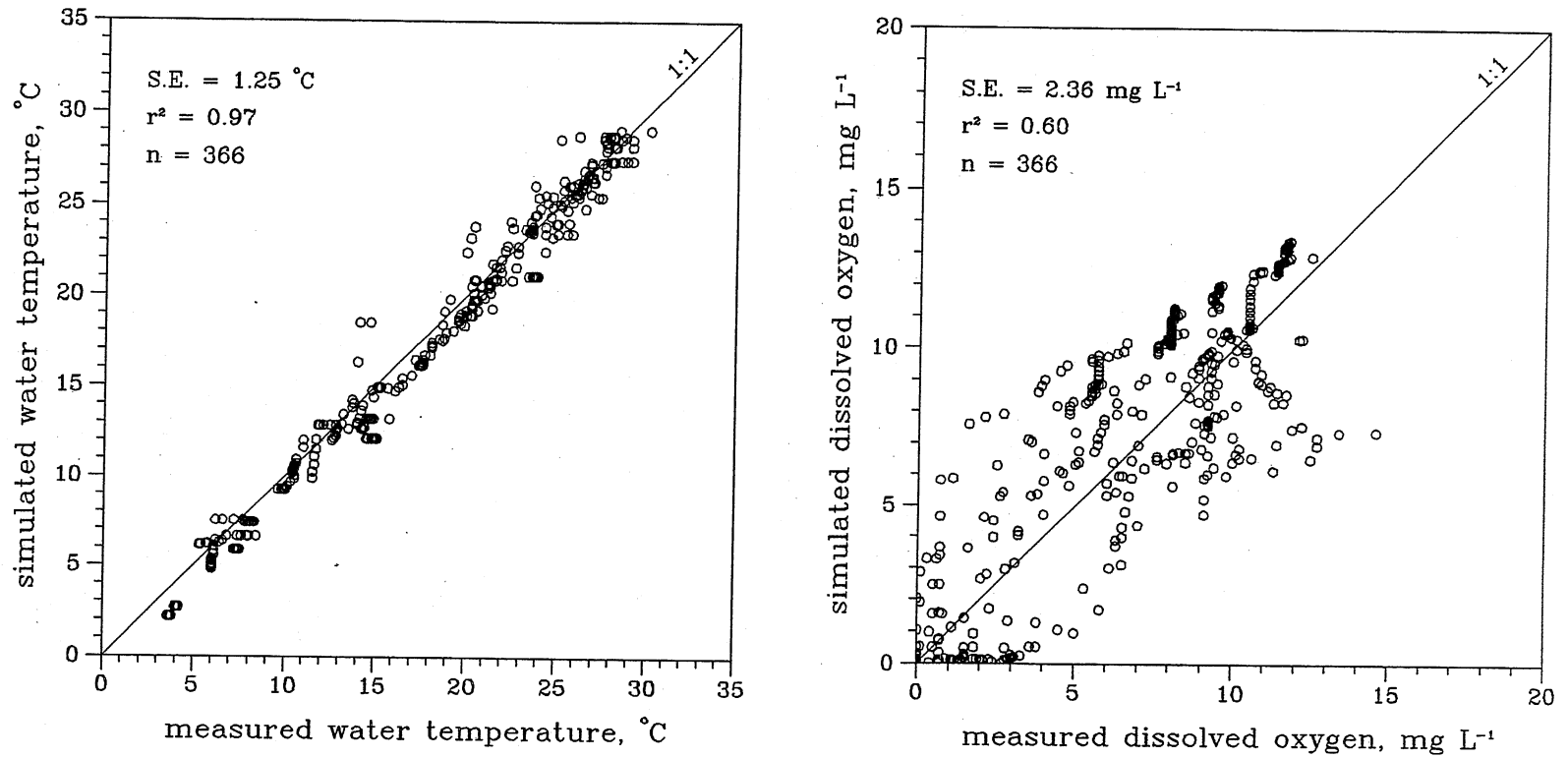


Fig. 5.10. Simulated versus measured temperature and dissolved oxygen in Jordan Reservoir (simulation #12, station B4030000).

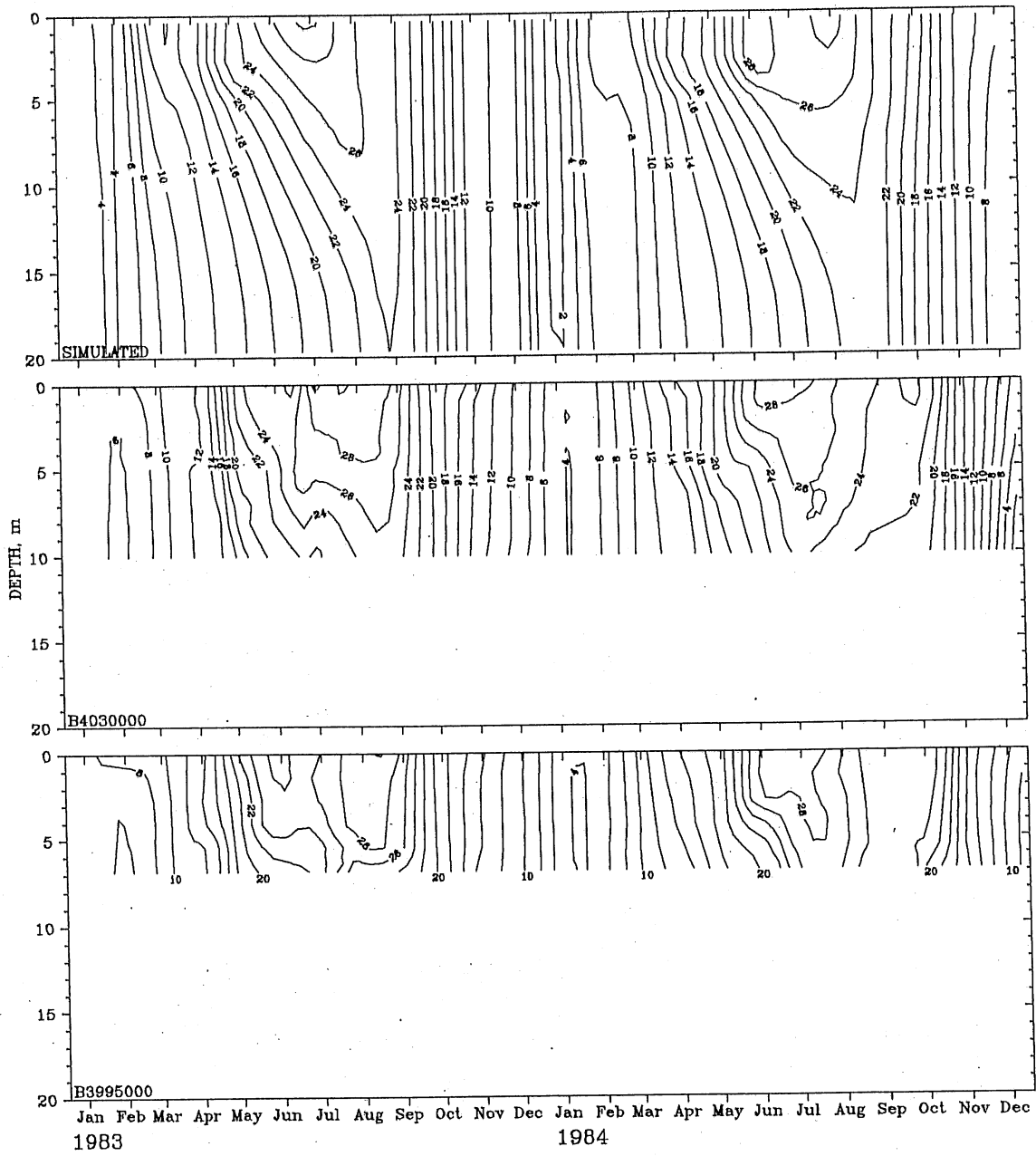


Fig. 5.11. Isotherms (°C) in Jordan Reservoir (1983-84) from simulation (top) and field data at stations B4030000 (middle) and B3995000 (bottom).

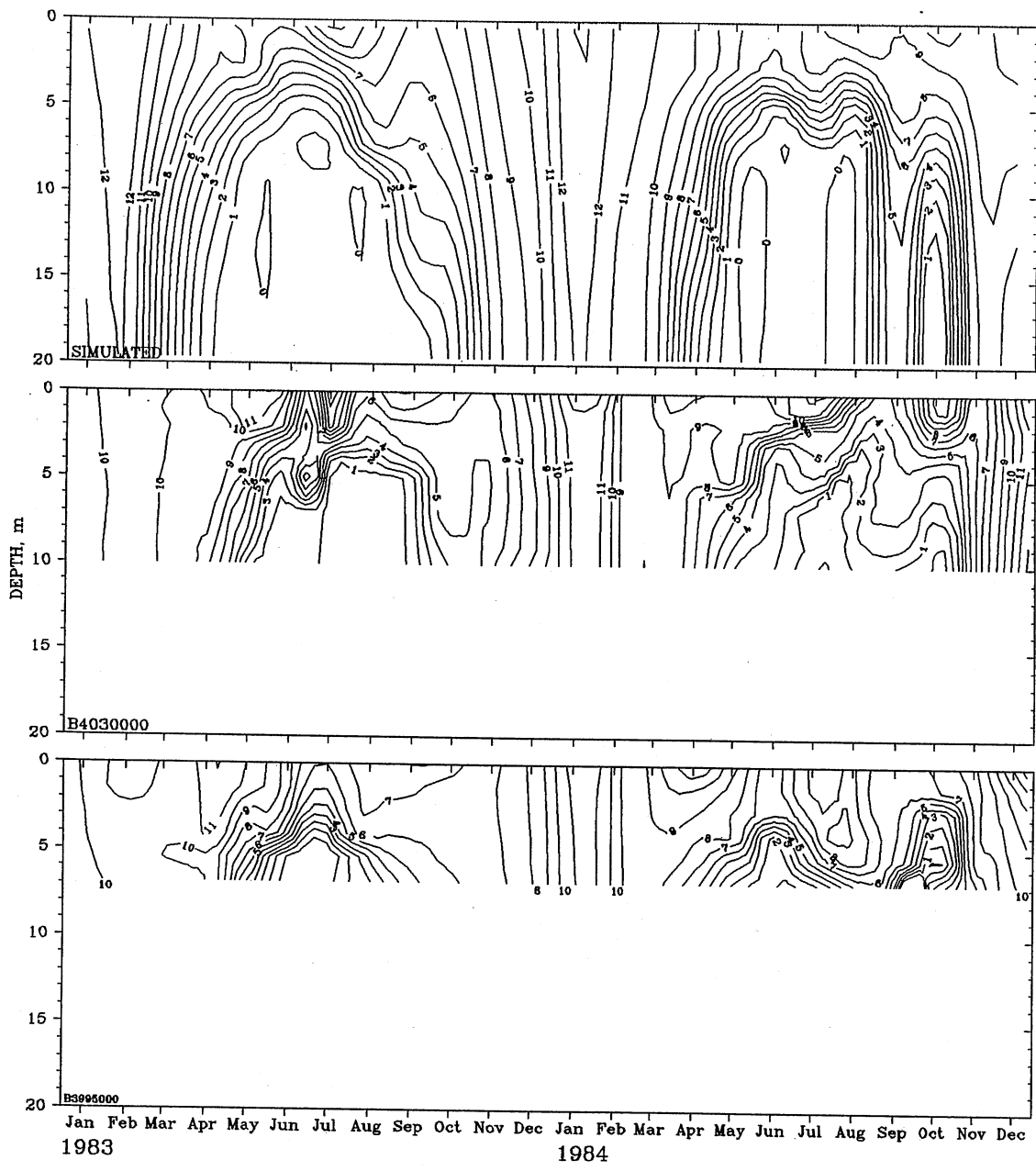


Fig. 5.12. Dissolved oxygen isopleths (mg L^{-1}) in Jordan Reservoir (1983-84) from simulation (top) and field data at stations B4030000 (middle) and B3995000 (bottom).

Specification of phytoplankton standing crop (chlorophyll-a concentrations)

During the initial trial simulation run for Jordan Reservoir for the years 1982-83, unsatisfactory DO results were obtained ($r^2 = -3.60$, S.E. = 6.49 mg L^{-1}) with respect to measurements on 16 days (127 data pairs) at station B3995000. The problem was traced to two extraordinarily high chlorophyll-a (chl-a) measurements on September 15 ($190 \mu\text{g L}^{-1}$) and October 4 ($280 \mu\text{g L}^{-1}$) in 1982. On those two dates, the simulated DO concentrations were much higher than the measured ones. The reason for these high chlorophyll-a concentrations is not known, but a localized algal bloom has been ruled out, since data from other stations in the reservoir (including in the Haw River arm) also reported unusually high chlorophyll-a concentrations on those days.

Strong algal blooms tend to occur when the weather is calm and sunny, and, hence, the surface mixed layer is shallow. A check of daily wind speeds showed that they were atypically low during the time of the high chlorophyll-a concentrations (Fig. 5.13). It can be shown (Stefan et al., 1976) that the standing crop of algae is inversely related to surface mixed layer depth and hence windspeed. Chlorophyll-a concentrations plotted against average wind speeds for 3 days, 1 week, and 2 weeks prior to the chlorophyll-a measurements (Fig. 5.14) indicated that chlorophyll-a is more or less inversely proportional to wind speed.

In the temperature and DO simulations of Jordan Reservoir with MINLAKE95, the chlorophyll-a concentration is specified as the average of the two adjacent field data values, except in three cases: (1) If the current day of simulation falls on a field measurement day, then the measured chlorophyll-a concentration is used; (2) if the current day is before the first field data day, the chlorophyll-a concentration used is equal to that of the first field measurement; (3) if the current day is after the last field data day in a year, the chlorophyll-a concentration used is equal to that of the last field measurement. For any year during the simulation without any field measurements, the chlorophyll-a values from the previous year are used.

When using MINLAKE95 to simulate lakes for extended time periods, such as to investigate water quality trends under different climate scenarios (see Chapter 6), chlorophyll-a concentrations in MINLAKE95 are specified by a summer mean value and a yearly standing crop cycle. Fang and Stefan (1994) used a "generalized" cycle on average summer chlorophyll-a concentrations. The cycle is based on an analysis of European and North American lakes by Marshall and Peters (1989).

At first, a constructed generic chlorophyll-a pattern for Jordan Reservoir was considered, but measurements did not show a consistent annual pattern (Fig. 5.15). The cycle given by Marshall and Peters (1989) was then superimposed on the average annual chlorophyll-a concentration for another simulation. This simulation (#11) was for the years 1983-87, and the field data were from sampling station B3995000. The r^2 values for simulated and measured temperature and DO values were 0.97 and 0.76, respectively. The standard errors between measurements and simulations were $1.32 \text{ }^\circ\text{C}$ and 1.63 mg L^{-1} ,

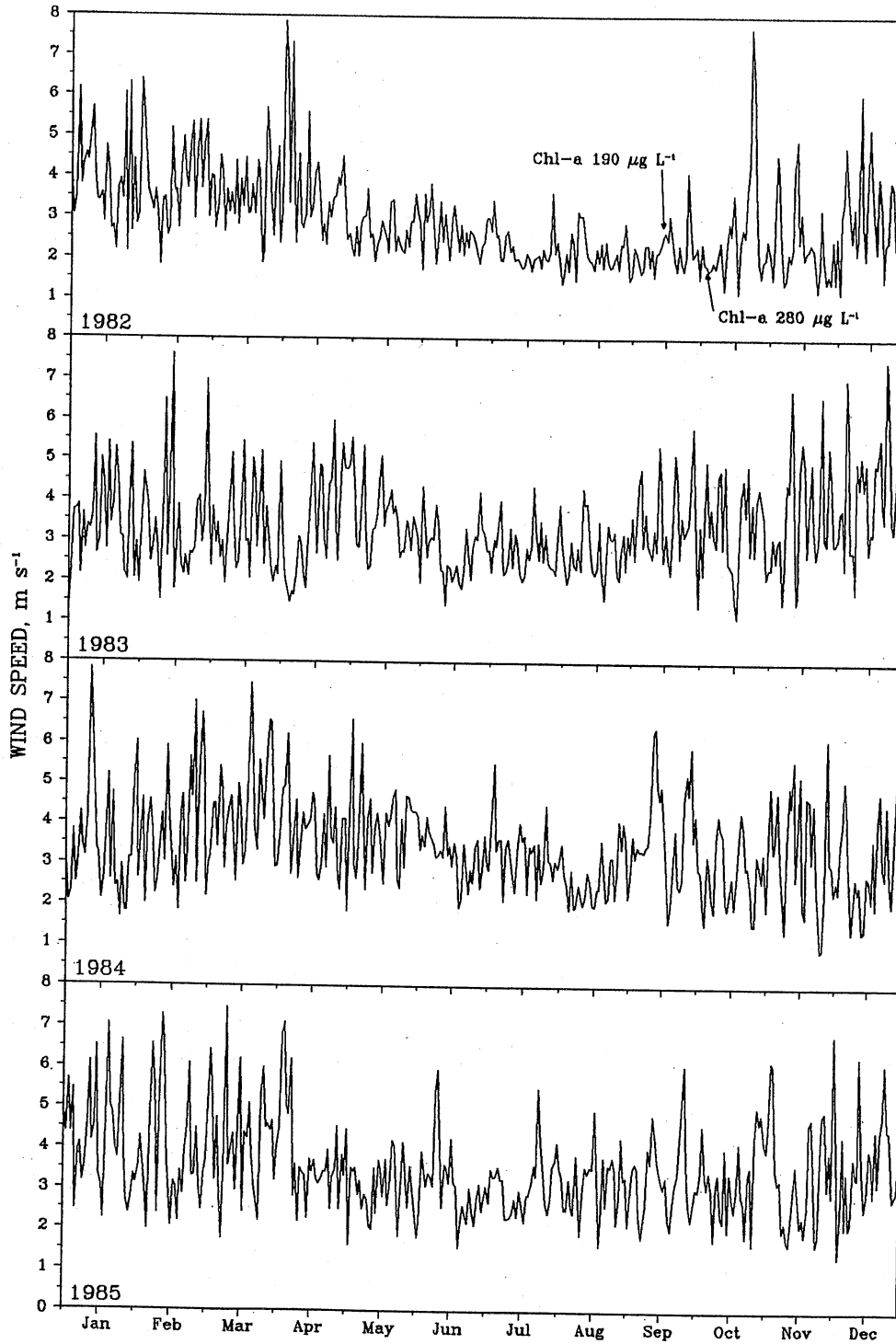


Fig. 5.13. Daily wind speeds at Raleigh, North Carolina (1982-85).

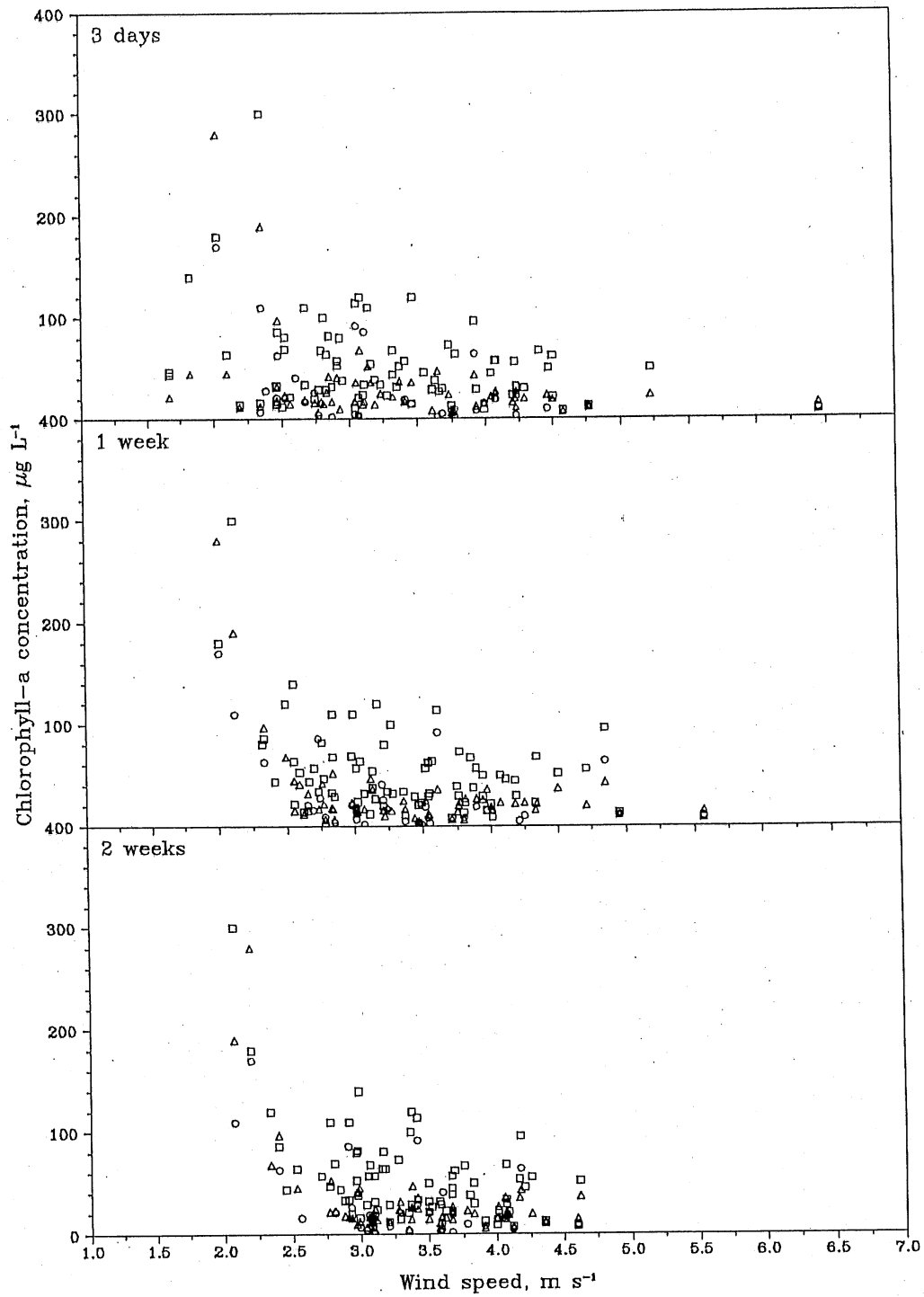


Fig. 5.14. Chlorophyll-a vs. average wind speed for 3 days, 1 week, and 2 weeks prior to measurement in Jordan Reservoir. Wind speeds were measured at Raleigh, NC.

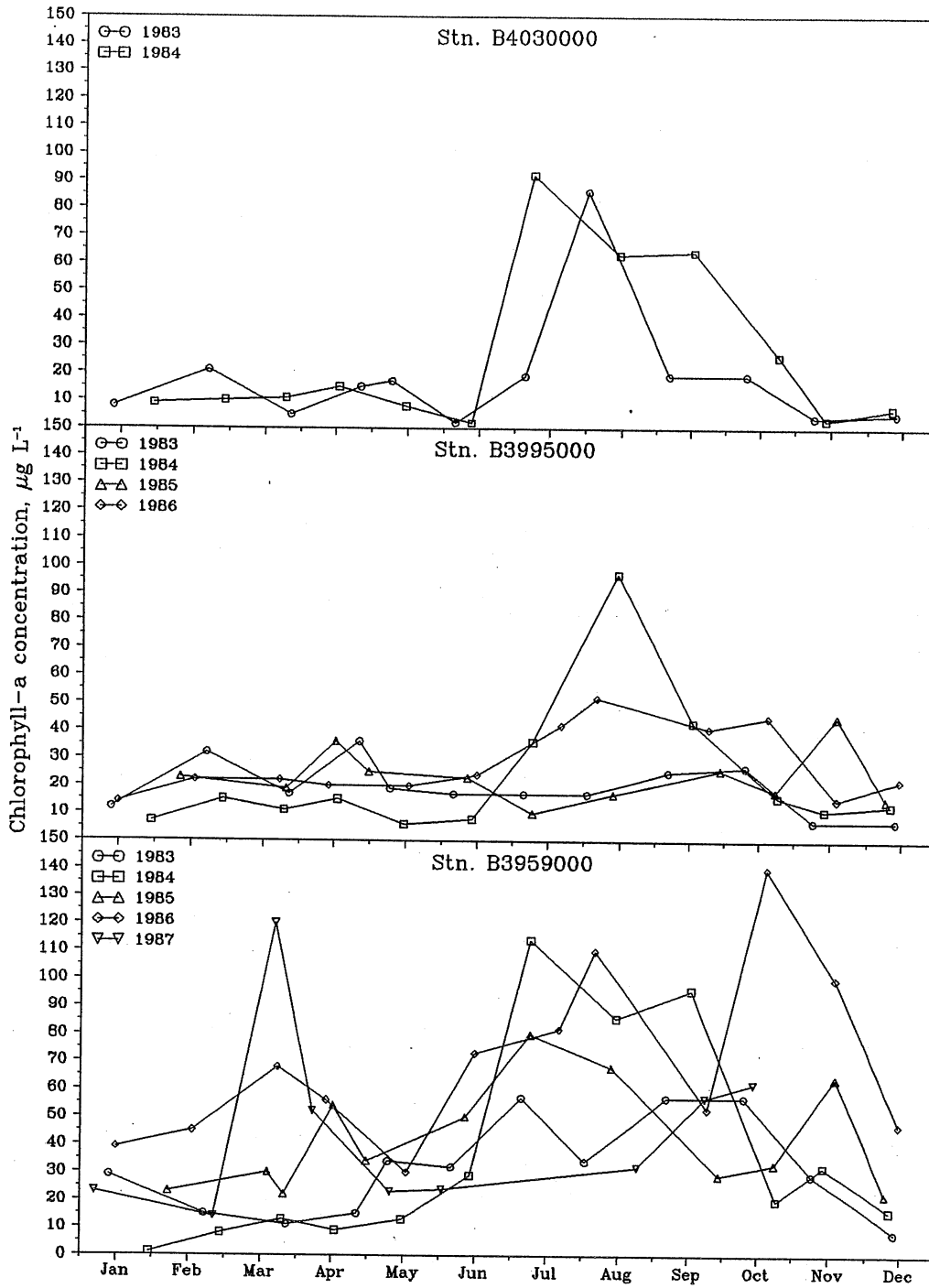


Fig. 5.15. Chlorophyll-a measurements during several years at field stations B3959000, B3995000, and B4030000 in Jordan Reservoir.

respectively. Time series plots are shown in Figs. 5.16 and 5.17, and plots of simulated versus measured values are given in Fig. 5.18. These overall results were virtually identical with a previous simulation (#10) in which actual chlorophyll-a measurements were used as input following the averaging procedure outlined earlier.

Another simulation (#7) with the superimposed generalized cycle function was done--this time necessitated by a lack of chlorophyll-a data--for the years 1987-1990 and checked against 15 days of field data from station B3995000. (Chlorophyll-a measurements at station B3995000 were available only for the first six months of 1987). The r^2 values for this simulation for temperature and DO were 0.95 and 0.65, respectively. The standard errors were 1.05 °C and 2.12 mg L⁻¹, respectively. Time series plots are shown in Figs. 5.19 and 5.20. The model simulated temperatures well, but it overestimated DO concentrations (Fig. 5.21).

A summary of results of all the simulations on Jordan Reservoir is shown in Table 5.5. The results (lines 2 and 3 in Table 5.5) indicate that the superimposed chlorophyll-a cycle is valid for use in modeling Jordan Reservoir. The validity of the use of the superimposed chlorophyll-a cycle is important, because none of the other lakes investigated in this study had sufficient chlorophyll-a field data to use as input. For the other four lakes (James, Santeélah, Phelps, and Waccamaw), an average chlorophyll-a concentration was determined for each from the few field data available, and then the generalized cycle was superimposed on this average. The results of these simulations are presented in the following sections.

A likely cause of the poor performance of the DO modeling effort is the averaging procedure between consecutive chlorophyll-a measurements. This procedure spread the influence of the atypically high values from 1982 over a span of weeks when actual periods of extremely high concentrations of chlorophyll-a may have lasted only a few days. The daily variability of wind paired with a short response time of algal growth to wind mixing would cause chlorophyll-a values to respond on a daily timescale. In the model, the long span of time (one month) between successive chlorophyll-a measurements kept the chlorophyll-a values too high for too long.

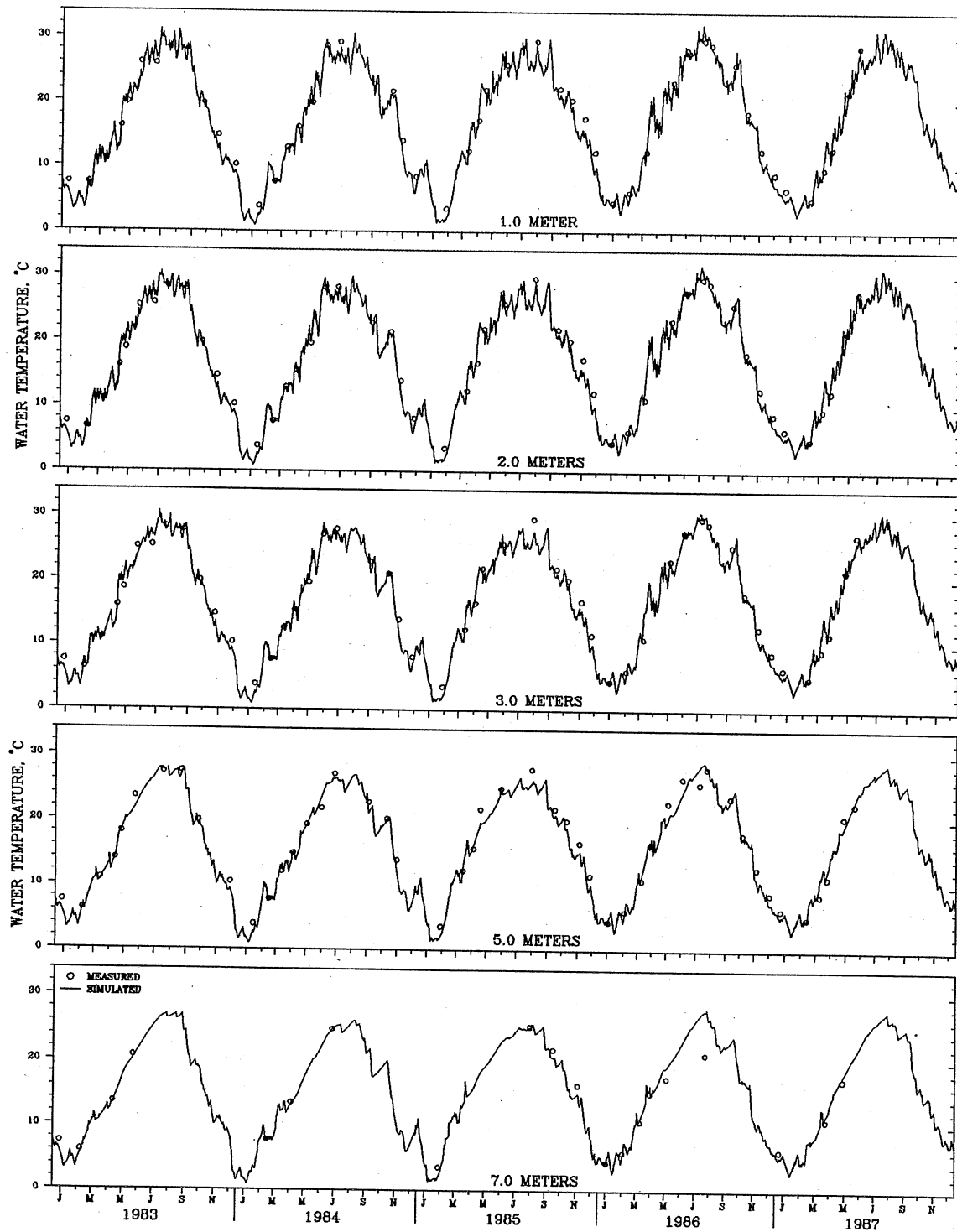


Fig. 5.16. Water temperature time series for Jordan Reservoir (1983-87), using chl-a cycle. Field data are from station B3995000 (simulation #11).

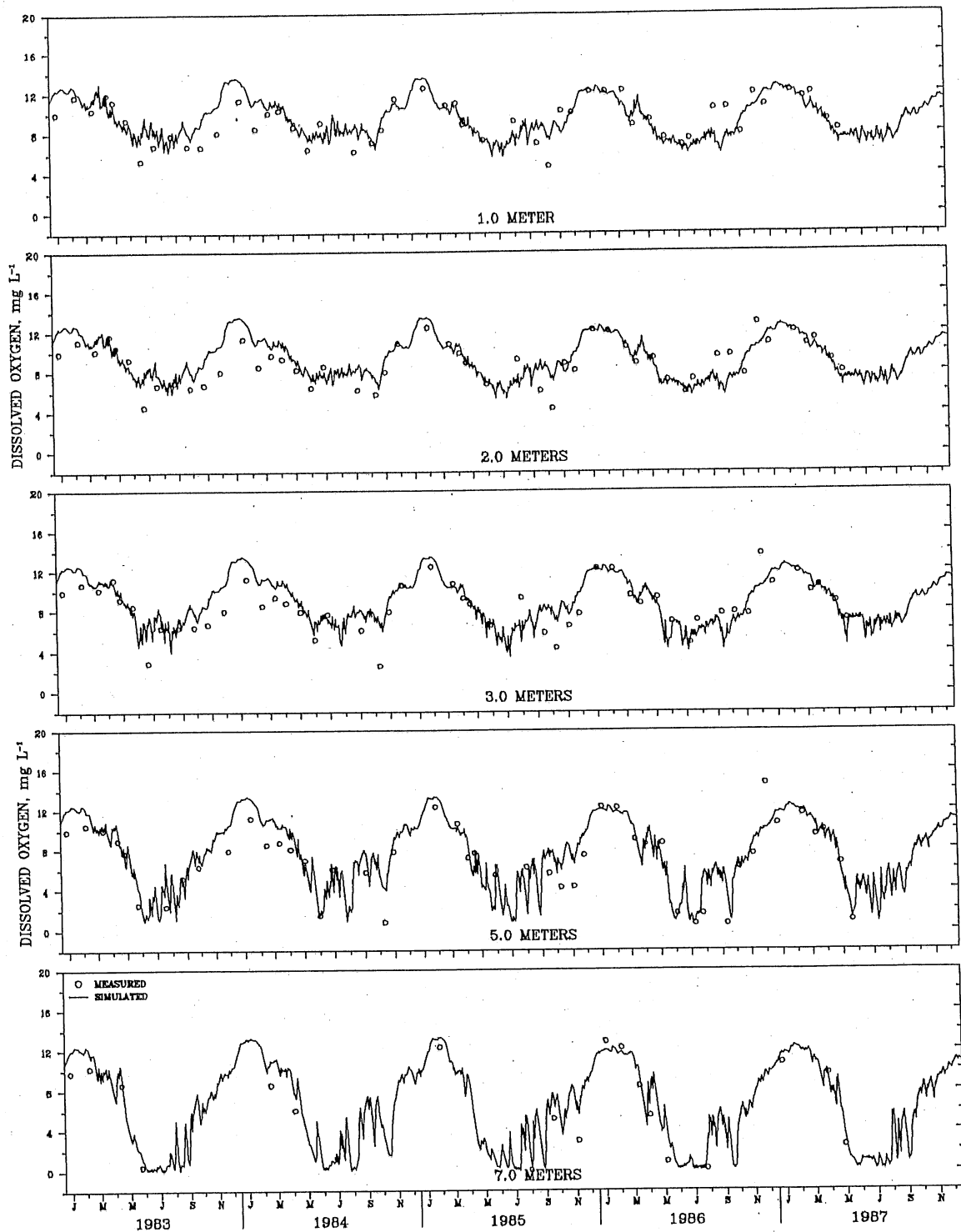


Fig. 5.17. Dissolved oxygen time series for Jordan Reservoir (1983-87), using chl-a cycle. Field data are from station B3995000 (simulation #11).

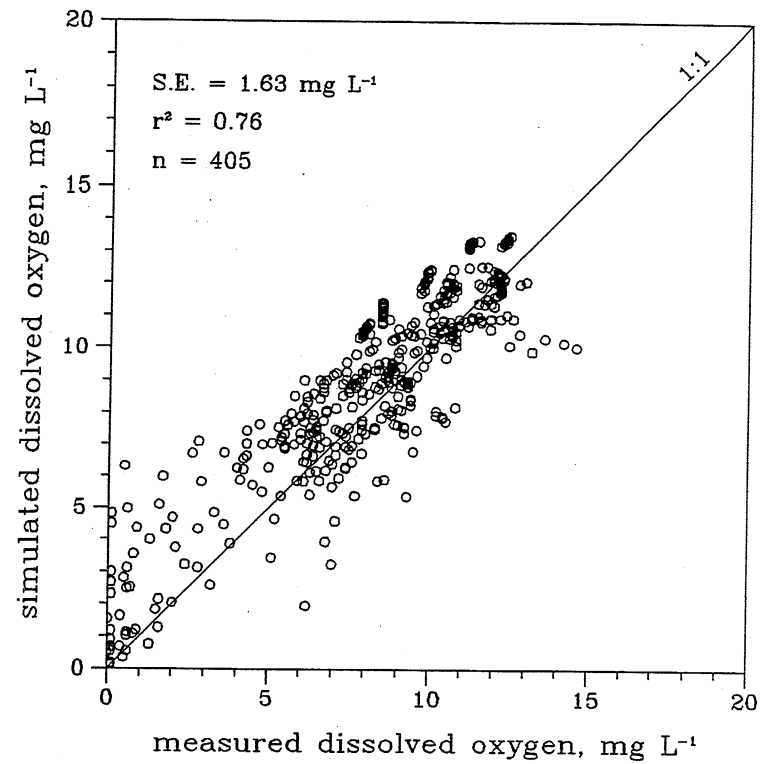
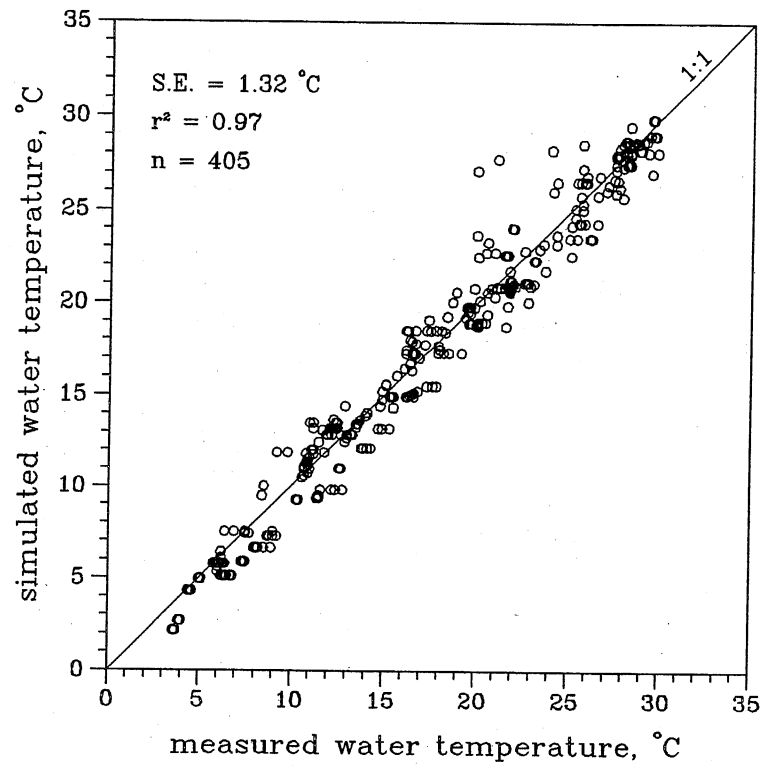


Fig. 5.18. Simulated versus measured temperature and dissolved oxygen in Jordan Reservoir (simulation #11, station B3995000).

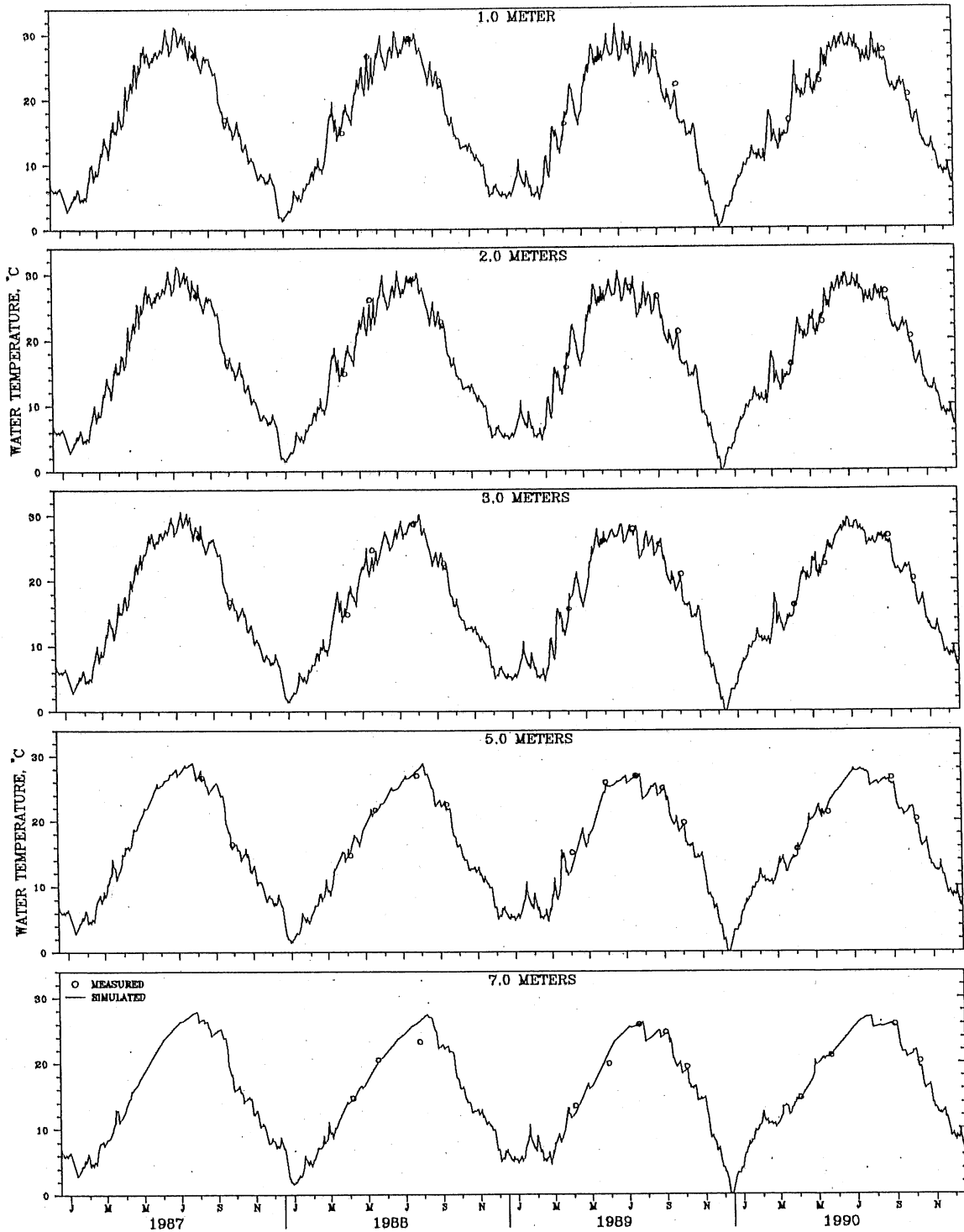


Fig. 5.19. Water temperature time series for Jordan Reservoir (1987-90), using chl-a cycle. Field data are from station B3995000 (simulation #7).

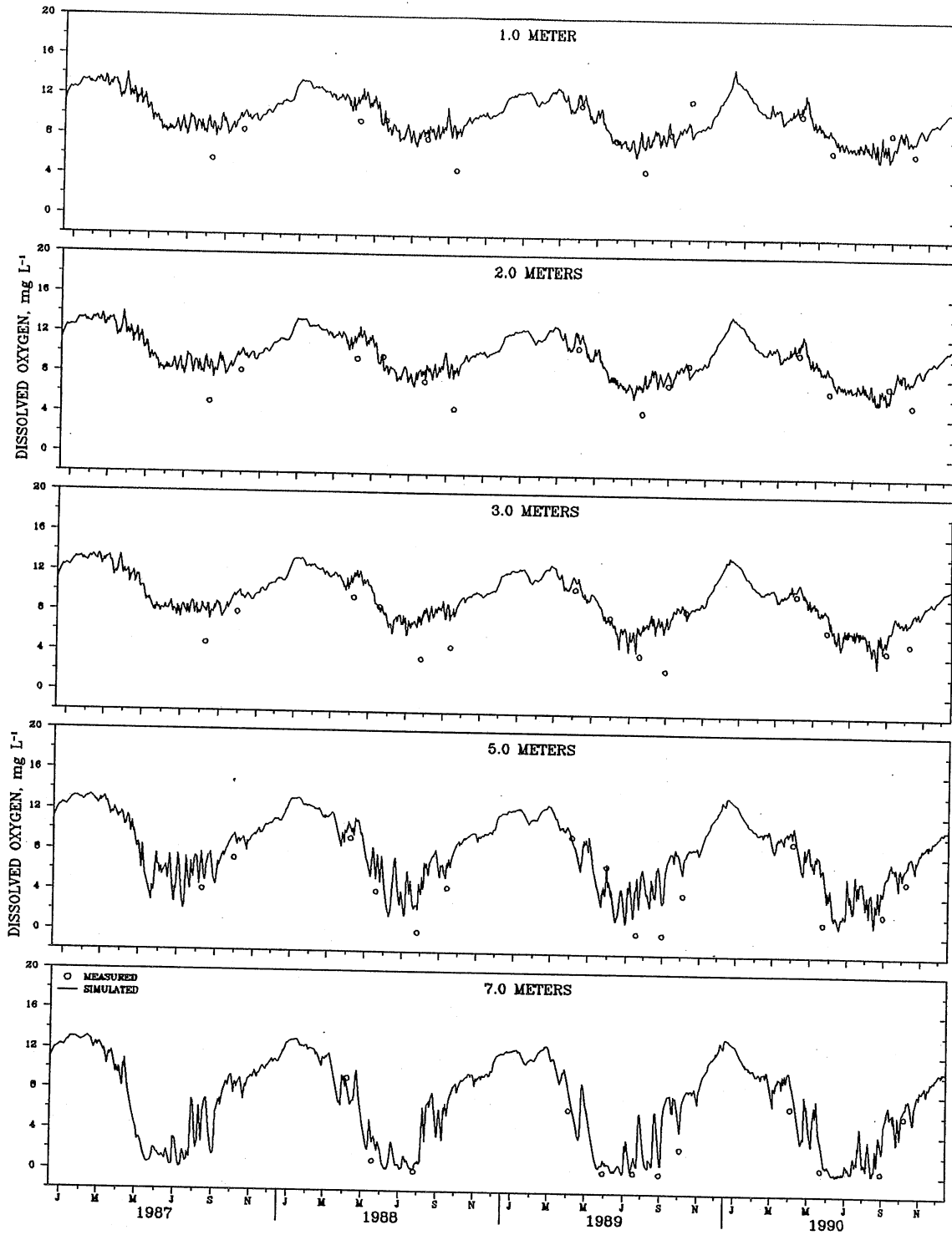


Fig. 5.20. Dissolved oxygen time series for Jordan Reservoir (1987-90), using chl-a cycle. Field data are from station B3995000 (simulation #7).

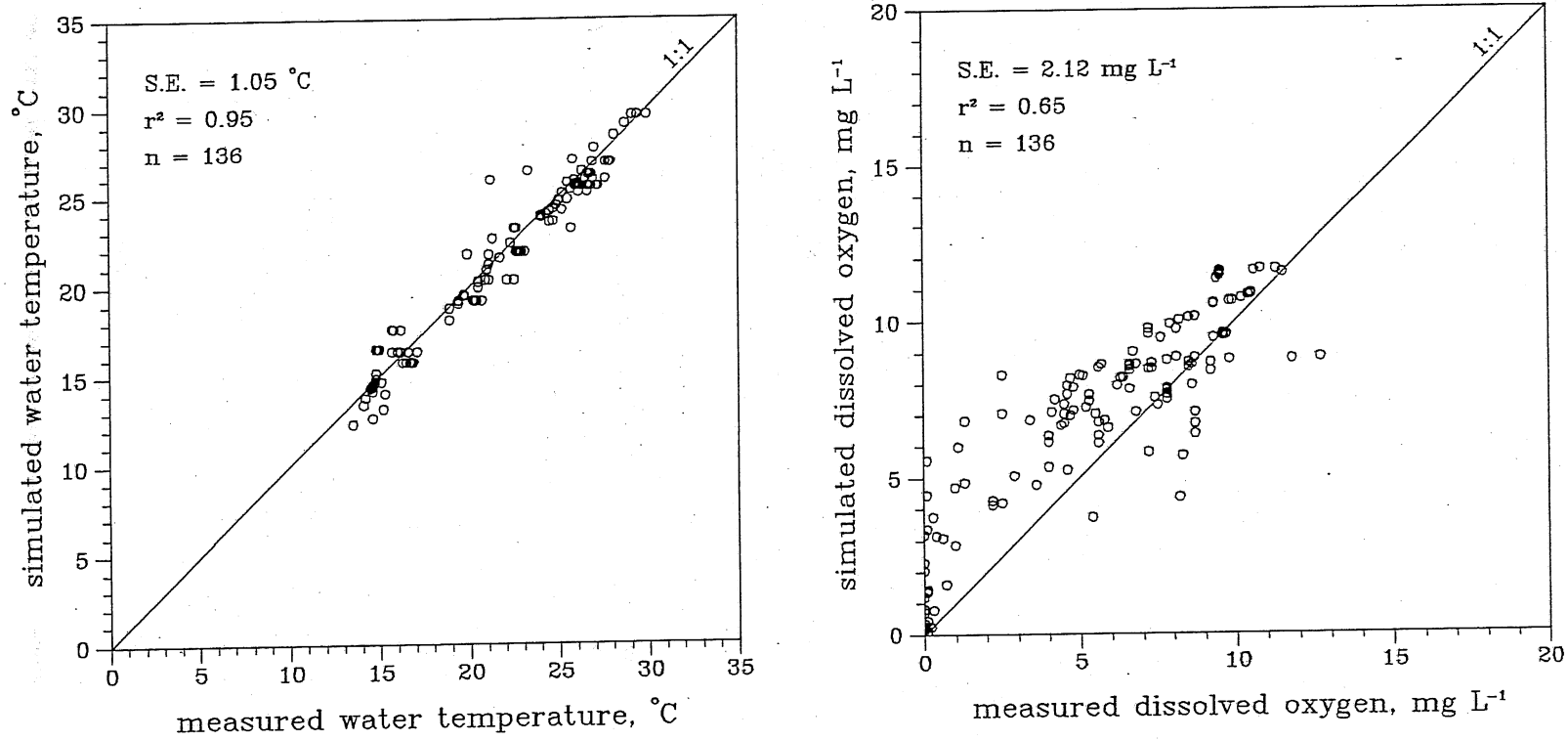


Fig. 5.21. Simulated versus measured temperature and dissolved oxygen in Jordan Reservoir (simulation #7, station B3995000).

Table 5.5. Summary statistics of simulations for B. Everett Jordan Reservoir.

Simulation no.	Station	Chl-a ¹	Years	No. of days ²	No. of data pairs	Temperature		Dissolved Oxygen	
						r ²	S.E. °C	r ²	S.E. mg L ⁻¹
7	B3995000	C	1987-90	15	136	0.95	1.05	0.65	2.12
10	B3995000	M	1983-87	51	405	0.97	1.32	0.74	1.67
11	B3995000	C	1983-87	51	405	0.97	1.32	0.76	1.63
12	B4030000	M	1983-85	29	366	0.97	1.25	0.60	2.36

¹M = chlorophyll-a field measurements were used; C = superimposed yearly chl-a cycle was used.

²Number of field measurement days.

5.5 Lake James

Lake James (Fig. 5.22) is a reservoir created in 1923 for hydropower and is located in the western mountains of North Carolina (Fig. 5.1). It has a surface area of 27 km², maximum and mean depths of 36 m and 14 m, respectively, and a mean hydraulic residence time of 208 days. Lake James is classified oligotrophic under the NCTSI. The associated weather station data were obtained from Asheville, which is about 300 m higher in elevation than Lake James.

Lake James temperatures and DO concentrations were simulated for the years 1981-1989 and checked against seven days of field measurements from sampling station C0730000. The values of W_{coef} and W_{str} were 1.0 and 0.6, respectively. The r² values for temperature and DO were 0.94 and 0.85, respectively. The standard errors were 1.56 °C and 1.23 mg L⁻¹, respectively. There were enough field data in 1982 (three days, one each in March, June, and August) to demonstrate that the model could acceptably simulate the warming trend (Fig. 5.23) and the associated decrease in DO (Fig. 5.24). Overall water temperatures were slightly underpredicted, while there was less precision in how well the model predicted DO (Fig. 5.25).

In the calibration process, the sedimentary oxygen demand (SOD) coefficient S_{b20} was adjusted by trial and error to 1.0 g m⁻² d⁻¹ to minimize simulation errors. This value is higher than the value of 0.2 g m⁻² d⁻¹ used for deep, oligotrophic lakes in Minnesota (Stefan et al., 1994) but is not out of line, considering that SOD values from 0.2 to 2 g m⁻² d⁻¹ are common (Thomann and Mueller, 1987). The higher SOD in Lake James may have a number of causes. One is that the trophic state classification is faulty. As mentioned in Chapter 2, North Carolina uses its own method of determining trophic state, while, for Minnesota lakes, Carlson's (1977) Trophic State Index was used. Based on measured Secchi depths, Lake James would be classified as mesotrophic under Carlson's scheme. This explanation for the increased S_{b20} is not sufficient, however, since the

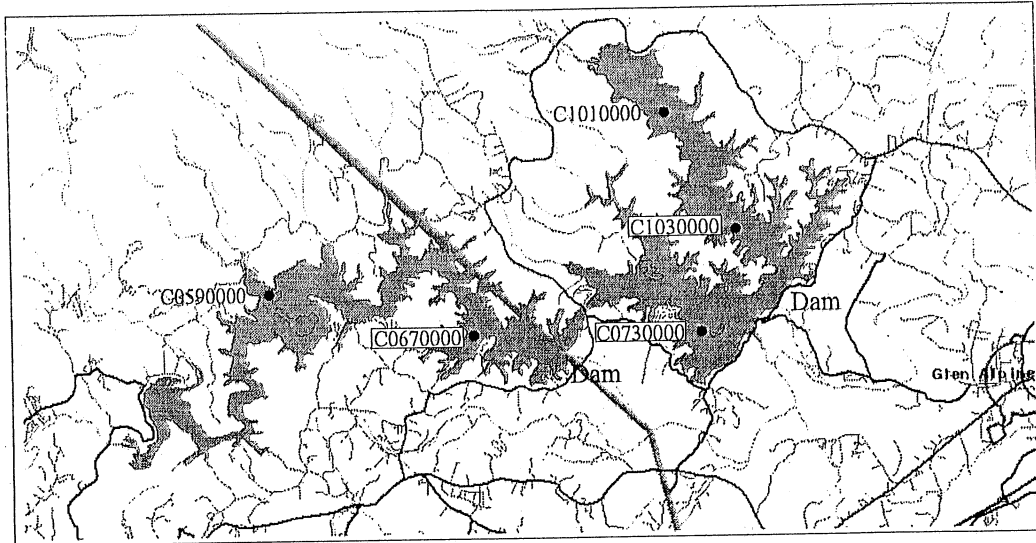


Fig. 5.22. Lake James with sampling stations. Data from station C0730000 were used to check simulation results.

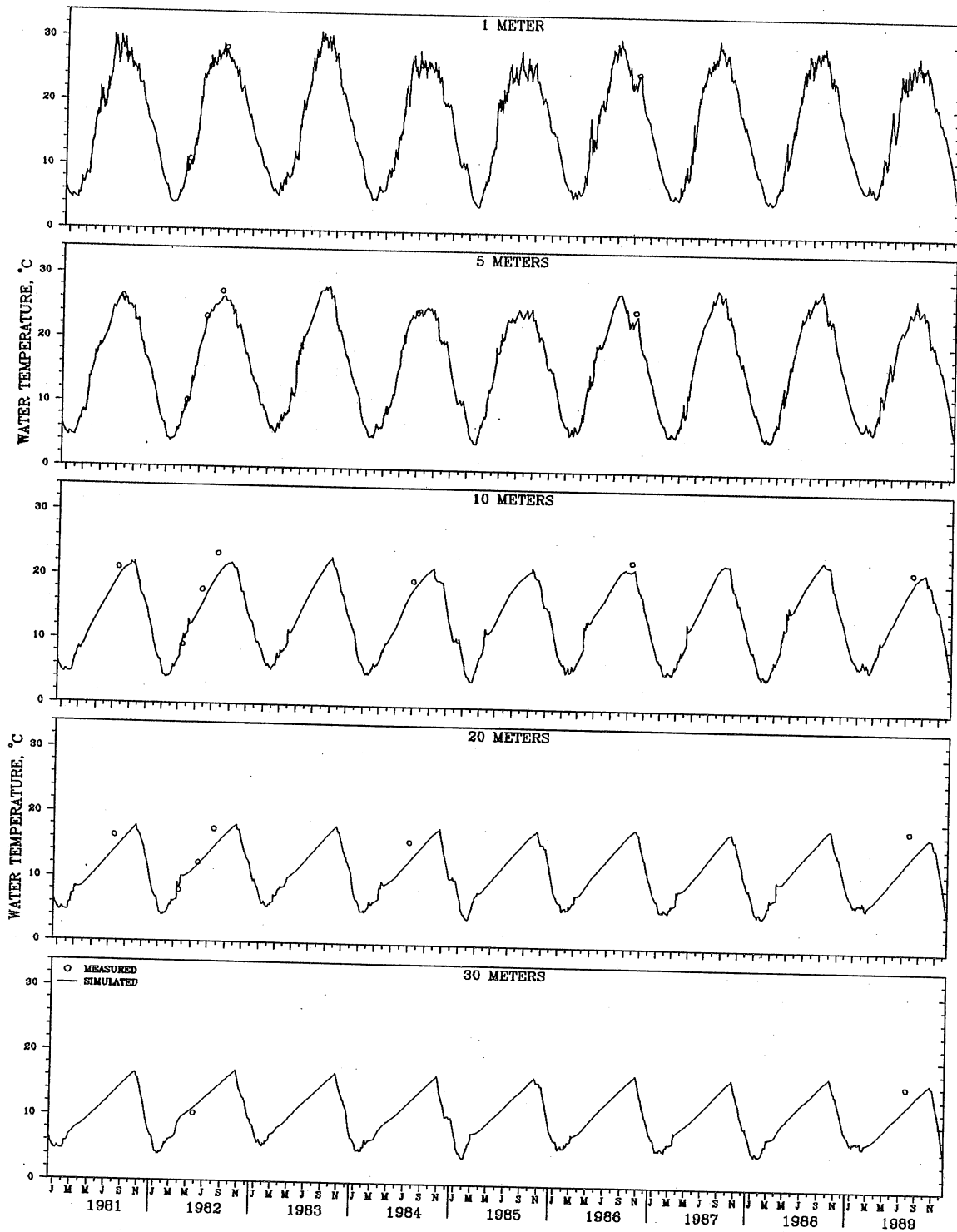


Fig. 5.23. Water temperature time series for Lake James (1981-89).

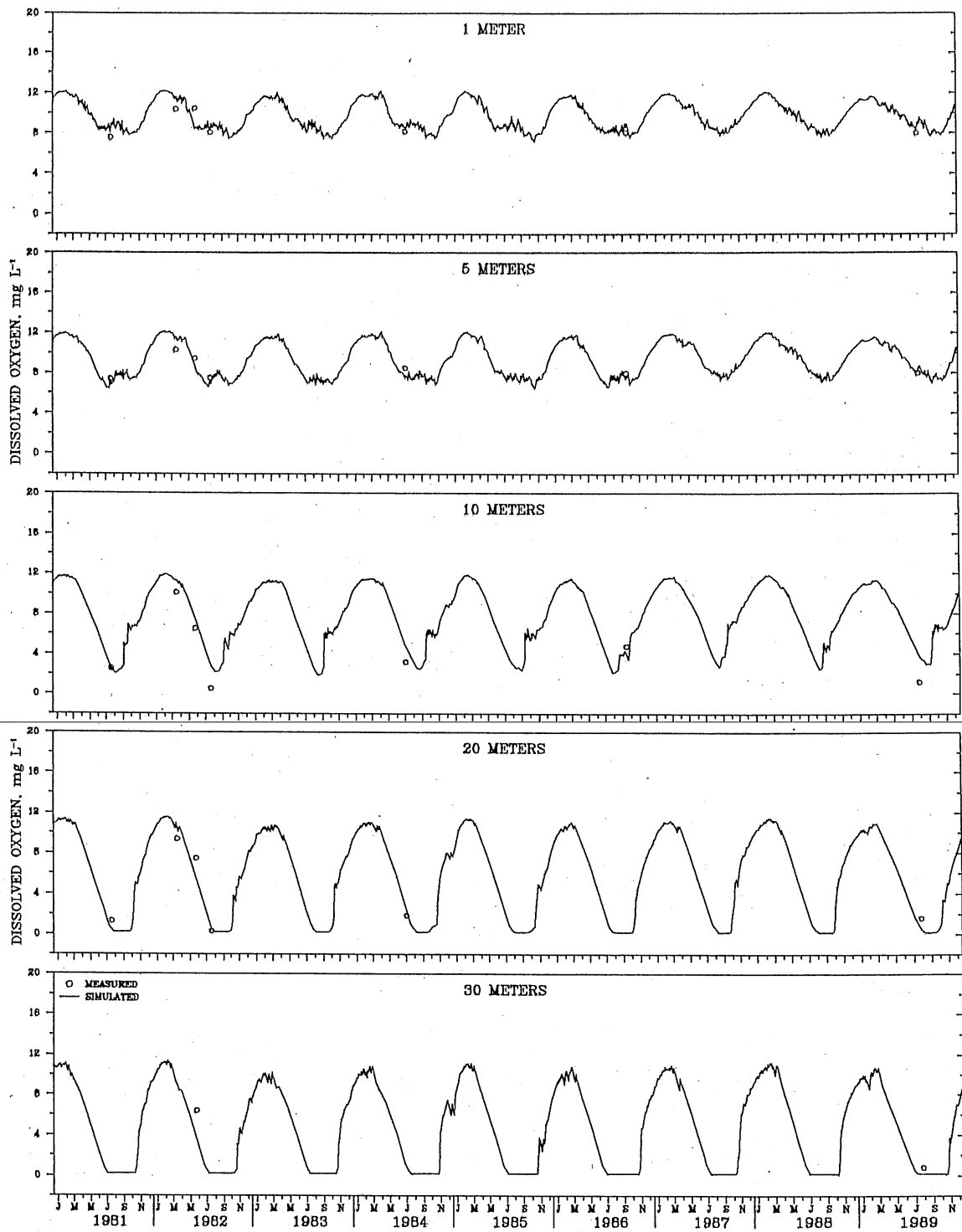


Fig. 5.24. Dissolved oxygen time series for Lake James (1981-89).

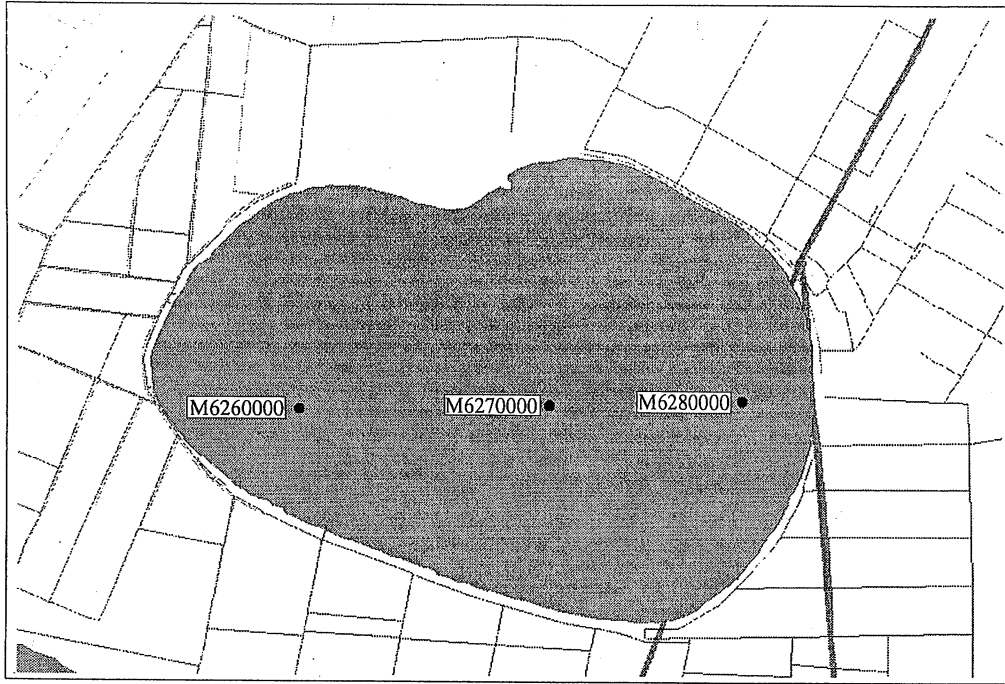


Fig. 5.30. Lake Phelps with sampling stations. Data from station M6270000 were used to check simulation results.

Lake Phelps was simulated for the years 1981-1989. Simulated temperatures and DO concentrations were checked against eight days of field measurements from sampling station M6270000. The values of W_{coef} and W_{str} were both 1.0, and S_{b20} was set at $0.5 \text{ g O}_2 \text{ m}^{-2} \text{ d}^{-1}$. The r^2 values, based on 19 data pairs, for water temperature and DO, all obtained during summer, were -0.57 and 0.13, respectively. The standard errors were $2.28 \text{ }^\circ\text{C}$ and 1.49 mg L^{-1} , respectively. The time series plots at various depths for temperature and DO, given in Figs. 5.31 and 5.32, respectively, show that Lake Phelps is well mixed throughout the year. The model overestimated temperature and underestimated DO (Fig. 5.33).

The water temperature results for Lake Phelps are not as good as would be expected for a natural lake. Unfortunately, the field data points were very clustered (Fig. 5.33). Investigations to explain the results in order to improve the simulations have been inconclusive and are described in the Appendix.

5.8 Lake Waccamaw

Lake Waccamaw (Fig. 5.34) is a natural coastal lake located in the southeastern portion of North Carolina (Fig. 5.1). It has a surface area of 36 km^2 , a maximum depth of 3.3 m, and a mean depth of 1.5 m. The residence time was not available, but Waccamaw was modeled since it is a natural lake with a presumably long hydraulic residence time. Lake Waccamaw is classified as oligotrophic under the NCTSI. Meteorological data were obtained from Wilmington.

Lake Waccamaw was simulated for the years 1983-1990. Simulated temperatures and DO concentrations were checked against four days of field measurements from sampling station I7710000. The values of W_{coef} and W_{str} were both 1.0, and S_{b20} was set at $0.5 \text{ g O}_2 \text{ m}^{-2} \text{ d}^{-1}$. The r^2 values for temperature and DO were 0.28 and -2.32, respectively, based upon 14 data pairs. The standard errors were $2.01 \text{ }^\circ\text{C}$ and 0.57 mg L^{-1} , respectively. These errors indicate goodness of fit only during summer, which is when all the field data were measured. The time series plots in Figs. 5.35 and 5.36 show the well mixed nature of Lake Waccamaw. Simulated water temperatures were higher than those measured, while simulated DO concentrations were good (Fig. 5.37), although the field data were clustered.

As with similar Lake Phelps, the temperature results for Lake Waccamaw are poorer than would be expected. Attempts to explain these results in order to improve the simulation have been inconclusive and are discussed in the Appendix.

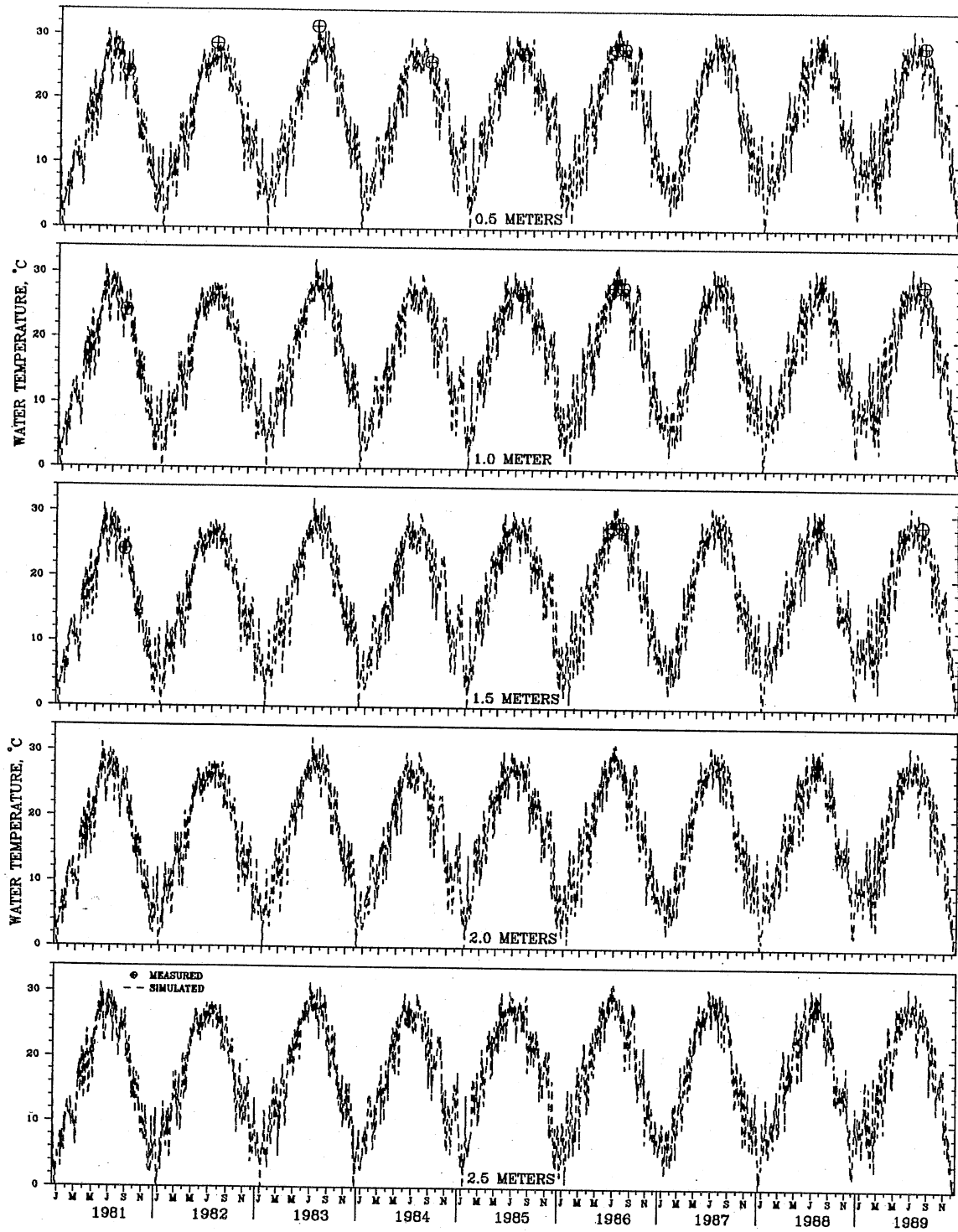


Fig. 5.31. Water temperature time series for Lake Phelps (1981-89).

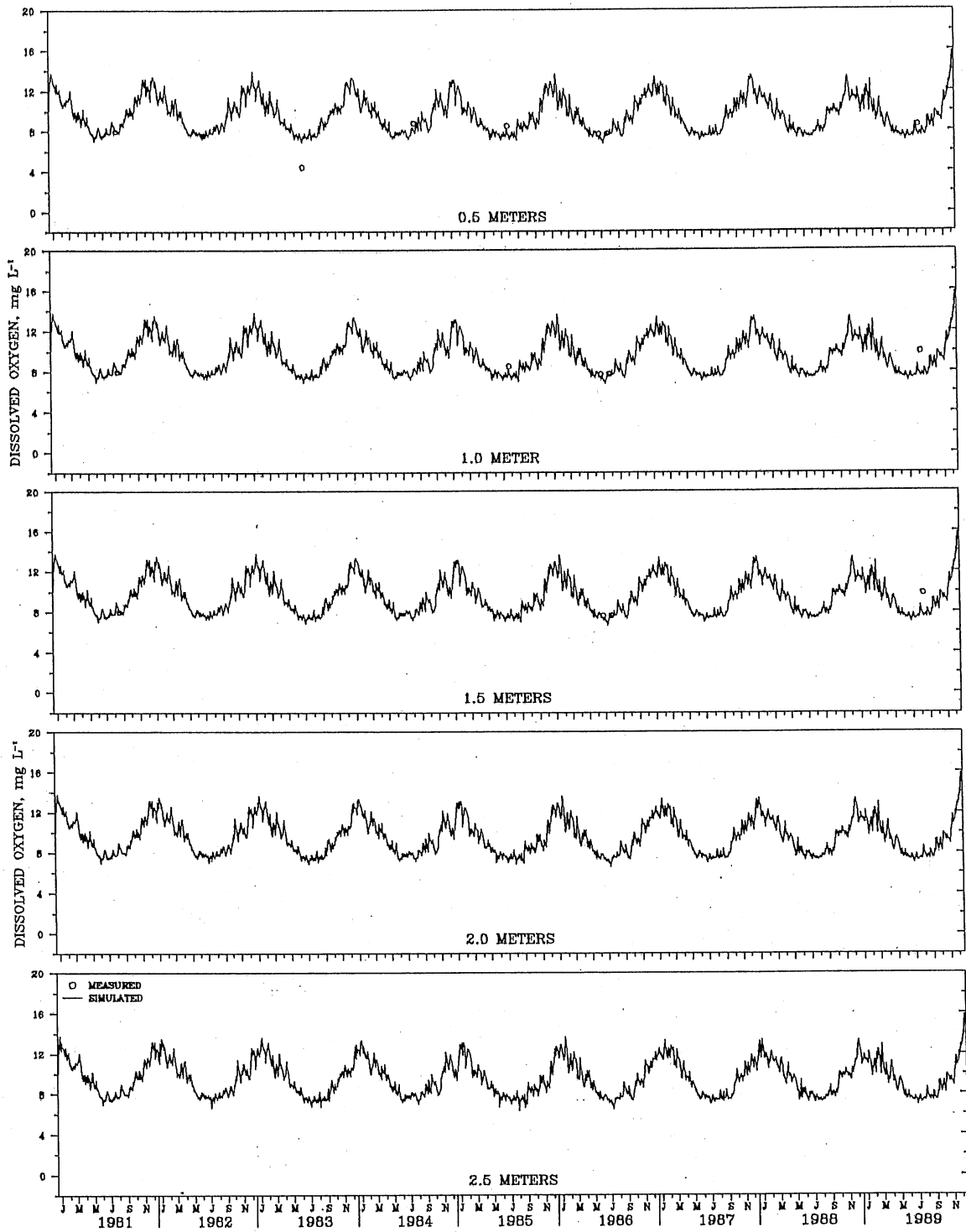


Fig. 5.32. Dissolved oxygen time series for Lake Phelps (1981-89).

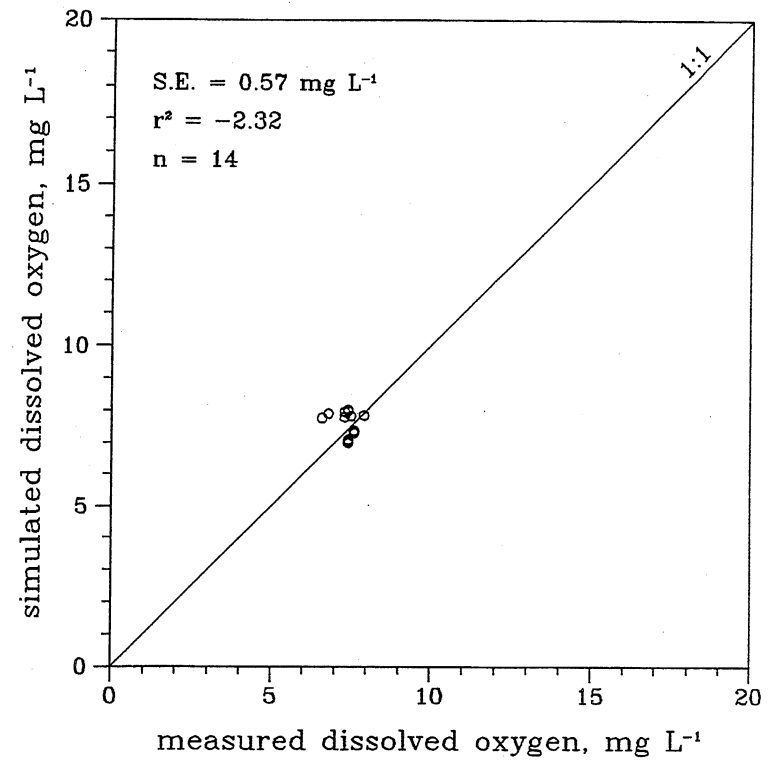
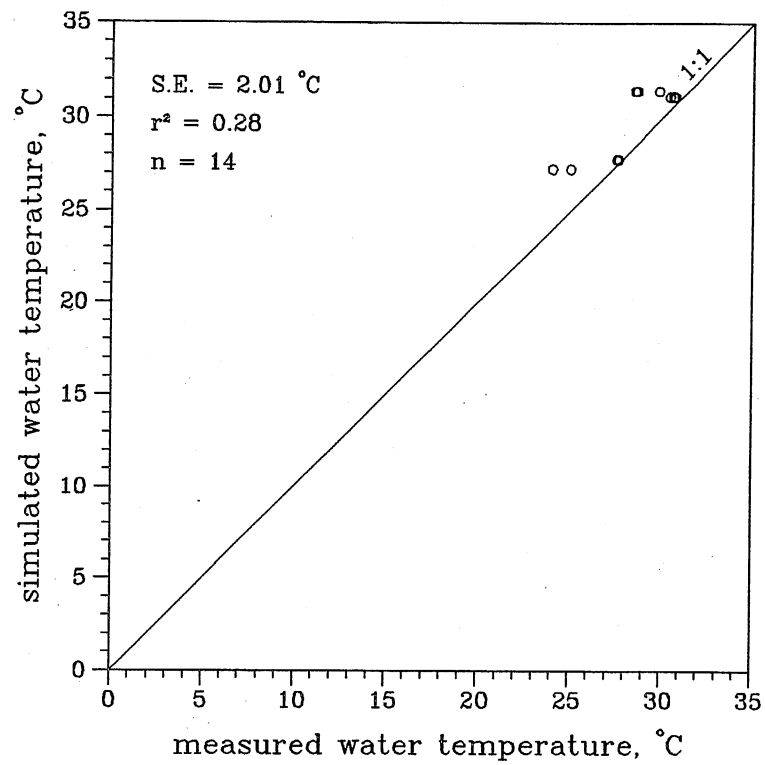


Fig. 5.37. Simulated versus measured temperatures and dissolved oxygen in Lake Waccamaw.

5.9 Discussion of simulation results

A summary of the simulation results is provided in Table 5.6. The average standard errors of simulation for temperature were 1.8 °C for the three reservoirs, 2.1 °C for the two natural lakes, and 2.0 °C overall. The standard errors of simulation for DO were 1.6 mg L⁻¹, 1.0 mg L⁻¹, and 1.4 mg L⁻¹, respectively. The results from the three reservoirs (Jordan, James, Santeetlah) were encouraging, given the types of modeling difficulties associated with such water bodies; these include dendritic shapes, significant advective transport, horizontal variations in water quality, and changes in lake stage (see Chapter 4). The reservoirs show strong stratification in summer accompanied by anoxic conditions in the hypolimnion. There is no permanent ice cover during winter, and each of the reservoirs remains well mixed or weakly stratified throughout winter. The simulations of the two natural lakes (Phelps, Waccamaw), however, gave poorer results than were expected. Investigations of such items as the effects of groundwater, wind, and sediment thermal properties did not yield significantly improved results and are discussed in detail in the Appendix. These shallow coastal lakes are generally well mixed and show no bottom anoxia. Weak stratifications can happen during calm conditions within a diurnal cycle but usually not at the mean daily time scale used by MINLAKE95.

Table 5.6. Summary statistics of simulation trials.

Lake	Field data		Water temp.		DO	
	Years	No. data pairs	r ²	S.E. °C	r ²	S.E. mg L ⁻¹
Jordan	83,84,85,86,87	405	0.97	1.32	0.74	1.67
James	81,82,84,86,89	100	0.94	1.56	0.85	1.23
Santeetlah	81,82,87,90	69	0.81	2.66	0.33	1.93
Phelps	81,82,83,84,85,86,89	19	-0.57	2.28	0.13	1.49
Waccamaw	83,86,87,90	14	0.28	2.01	-2.32	0.57

CHAPTER 6

SIMULATIONS FOR EXTENDED TIME PERIODS UNDER TWO CLIMATE SCENARIOS

6.1 Methodology for simulations with 1xCO₂ and 2xCO₂ climate scenarios

Of concern in this study is the change in lake water temperatures and dissolved oxygen (DO) under a projected climate scenario for a doubling of atmospheric carbon dioxide. The reference climate condition (1xCO₂, past) was taken to be the 19-year period 1961-1979. Meteorological data used in this study were from the Solar and Meteorological Surface Observation Network for the years 1961-1990, compiled by the National Climatic Data Center (Asheville, North Carolina). Jones et al. (1986) showed that annual global temperatures between the late 1930s and the mid 1970s varied little from the 134-year (1861-1984) annual global mean and that a warming trend started in the late 1970s. The cutoff year to characterize the reference climate conditions was chosen to be 1979, as has been done in previous studies (Hondzo and Stefan, 1992; Fang and Stefan, 1994; Stefan and Fang, 1995). Weather in the 1961-1979 time period is assumed to be representative of past atmospheric carbon dioxide conditions (1xCO₂) (Hondzo and Stefan, 1992).

The projected climate scenario after a doubling of atmospheric carbon dioxide (2xCO₂) was generated by applying the Canadian Climate Centre General Circulation Model (CCC-GCM) 2xCO₂ adjustments (Canadian Climate Centre, 4905 Dufferin Street, Downsview, Ontario; discussed by Boer et al., 1992, and McFarlane et al., 1992) to the past (1961-1979) weather. The output from the CCC-GCM grid point closest to a particular weather station was used. Monthly averaged differences or ratios (see Section 3.2) were applied to the past daily values to get the projected 2xCO₂ climate.

All five lakes were simulated twice over the aforementioned 19-year period, once for the 1xCO₂ climate scenario and once for the 2xCO₂ climate scenario. Thirteen parameters related to temperature and dissolved oxygen were obtained for each lake from each simulation. The majority of these parameters are useful in characterizing a lake with respect to fish habitat. Any statistically significant differences between the two simulation results for a given lake reflect the change in meteorological forcing and may signify a change in fish habitat. The 13 selected lake characteristics are discussed in detail in the next section. Values for each of these 13 parameters were determined for each year of

a simulation, and the resulting 19 values were then statistically analyzed to determine means, standard deviations, and whether or not there was a change between the two climate scenario simulations.

Daily temperature and dissolved oxygen profiles were selected every seven days (for Phelps and Waccamaw) or 14 days (for Jordan, James, and Santeetlah) and used to compile average profiles for 19 years for each lake under each climate scenario. A mean and standard deviation were calculated at five depths for the weekly profiles and at 11 depths for the biweekly profiles. Isolines of temperature and DO for an average year for each lake were then generated using Plot-IT, which uses a fifth-order interpolation scheme and can handle up to 300 original data points. Isopleth plots of standard deviation (σ) and mean $\pm 2\sigma$ were also generated. All of these plots are shown in Figs. 6.1 to 6.20.

6.2 Simulated selective lake characteristics

Thirteen parameters useful in characterizing a lake were investigated for each lake under each climate scenario simulation. Twelve of the characteristics are useful in describing fish habitat and are related to either temperature or dissolved oxygen, while the last is the evaporative water loss. They are defined below.

The **maximum epilimnetic temperature** (T_{epi}) is the maximum temperature simulated in the surface mixed layer. The **maximum hypolimnetic temperature** (T_{hyp}) is the maximum temperature occurring each year in the bottom layer. The **maximum temperature difference** (T_{diff}) is the maximum difference between the temperatures in the surface and bottom layers occurring on a single day.

The **minimum hypolimnetic DO** (DO_{hyp}) is the minimum dissolved oxygen concentration simulated in the bottom layer. $DOV_{0.1}$, $DOV_{2.0}$, $DOV_{2.5}$, and $DOV_{3.0}$ are the **maximum percentages of lake volume** with DO concentrations of less than 0.1, 2.0, 2.5, and 3.0 mg L⁻¹, respectively. The volume of all of the layers with DO less than the cutoff values, as opposed to an interpolated volume based on interpolated DO concentrations, was used to determine the volume percentages. $DAY_{0.1}$, $DAY_{2.0}$, $DAY_{2.5}$, and $DAY_{3.0}$ are the **maximum number of consecutive days** with DO concentrations of less than 0.1, 2.0, 2.5, and 3.0 mg L⁻¹, respectively, in the bottom layer.

The **evaporative water loss** ($EVAP$) is the total depth of water lost to evaporation each year. This was calculated from the cumulative annual evaporative heat flux, using 590×10^3 kcal m⁻³ for the latent heat of vaporization for water. The cumulative annual evaporative heat flux is the sum of each year's daily evaporative heat loss values.

Warm water surface temperatures drive cold- and coolwater fish deeper into a lake, while low hypolimnetic DO levels drive them upward. These conditions limit suitable habitat for fish. Hence, any changes caused by climate change can affect the species

composition of the fish population. Most fish do not thrive at DO levels below about 2.5 to 3 mg L⁻¹. Eaton et al. (1995) give a detailed discussion of temperature tolerances of fish. Temperature differences between the surface and bottom indicate the strength of stratification. Changes in the amount of water lost to evaporation can alter the water budget.

6.3 Simulations for 1xCO₂ climate scenario

Each lake was simulated for the 19-year period 1961-1979, which was considered to be characteristic of 1xCO₂ (past) climate conditions. The simulation produced daily vertical profiles of water temperature and DO. Values for the lake characteristics defined in Section 6.2 were determined for each of the 19 years, and averages and standard deviations were then calculated.

The average maximum epilimnetic and hypolimnetic temperatures were 30.5 and 23.8 °C, respectively, in **B. Everett Jordan Reservoir** (Table 6.1). The maximum temperature difference between the surface and bottom was 12.3 °C. The minimum bottom DO was 0 mg L⁻¹, as expected for a monomictic, eutrophic lake. The maximum percent of the lake volume with anoxic conditions (<0.1 mg L⁻¹) was 8%. The values of $DOV_{2.0}$, $DOV_{2.5}$, and $DOV_{3.0}$ were 37%, 40%, and 44%, respectively. Average number of days for $DAY_{0.1}$, $DAY_{2.0}$, $DAY_{2.5}$, and $DAY_{3.0}$ were 11, 156, 158, and 163, respectively. The average cumulative annual evaporative water loss was 1151 mm yr⁻¹. Isopleths of temperature and DO for an average year and extreme years (mean ± 2σ) are shown in Figs. 6.1 and 6.2, respectively. Most of the variability occurred during winter near the surface for temperature, while for DO it occurred around the onset of stratification in spring.

For **Lake James** (Table 6.2), the averages of T_{epi} and T_{hyp} were 28.7 °C and 16.7 °C, respectively. T_{diff} was 16.5 °C. The minimum bottom DO was 0 mg L⁻¹, as expected for a deep lake. The maximum percent of the lake volume with anoxic conditions was less than 1%, and the percentage volumes for $DOV_{2.0}$, $DOV_{2.5}$, and $DOV_{3.0}$ were 37%, 40%, and 44%, respectively. The numbers of consecutive days with bottom DO less than 0.1, 2, 2.5, and 3 mg L⁻¹ were 2, 147, 152, and 158, respectively. The average cumulative annual evaporative water loss was 787 mm yr⁻¹. Even at the extremes, Lake James still stratifies strongly in summer (Figs. 6.3 and 6.4).

The maximum epilimnetic and hypolimnetic temperatures under the 1xCO₂ climate scenario were 27.7 °C and 9.2 °C, respectively, in **Santeetlah Lake** (Table 6.3). The maximum temperature difference between the surface and bottom was 20.7 °C. The average minimum bottom DO was 0 mg L⁻¹. The maximum percent of the lake volume with anoxic conditions was virtually 0% due to the extreme depth of the reservoir, while 52% of the lake volume went below 2 mg L⁻¹ DO and 56% was below 3 mg L⁻¹. The values of $DAY_{0.1}$, $DAY_{2.0}$, $DAY_{2.5}$, $DAY_{3.0}$, were 2, 261, 266, and 271, respectively. The

Table 6.1. Selected characteristics from simulation of Jordan Reservoir under the 1xCO₂ (past, 1961-1979) climate scenario. Each is a daily extreme value for a particular year (except EVAP, which is cumulative).

Year	T _{epi} °C	T _{hyp} °C	T _{diff} °C	DO _{hyp} mg L ⁻¹	EVAP mm
1 (1961)	31.1	23.7	11.6	0.0	1192
2	30.3	23.6	14.5	0.0	1161
3	32.4	23.6	15.6	0.0	1212
4	29.9	23.4	13.0	0.0	1108
5	29.8	23.5	12.1	0.1	1165
6	30.5	24.1	12.4	0.0	1256
7	29.7	23.1	10.9	0.0	1178
8	31.7	23.5	10.3	0.0	1254
9	31.0	23.7	12.3	0.0	1154
10	28.3	24.0	10.3	0.0	1185
11	29.2	23.9	13.1	0.0	1121
12	31.7	23.0	12.5	0.0	1129
13	30.9	24.2	11.9	0.0	1095
14	29.4	23.5	11.8	0.0	1059
15	31.0	23.9	14.1	0.1	1093
16	29.6	23.8	11.2	0.0	1236
17	31.8	24.7	12.0	0.0	1150
18	31.6	24.6	13.4	0.0	1105
19 (1979)	30.5	24.1	10.5	0.0	1026
average	30.5	23.8	12.3	0.01	1151
std. dev.	1.04	0.43	1.39	0.03	62
coef. var.	0.03	0.02	0.11	3.0	0.05

Definitions:

T_{epi} = maximum epilimnetic temperature, °C

T_{hyp} = maximum hypolimnetic temperature, °C

T_{diff} = maximum temperature difference between surface and bottom, °C

DO_{hyp} = minimum hypolimnetic DO, mg L⁻¹

EVAP = annual total depth of water lost to evaporation, mm

Table 6.2. (cont'd.)

Year	DOV _{0.1} %	DOV _{2.0} %	DOV _{2.5} %	DOV _{3.0} %	DAY _{0.1}	DAY _{2.0}	DAY _{2.5}	DAY _{3.0}
1 (1961)	0.05	33.5	37.3	41.3	1	132	136	142
2	0.30	33.5	37.3	41.3	1	133	138	144
3	0.30	33.5	37.3	41.3	2	143	148	153
4	0.15	33.5	33.5	37.3	1	139	145	150
5	0.30	37.3	41.3	41.3	1	144	149	157
6	0.30	33.5	37.3	41.3	2	132	137	144
7	0.30	33.5	37.3	41.3	1	148	154	161
8	0.54	41.3	41.3	45.6	2	143	149	155
9	0.15	37.3	41.3	45.6	2	138	144	149
10	0.05	41.3	41.3	45.6	1	147	155	160
11	0.30	37.3	41.3	45.6	1	155	161	167
12	0.30	37.3	41.3	45.6	2	155	162	168
13	0.15	41.3	41.3	45.6	2	148	153	161
14	0.54	37.3	41.3	45.6	2	167	173	179
15	0.15	41.3	41.3	45.6	2	152	156	162
16	0.30	37.3	41.3	45.6	1	159	164	170
17	0.30	37.3	41.3	45.6	2	151	156	161
18	0.15	41.3	41.3	45.6	1	153	159	164
19 (1979)	0.15	41.3	41.3	45.6	1	153	158	164
average	0.3	37.4	39.9	43.8	1.5	147	152	158
std. dev.	0.1	3.1	2.3	2.5	0.5	9	10	9
coef. var.	0.33	0.08	0.06	0.06	0.33	0.06	0.07	0.06

See Table 6.1 for the definition of each characteristic.

Table 6.3. Selected characteristics from simulation of Santeetlah Lake under the 1xCO₂ (past, 1961-1979) climate scenario. Each is a daily extreme value for a particular year (except EVAP, which is cumulative).

Year	T _{epi} °C	T _{hyp} °C	T _{diffr} °C	DO _{hyp} mg L ⁻¹	EVAP mm
1 (1961)	26.1	10.8	17.3	0.1	815
2	27.0	9.4	19.8	0.0	879
3	27.7	9.1	20.6	0.1	917
4	27.6	9.0	20.5	0.0	776
5	26.3	9.3	19.4	0.1	853
6	26.9	8.1	21.4	0.0	795
7	25.6	8.8	19.4	0.0	811
8	29.7	8.7	22.6	0.1	893
9	29.5	8.4	23.4	0.1	922
10	27.8	9.0	21.4	0.1	864
11	26.7	9.8	19.3	0.0	817
12	28.1	9.8	20.6	0.0	867
13	26.9	9.5	20.4	0.0	853
14	27.1	9.9	19.3	0.0	873
15	27.5	10.4	18.3	0.0	853
16	27.4	9.3	20.3	0.1	952
17	29.9	8.4	24.1	0.0	937
18	29.0	8.5	23.1	0.0	894
19 (1979)	29.6	9.1	22.7	0.1	821
average	27.7	9.2	20.7	0.04	863
std. dev.	1.25	0.68	1.76	0.05	48
coef. var.	0.05	0.07	0.09	1.25	0.06

See Table 6.1 for the definition of each characteristic.

Table 6.3. (cont'd.)

Year	DOV _{0.1} %	DOV _{2.0} %	DOV _{2.5} %	DOV _{3.0} %	DAY _{0.1}	DAY _{2.0}	DAY _{2.5}	DAY _{3.0}
1 (1961)	0.001	52.9	52.9	552.9	1	253	262	266
2	0.001	52.9	52.9	52.9	1	235	238	242
3	0.009	52.9	52.9	52.9	3	235	237	242
4	0.009	45.9	52.9	52.9	4	253	258	278
5	0.001	52.9	52.9	52.9	2	257	260	263
6	0.001	52.9	52.9	52.9	1	256	259	263
7	0.001	45.9	52.9	52.9	3	263	273	275
8	0.001	52.9	52.9	52.9	1	244	246	250
9	0.001	52.9	52.9	52.9	1	242	246	250
10	0.001	52.9	60.4	60.4	1	275	279	283
11	0.009	52.9	52.9	60.4	4	299	302	304
12	0.009	52.9	52.9	60.4	4	286	289	296
13	0.001	52.9	60.4	60.4	1	275	280	284
14	0.001	52.9	52.9	60.4	3	273	276	284
15	0.001	52.9	52.9	60.4	1	258	263	266
16	0.001	52.9	52.9	52.9	1	276	283	286
17	0.001	52.9	52.9	60.4	1	257	261	266
18	0.001	52.9	52.9	60.4	1	256	259	262
19 (1979)	0.001	52.9	52.9	60.4	2	275	278	283
average	0.003	52.1	53.7	56.4	1.9	261	266	271
std. dev.	0.003	2.1	2.3	3.8	1.2	17	17	17
coef. var.	1.0	0.04	0.04	0.07	0.63	0.07	0.06	0.06

See Table 6.1 for the definition of each characteristic.

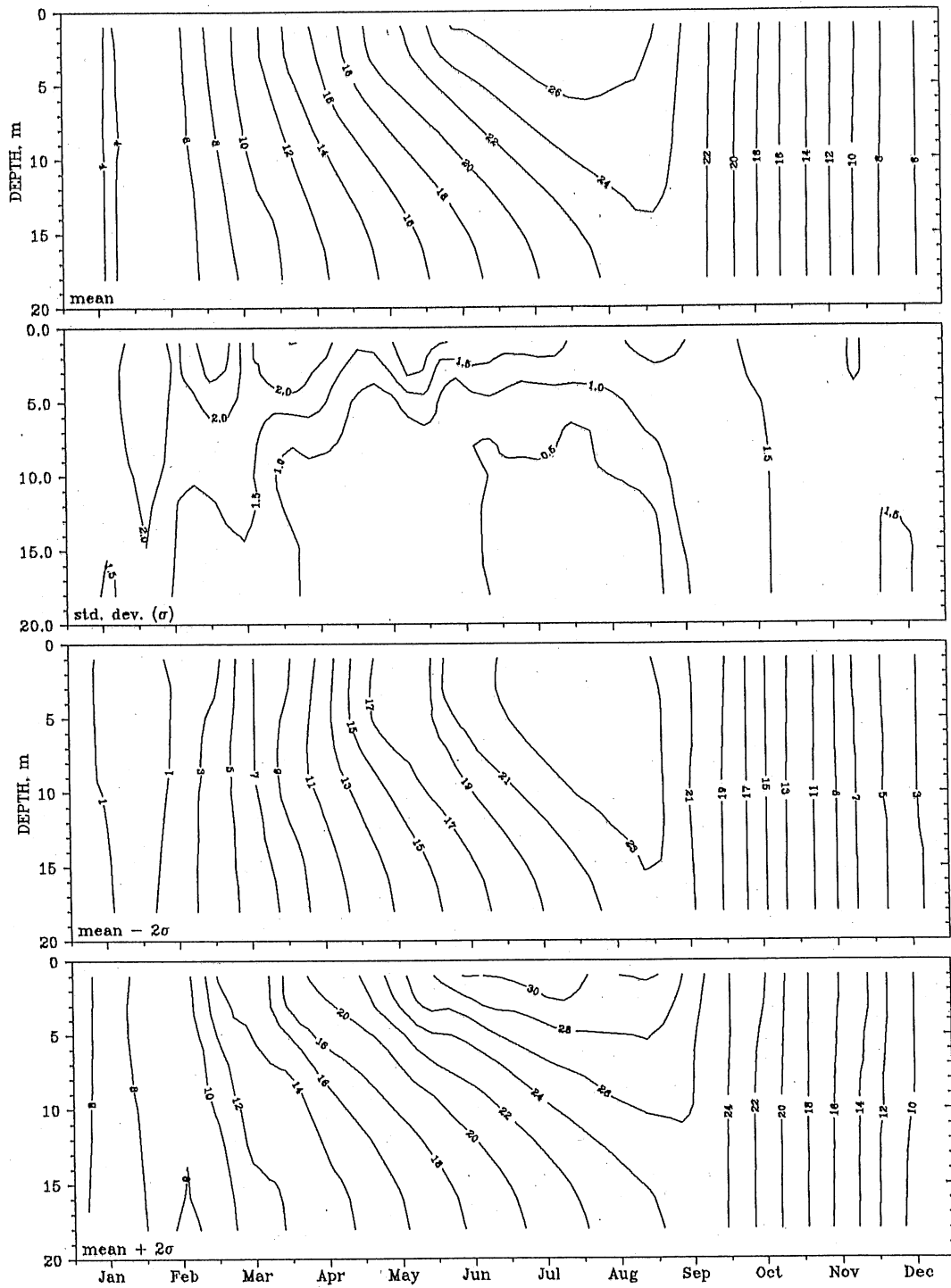


Fig. 6.1. Isotherms ($^{\circ}\text{C}$) in Jordan Reservoir for an average year under the $1\times\text{CO}_2$ climate scenario (top) with isopleths of standard deviations (σ) and isotherms for extreme (mean $\pm 2\sigma$) events.

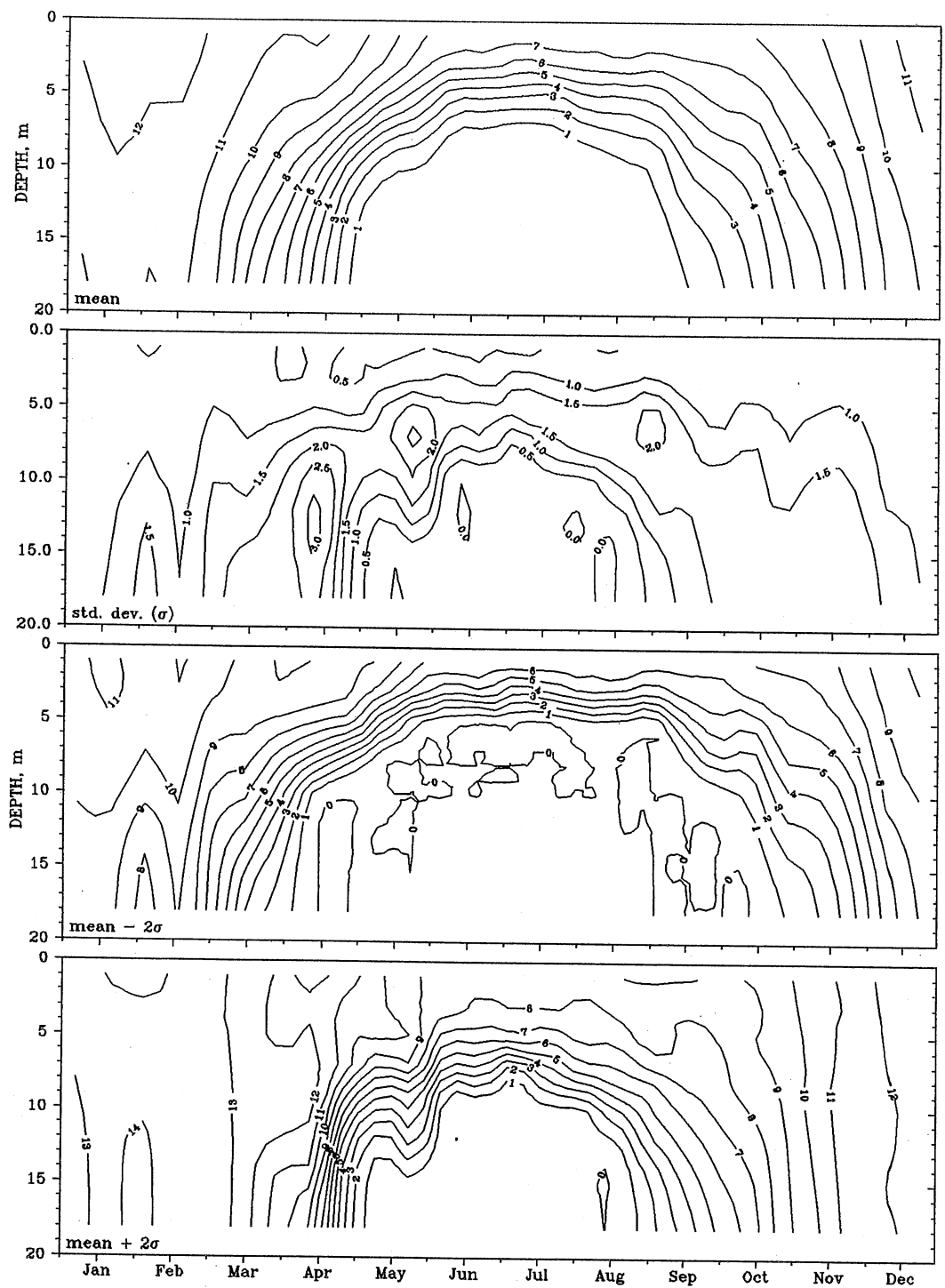


Fig. 6.2. DO isopleths (mg L⁻¹) in Jordan Reservoir for an average year under the 1xCO₂ climate scenario (top) with isopleths of standard deviations (σ) and of DO for extreme (mean ± 2σ) events.

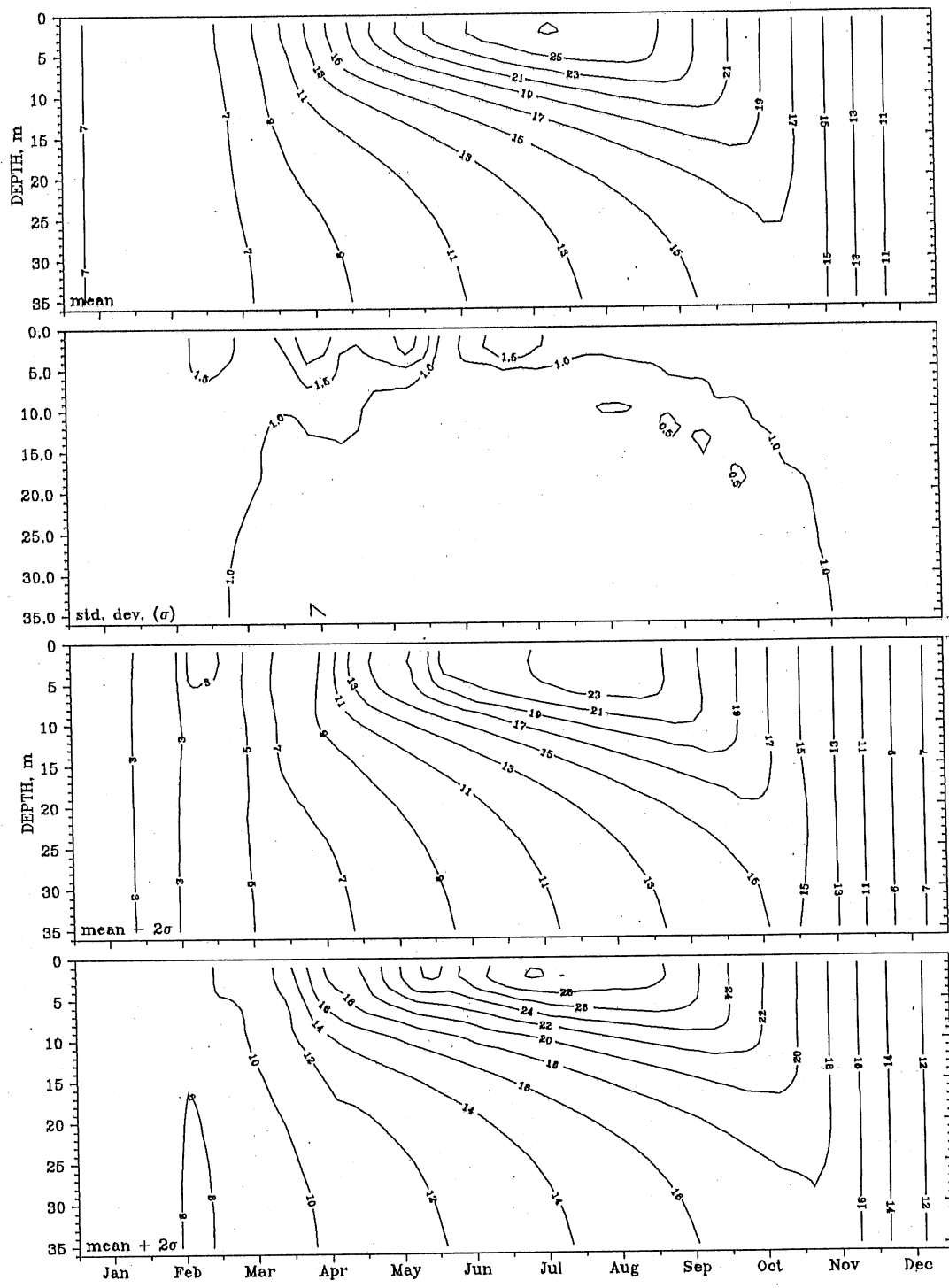


Fig. 6.3. Isotherms ($^{\circ}\text{C}$) in Lake James for an average year under the $1\times\text{CO}_2$ climate scenario (top) with isopleths of standard deviations (σ) and isotherms for extreme (mean $\pm 2\sigma$) events.

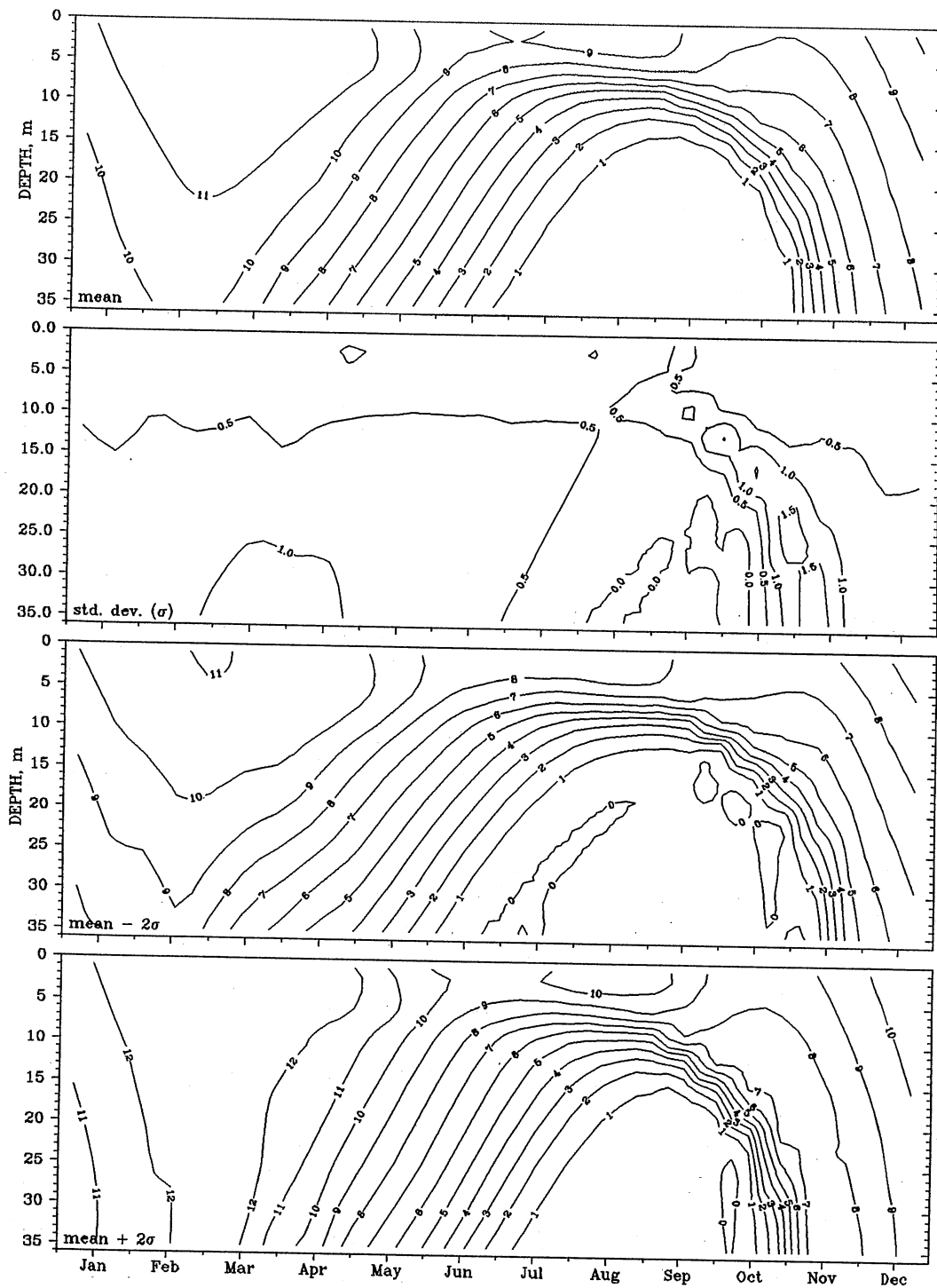


Fig. 6.4. DO isopleths (mg L^{-1}) in Lake James for an average year under the $1\times\text{CO}_2$ climate scenario (top) with isopleths of standard deviations (σ) and of DO for extreme ($\text{mean} \pm 2\sigma$) events.

average cumulative annual evaporative water loss was 863 mm yr⁻¹. Santeetlah Lake has a long stratification season (Fig. 6.5), but the exact length of stratification has a large effect on hypolimnetic DO (Fig. 6.6).

In shallow **Lake Phelps** (Table 6.4), T_{epi} and T_{hyp} were both 32.1 °C. The maximum temperature difference between the surface and bottom was 0.6 °C, as expected for a shallow polymictic lake. The minimum bottom DO was 6.3 mg L⁻¹. There was no portion of the lake that had DO less than 3 mg L⁻¹ for any number of days. The average cumulative annual evaporative water loss was 1191 mm yr⁻¹. The temperature and DO isopleths shown in Figs. 6.7 and 6.8, respectively, show the well mixed nature of Lake Phelps. The water temperatures in the entire volume of polymictic lakes are very sensitive to atmospheric conditions, as shown by the high variance of temperature (Fig. 6.7).

Lake Waccamaw (Table 6.5) behaved as would be expected for a polymictic lake. The maximum epilimnetic and hypolimnetic temperatures were 32.2 °C and 32.0 °C, respectively, and the maximum difference between the surface and bottom was 1.9 °C. The minimum bottom DO was 5.4 mg L⁻¹. There was no portion of the lake volume with DO less than 3 mg L⁻¹, nor were there any days for which the bottom DO went below 3 mg L⁻¹. The average cumulative annual evaporative water loss was 1217 mm yr⁻¹. Well mixed conditions with interspersed short periods of weak stratification are exhibited in Lake Waccamaw for both temperature and DO (Figs. 6.9 and 6.10).

A comparison of all five lakes for the various parameters under the 1xCO₂ scenario is shown in Table 6.6. The lower averages of maximum epilimnetic and hypolimnetic temperatures and of evaporation for James and Santeetlah lakes reflect the fact that both are at higher, colder altitudes in the mountainous region of North Carolina, while the other three lakes are in warmer areas. The three reservoirs show definite strong summer stratification, as can be seen from the maximum temperature difference between the surface and bottom, while the two shallow coastal lakes seem to be well mixed in general, though Lake Waccamaw showed weak stratification. The strength of stratification increases with increasing maximum depth. Absence or presence of summer stratification also affects the minimum hypolimnetic DO concentration as well as the length of time when the lake bottom is anoxic. Volumes of anoxic water, while occurring in each of the stratified reservoirs, were greater in eutrophic Jordan Reservoir, mainly due to higher sediment oxygen demand there.

Some of the characteristics are relatively constant from year to year, while others are more variable. Relative variability can be described by the coefficient of variation, which is the standard deviation divided by the mean. Coefficients of variation were small, typically less than 0.05, for maximum epilimnetic and hypolimnetic temperatures (T_{epi} and T_{hyp}) and annual evaporation (*EVAP*); they were slightly higher, on the order of 0.15 or less, for volume percentages and durations of low DO values at the 2 to 3 mg L⁻¹ level ($DOV_{2.0}$ to $DOV_{3.0}$ and $DAY_{2.0}$ to $DAY_{3.0}$). Coefficients of variation for the maximum

Table 6.4. Selected characteristics from simulation of Lake Phelps under the 1xCO₂ (past, 1961-1979) climate scenario. Each is a daily extreme value for a particular year (except EVAP, which is cumulative).

Year	T _{epi} °C	T _{hyp} °C	T _{diff} °C	DO _{hyp} mg L ⁻¹	EVAP mm
1 (1961)	32.2	32.2	0.6	6.9	1213
2	32.7	32.7	0.7	6.8	1171
3	31.8	31.8	0.6	6.4	1126
4	30.6	30.6	0.5	6.4	1108
5	30.8	30.8	0.6	6.1	1210
6	31.5	31.5	0.5	6.8	1238
7	30.9	30.9	0.5	6.7	1310
8	33.8	33.8	0.6	6.4	1281
9	32.7	32.5	0.5	5.6	1155
10	32.6	32.2	0.5	5.4	1152
11	31.9	31.9	0.7	6.4	1165
12	32.5	32.5	0.3	6.4	1143
13	31.5	31.5	0.7	6.0	1213
14	31.2	31.2	0.7	6.1	1147
15	32.1	32.1	0.4	6.5	1173
16	31.5	31.5	0.7	6.4	1218
17	33.5	33.5	0.4	6.3	1258
18	32.5	32.5	0.9	6.5	1177
19 (1979)	33.7	33.7	0.5	6.4	1172
average	32.1	32.1	0.6	6.3	1191
std. dev.	0.92	0.91	0.14	0.37	52
coef. var.	0.03	0.03	0.23	0.06	0.04

See Table 6.1 for the definition of each characteristic.

Table 6.4. (cont'd.)

Year	DOV _{0.1} %	DOV _{2.0} %	DOV _{2.5} %	DOV _{3.0} %	DAY _{0.1}	DAY _{2.0}	DAY _{2.5}	DAY _{3.0}
1 (1961)	0	0	0	0	0	0	0	0
2	0	0	0	0	0	0	0	0
3	0	0	0	0	0	0	0	0
4	0	0	0	0	0	0	0	0
5	0	0	0	0	0	0	0	0
6	0	0	0	0	0	0	0	0
7	0	0	0	0	0	0	0	0
8	0	0	0	0	0	0	0	0
9	0	0	0	0	0	0	0	0
10	0	0	0	0	0	0	0	0
11	0	0	0	0	0	0	0	0
12	0	0	0	0	0	0	0	0
13	0	0	0	0	0	0	0	0
14	0	0	0	0	0	0	0	0
15	0	0	0	0	0	0	0	0
16	0	0	0	0	0	0	0	0
17	0	0	0	0	0	0	0	0
18	0	0	0	0	0	0	0	0
19 (1979)	0	0	0	0	0	0	0	0
average	0	0	0	0	0	0	0	0
std. dev.	0	0	0	0	0	0	0	0
coef. var.	-	-	-	-	-	-	-	-

See Table 6.1 for the definition of each characteristic.

Table 6.5. Selected characteristics from simulation of Lake Waccamaw under the 1xCO₂ (past, 1961-1979) climate scenario. Each is a daily extreme value for a particular year (except EVAP, which is cumulative).

Year	T _{epi} °C	T _{hyp} °C	T _{diff} °C	DO _{hyp} mg L ⁻¹	EVAP mm
1 (1961)	32.3	32.3	1.7	6.1	1239
2	32.7	31.8	1.7	6.0	1196
3	31.8	31.7	2.0	5.2	1150
4	30.7	30.7	2.3	5.3	1132
5	30.9	30.8	2.2	5.1	1235
6	31.6	31.6	2.0	5.2	1264
7	31.0	30.7	3.7	6.1	1336
8	33.9	33.7	1.5	5.2	1308
9	32.9	32.4	1.5	5.3	1180
10	32.8	32.3	1.3	4.6	1178
11	32.0	32.0	2.9	3.8	1191
12	32.6	32.1	1.4	5.7	1169
13	31.5	31.1	2.0	4.7	1239
14	31.3	31.3	1.8	5.4	1172
15	32.2	31.8	1.6	5.2	1199
16	31.6	31.6	1.5	5.1	1244
17	33.6	33.4	1.5	5.8	1285
18	32.5	32.5	1.9	6.0	1203
19 (1979)	33.8	33.3	1.4	6.2	1198
average	32.2	32.0	1.9	5.4	1217
std. dev.	0.93	0.85	0.57	0.59	52
coef. var.	0.03	0.03	0.30	0.11	0.04

See Table 6.1 for the definition of each characteristic.

Table 6.5. (cont'd.)

Year	DOV _{0.1} %	DOV _{2.0} %	DOV _{2.5} %	DOV _{3.0} %	DAY _{0.1}	DAY _{2.0}	DAY _{2.5}	DAY _{3.0}
1 (1961)	0	0	0	0	0	0	0	0
2	0	0	0	0	0	0	0	0
3	0	0	0	0	0	0	0	0
4	0	0	0	0	0	0	0	0
5	0	0	0	0	0	0	0	0
6	0	0	0	0	0	0	0	0
7	0	0	0	0	0	0	0	0
8	0	0	0	0	0	0	0	0
9	0	0	0	0	0	0	0	0
10	0	0	0	0	0	0	0	0
11	0	0	0	0	0	0	0	0
12	0	0	0	0	0	0	0	0
13	0	0	0	0	0	0	0	0
14	0	0	0	0	0	0	0	0
15	0	0	0	0	0	0	0	0
16	0	0	0	0	0	0	0	0
17	0	0	0	0	0	0	0	0
18	0	0	0	0	0	0	0	0
19 (1979)	0	0	0	0	0	0	0	0
average	0	0	0	0	0	0	0	0
std. dev.	0	0	0	0	0	0	0	0
coef. var.	-	-	-	-	-	-	-	-

See Table 6.1 for the definition of each characteristic.

Table 6.6. Results of simulation under the 1xCO₂ climate scenario showing averages, standard deviations, and coefficients of variation of selected characteristics for each lake.

Lake	T _{epi} °C	T _{hyp} °C	T _{diff} °C	DO _{hyp} mg L ⁻¹	EVAP mm	DOV _{0.1} %	DOV _{2.0} %	DOV _{2.5} %	DOV _{3.0} %	DAY _{0.1}	DAY _{2.0}	DAY _{2.5}	DAY _{3.0}
Averages													
Jordan	30.5	23.8	12.3	0.01	1151	7.7	37.2	39.5	43.8	11	156	158	163
James	28.7	16.7	16.5	0.0	787	0.3	37.4	39.9	43.8	1.5	147	152	158
Santeetlah	27.7	9.2	20.7	0.04	863	0.003	52.1	53.7	56.4	1.9	261	266	271
Phelps	32.1	32.1	0.6	6.34	1191	0	0	0	0	0	0	0	0
Waccamaw	32.2	32.0	1.9	5.37	1217	0	0	0	0	0	0	0	0
Standard deviations													
Jordan	1.04	0.43	1.39	0.03	62	4.5	5.4	5.0	6.2	6	15	16	17
James	1.33	0.50	1.80	0.0	43	0.1	3.1	2.3	2.5	0.5	9	10	9
Santeetlah	1.25	0.68	1.76	0.05	48	0.003	2.1	2.3	3.8	1.2	17	17	17
Phelps	0.92	0.91	0.14	0.37	52	0	0	0	0	0	0	0	0
Waccamaw	0.93	0.85	0.57	0.59	52	0	0	0	0	0	0	0	0
Coefficients of variation													
Jordan	0.03	0.02	0.11	3.0	0.05	0.58	0.15	0.13	0.14	0.55	0.10	0.10	0.10
James	0.05	0.03	0.11	-	0.06	0.33	0.08	0.06	0.06	0.33	0.06	0.07	0.06
Santeetlah	0.05	0.07	0.09	1.25	0.06	1.0	0.04	0.04	0.07	0.63	0.07	0.06	0.06
Phelps	0.03	0.03	0.23	0.06	0.04	-	-	-	-	-	-	-	-
Waccamaw	0.03	0.03	0.30	0.11	0.04	-	-	-	-	-	-	-	-

See Table 6.1 for the definition of each characteristic.

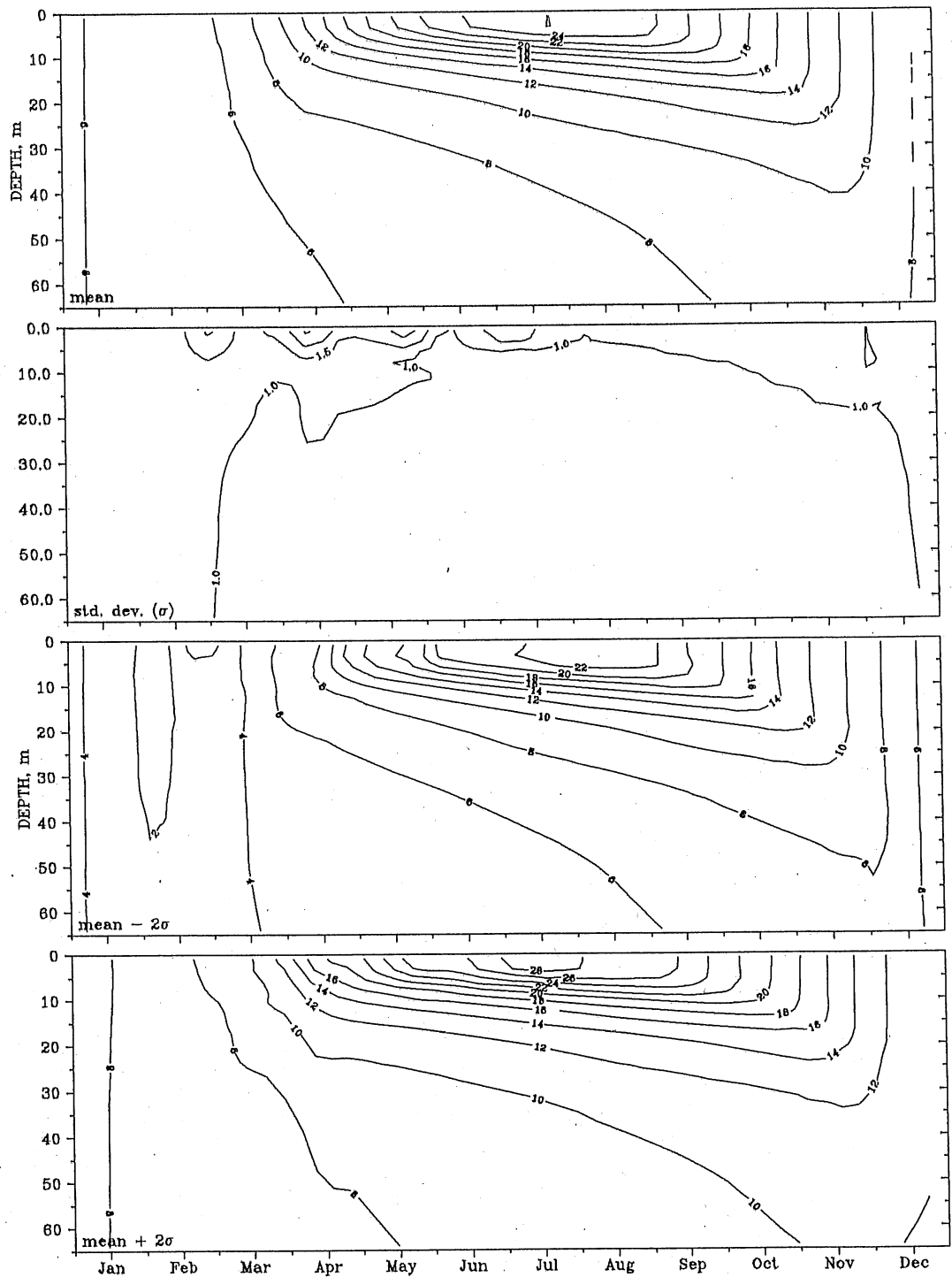


Fig. 6.5. Isotherms ($^{\circ}\text{C}$) in Santeetlah Lake for an average year under the $1x\text{CO}_2$ climate scenario (top) with isopleths of standard deviations (σ) and isotherms for extreme (mean $\pm 2\sigma$) events.

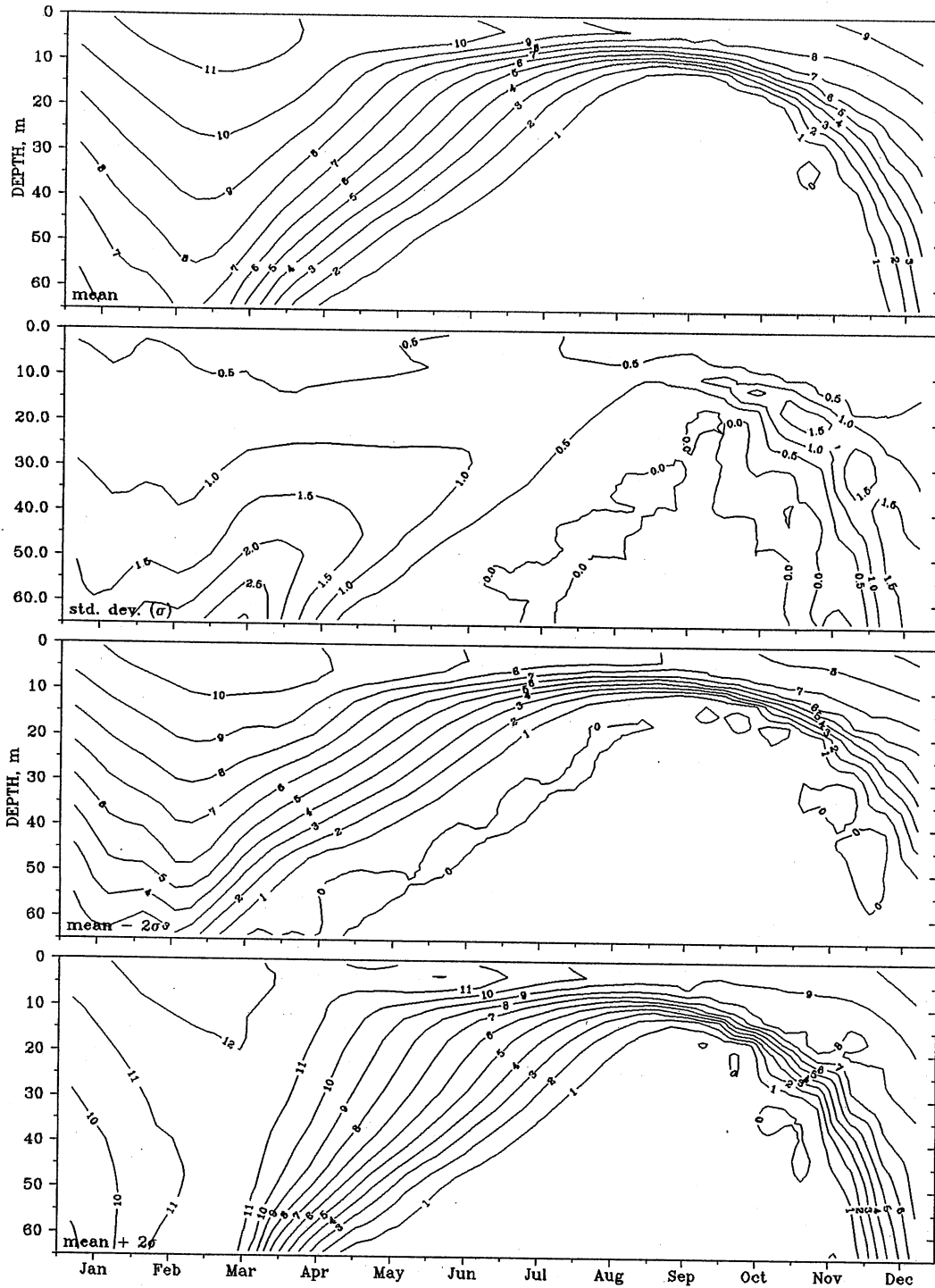


Fig. 6.6. DO isopleths (mg L^{-1}) in Santeetlah Lake for an average year under the $1\times\text{CO}_2$ climate scenario (top) with isopleths of standard deviations (σ) and of DO for extreme ($\text{mean} \pm 2\sigma$) events.

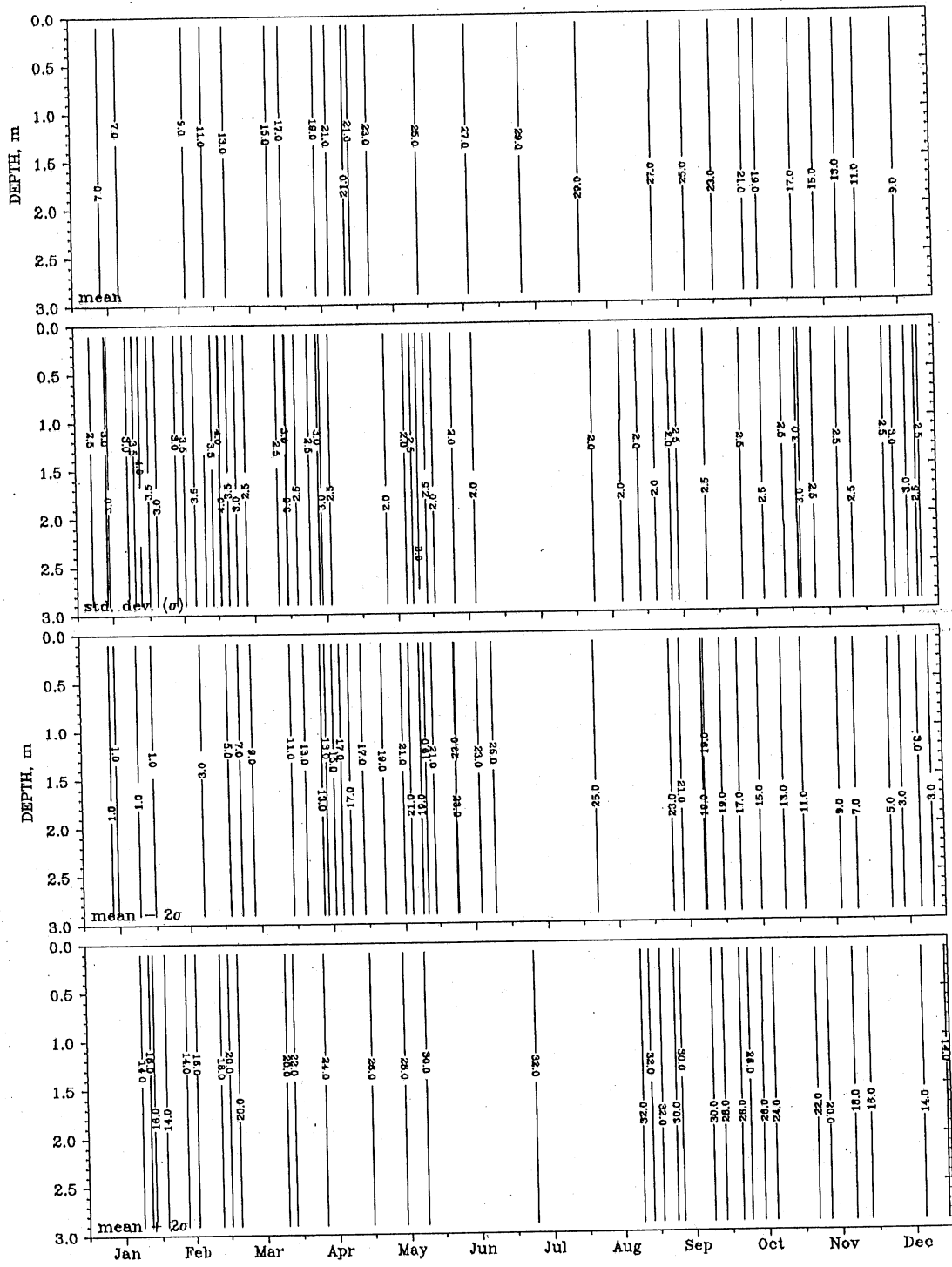


Fig. 6.7. Isotherms ($^{\circ}\text{C}$) in Lake Phelps for an average year under the $1x\text{CO}_2$ climate scenario (top) with isopleths of standard deviations (σ) and isotherms for extreme (mean $\pm 2\sigma$) events.

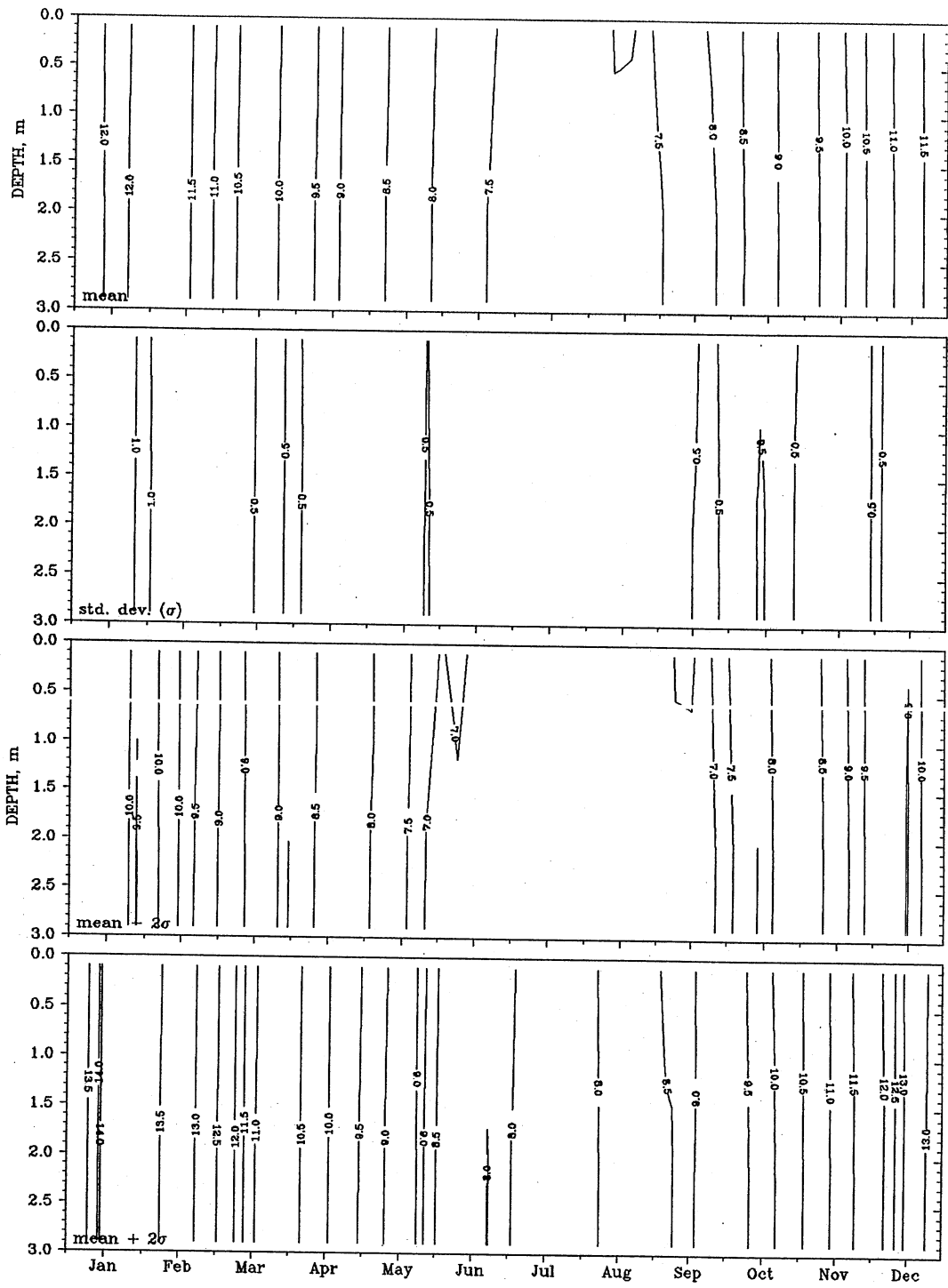


Fig. 6.8. DO isopleths (mg L^{-1}) in Lake Phelps for an average year under the $1x\text{CO}_2$ climate scenario (top) with isopleths of standard deviations (σ) and of DO for extreme ($\text{mean} \pm 2\sigma$) events.

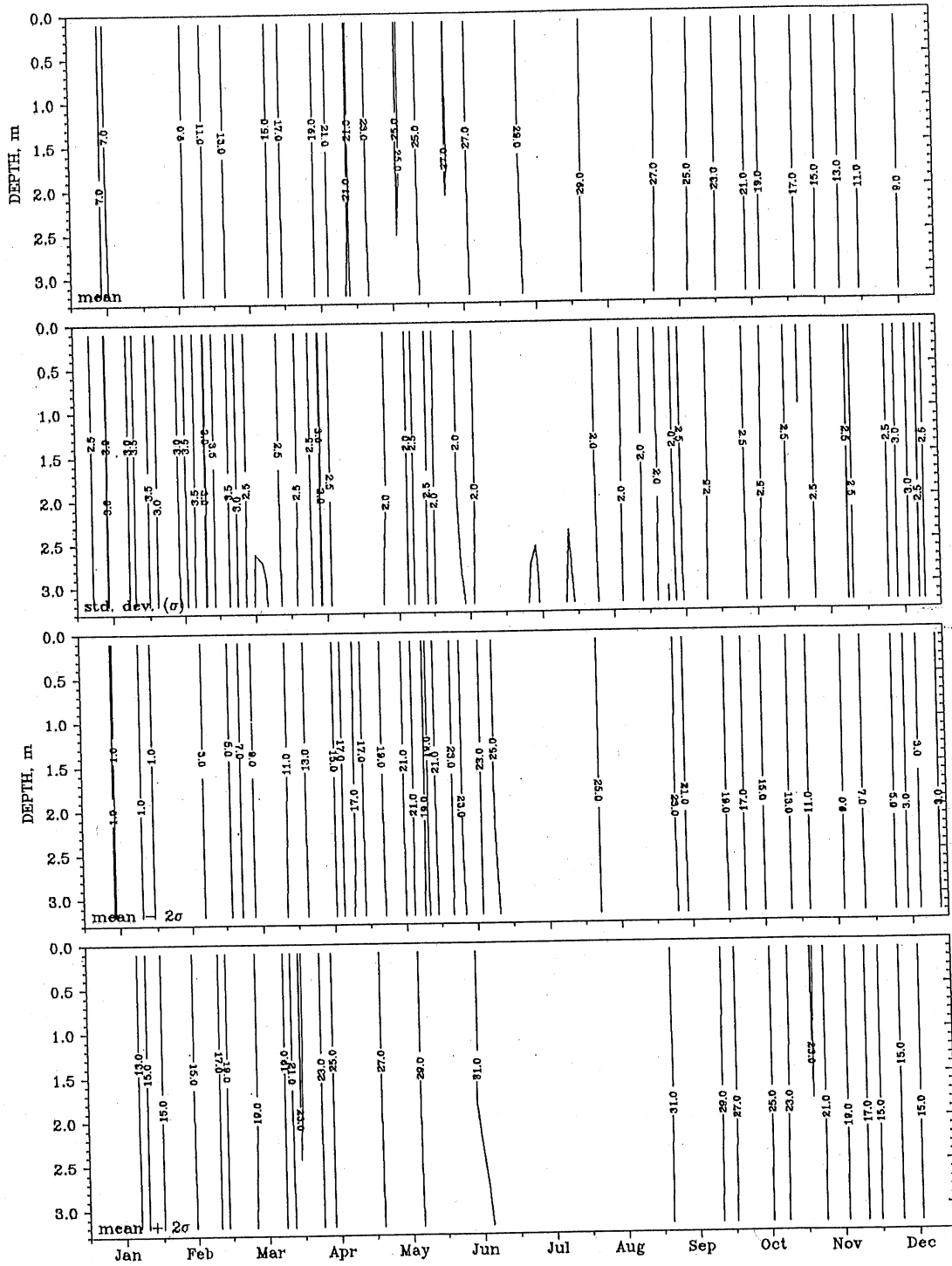


Fig. 6.9. Isotherms ($^{\circ}\text{C}$) in Lake Waccamaw for an average year under the $1x\text{CO}_2$ climate scenario (top) with isopleths of standard deviations (σ) and isotherms for extreme (mean $\pm 2\sigma$) events.

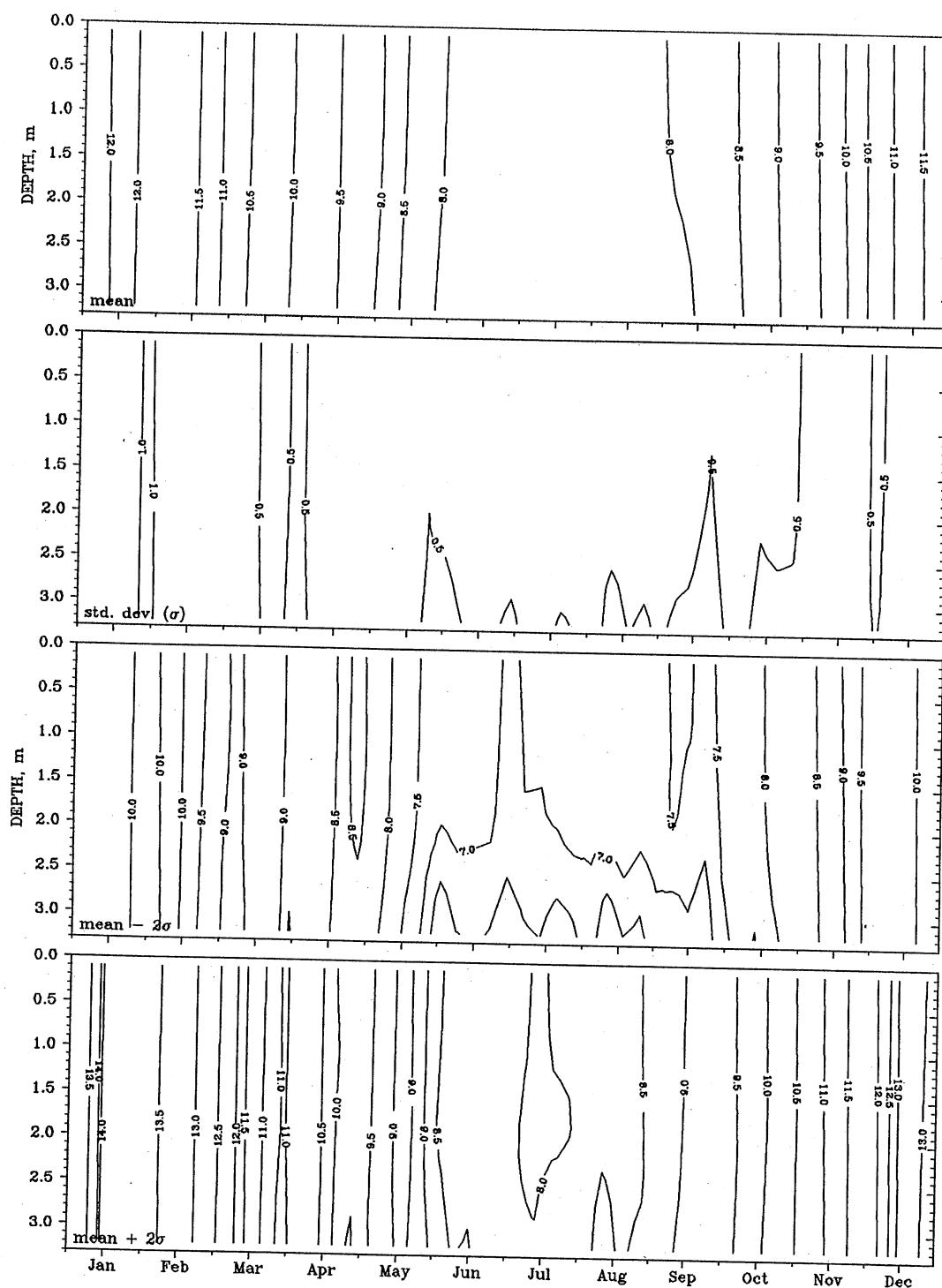


Fig. 6.10. DO isopleths (mg L^{-1}) in Lake Waccamaw for an average year under the $1x\text{CO}_2$ climate scenario (top) with isopleths of standard deviations (σ) and of DO for extreme (mean $\pm 2\sigma$) events.

temperature difference between the surface and bottom were about 0.1 in the reservoirs but higher, an average of 0.27, in the natural lakes. This higher value in the shallow lakes is due to their polymictic nature, which causes bottom temperatures to be rather responsive to meteorological forcing. The low variability of these parameters, which are used for fish habitat interpretations, indicates that mean values are reasonable predictors of habitat suitability. It depends, of course, on how close the parameter values are to fish tolerance values.

Another way to account for variability from year to year is with the contour plots shown in Figs. 6.1 to 6.10. These figures show when and at what depths variations are the strongest. The trends in the three deep reservoirs are distinct from the natural shallow lakes. Since MINLAKE95 is a daily model, the variations do not indicate diurnal effects. Standard deviations of water temperatures in the three reservoirs are from about 0.5 to 2 °C. They are greatest in the surface mixed layer during late winter to early summer, indicating the sensitivity to the meteorological conditions that force the onset of stratification and which themselves are variable. Temperatures are least variable in the hypolimnion during summer stratification. Standard deviations of DO concentrations in the reservoirs range from 0 to 3 mg L⁻¹. They are the highest during spring (Jordan, Santeetlah) or fall (James) in about the bottom half of each reservoir and are the lowest during summer in the anoxic hypolimnion. Low standard deviations of DO (0.5 mg L⁻¹) are found throughout the year near the surface. In the two shallow, natural lakes, standard deviations of water temperature vary from 2.0 °C during summer to 3.5 °C during winter and spring. Standard deviations of DO concentrations in these coastal lakes are 1.0 mg L⁻¹ during winter and only 0.5 mg L⁻¹ during the rest of the year.

6.4 Simulation for 2xCO₂ climate scenario

The effect of the projected 2xCO₂ climate scenario on each lake was also simulated for a 19-year period, producing daily vertical profiles of temperature and DO. The lake characteristics defined in Section 6.2 were determined for each of the 19 years, and averages and standard deviations were then calculated.

The maximum epilimnetic and hypolimnetic temperatures were 33.5 °C and 25.8 °C, respectively, in **B. Everett Jordan Reservoir** (Table 6.7). The maximum temperature difference between the surface and bottom was 13.6 °C. The minimum bottom DO was 0 mg L⁻¹. The maximum percent of the lake volume with anoxic conditions was 13.8%. The values of $DOV_{2.0}$, $DOV_{2.5}$, and $DOV_{3.0}$ were 46%, 50%, and 53%, respectively. Average values of $DAY_{0.1}$, $DAY_{2.0}$, $DAY_{2.5}$, and $DAY_{3.0}$ were 22, 182, 193, and 205 days, respectively. The average cumulative annual evaporative water loss was 1381 mm yr⁻¹. Isotherms for an average 2xCO₂ year are given in Fig. 6.11 and show the same pattern for Jordan Reservoir as under the 1xCO₂ scenario except at higher temperatures. These higher temperatures affect the DO concentrations, as shown in Fig. 6.12.

Table 6.7. Selected characteristics from simulation of Jordan Reservoir under the CCC 2xCO₂ climate scenario. Each is a daily extreme value for a particular year (except EVAP, which is cumulative).

Year	T _{epi} °C	T _{hyp} °C	T _{diff} °C	DO _{hyp} mg L ⁻¹	EVAP mm
1	33.6	25.4	12.5	0.0	1413
2	33.0	25.6	16.3	0.0	1387
3	34.7	25.4	16.6	0.0	1436
4	32.5	25.3	14.9	0.0	1332
5	33.4	25.7	14.0	0.0	1398
6	33.3	25.9	12.9	0.0	1484
7	32.7	25.1	11.6	0.0	1414
8	34.9	25.7	11.5	0.0	1486
9	33.6	25.6	14.3	0.0	1380
10	31.5	26.2	11.8	0.0	1431
11	31.7	25.9	14.3	0.0	1359
12	34.6	25.2	13.7	0.0	1356
13	34.1	26.5	12.9	0.0	1323
14	33.0	25.5	13.0	0.0	1282
15	34.4	25.8	15.5	0.0	1316
16	33.1	26.1	13.0	0.0	1462
17	34.3	26.9	13.3	0.1	1407
18	34.5	26.5	14.8	0.0	1324
19	33.6	26.1	12.3	0.0	1247
average	33.5	25.8	13.6	0.005	1381
std. dev.	0.95	0.47	1.46	0.022	65

Definitions:

T_{epi} = maximum epilimnetic temperature, °C

T_{hyp} = maximum hypolimnetic temperature, °C

T_{diff} = maximum temperature difference between surface and bottom, °C

DO_{hyp} = minimum hypolimnetic DO, mg L⁻¹

EVAP = annual total depth of water lost to evaporation, mm

Table 6.7. (cont'd.)

Year	DOV _{0.1} %	DOV _{2.0} %	DOV _{2.5} %	DOV _{3.0} %	DAY _{0.1}	DAY _{2.0}	DAY _{2.5}	DAY _{3.0}
1	32.1	42.9	55.8	55.8	18	168	171	195
2	23.3	42.9	55.8	55.8	45	173	174	186
3	11.1	55.8	55.8	55.8	11	182	202	213
4	16.4	42.9	42.9	55.8	12	147	171	174
5	16.4	42.9	42.9	55.8	22	173	178	179
6	11.1	55.8	55.8	55.8	16	193	197	212
7	7.9	42.9	42.9	55.8	19	173	175	212
8	11.1	42.9	42.9	42.9	14	188	190	211
9	11.1	42.9	42.9	42.9	24	166	168	171
10	16.4	32.1	42.9	42.9	58	162	166	172
11	11.1	42.9	42.9	42.9	39	165	167	168
12	11.1	42.9	55.8	55.8	14	173	197	200
13	23.3	55.8	55.8	55.8	19	219	222	225
14	16.4	42.9	55.8	55.8	14	185	221	225
15	7.9	42.9	55.8	55.8	14	163	223	226
16	16.4	42.9	55.8	55.8	30	227	233	236
17	11.1	55.8	55.8	55.8	32	205	207	213
18	2.1	55.8	55.8	55.8	2	197	200	237
19	5.8	42.9	42.9	55.8	8	208	211	237
average	13.8	45.7	50.4	53.1	22	182	193	205
std. dev.	6.8	6.5	6.4	5.3	13	21	21	23

Definitions:

DOV_{0.1} = maximum percentage of total lake volume with DO < 0.1 mg L⁻¹

DOV_{2.0} = maximum percentage of total lake volume with DO < 2.0 mg L⁻¹

DOV_{2.5} = maximum percentage of total lake volume with DO < 2.5 mg L⁻¹

DOV_{3.0} = maximum percentage of total lake volume with DO < 3.0 mg L⁻¹

DAY_{0.1} = maximum number of consecutive days with bottom DO < 0.1 mg L⁻¹

DAY_{2.0} = maximum number of consecutive days with bottom DO < 2 mg L⁻¹

DAY_{2.5} = maximum number of consecutive days with bottom DO < 2.5 mg L⁻¹

DAY_{3.0} = maximum number of consecutive days with bottom DO < 3.0 mg L⁻¹

Table 6.8. Selected characteristics from simulation of Lake James under the CCC 2xCO₂ climate scenario. Each is a daily extreme value for a particular year (except EVAP, which is cumulative).

Year	T _{epi} °C	T _{hyp} °C	T _{diff} °C	DO _{hyp} mg L ⁻¹	EVAP mm
1	29.9	18.6	15.1	0.0	860
2	30.6	18.3	16.7	0.0	959
3	32.0	18.6	17.3	0.0	997
4	31.3	18.4	18.6	0.0	861
5	30.7	18.6	15.6	0.0	948
6	30.5	17.6	17.0	0.0	886
7	29.3	18.3	16.3	0.0	899
8	33.9	18.4	18.7	0.0	982
9	33.4	18.2	20.9	0.0	1012
10	32.1	18.7	17.7	0.0	962
11	30.4	19.1	16.7	0.0	924
12	31.5	19.2	16.4	0.0	964
13	31.0	18.7	16.6	0.0	943
14	31.3	19.8	15.2	0.0	968
15	32.0	19.9	15.7	0.0	946
16	31.1	18.7	16.1	0.0	1038
17	33.5	18.2	20.2	0.0	1026
18	32.9	18.4	20.8	0.0	986
19	33.8	18.5	19.0	0.0	923
average	31.6	18.6	17.4	0.0	952
std. dev.	1.31	0.53	1.77	0.0	50

See Table 6.7 for the definition of each characteristic.

Table 6.8. (cont'd.)

Year	DOV _{0.1} %	DOV _{2.0} %	DOV _{2.5} %	DOV _{3.0} %	DAY _{0.1}	DAY _{2.0}	DAY _{2.5}	DAY _{3.0}
1	0.30	41.3	45.6	50.2	2	178	184	192
2	0.30	45.6	45.6	50.2	2	172	178	186
3	0.30	41.3	45.6	50.2	2	175	180	185
4	0.30	41.3	45.6	45.6	1	180	186	194
5	0.30	45.6	50.2	50.2	1	185	193	200
6	0.15	45.6	45.6	50.2	1	175	182	190
7	0.30	41.3	45.6	50.2	1	185	191	198
8	0.15	50.2	50.2	55.0	1	181	187	196
9	0.15	45.6	50.2	55.0	1	176	182	188
10	0.54	50.2	50.2	55.0	2	196	203	209
11	0.54	45.6	50.2	50.2	1	208	216	226
12	0.54	45.6	50.2	50.2	2	210	219	229
13	0.30	50.2	50.2	55.0	2	197	203	215
14	0.15	45.6	50.2	50.2	1	217	228	235
15	0.30	45.6	50.2	50.2	2	182	192	198
16	0.15	45.6	50.2	50.2	1	203	209	215
17	0.30	45.6	50.2	55.0	1	188	194	202
18	0.15	45.6	50.2	50.2	1	188	195	206
19	0.15	50.2	50.2	55.0	1	195	201	207
average	0.3	45.7	48.7	51.4	1.4	189	196	204
std. dev.	0.1	2.9	2.1	2.6	0.5	13	14	14

See Table 6.7 for the definition of each characteristic.

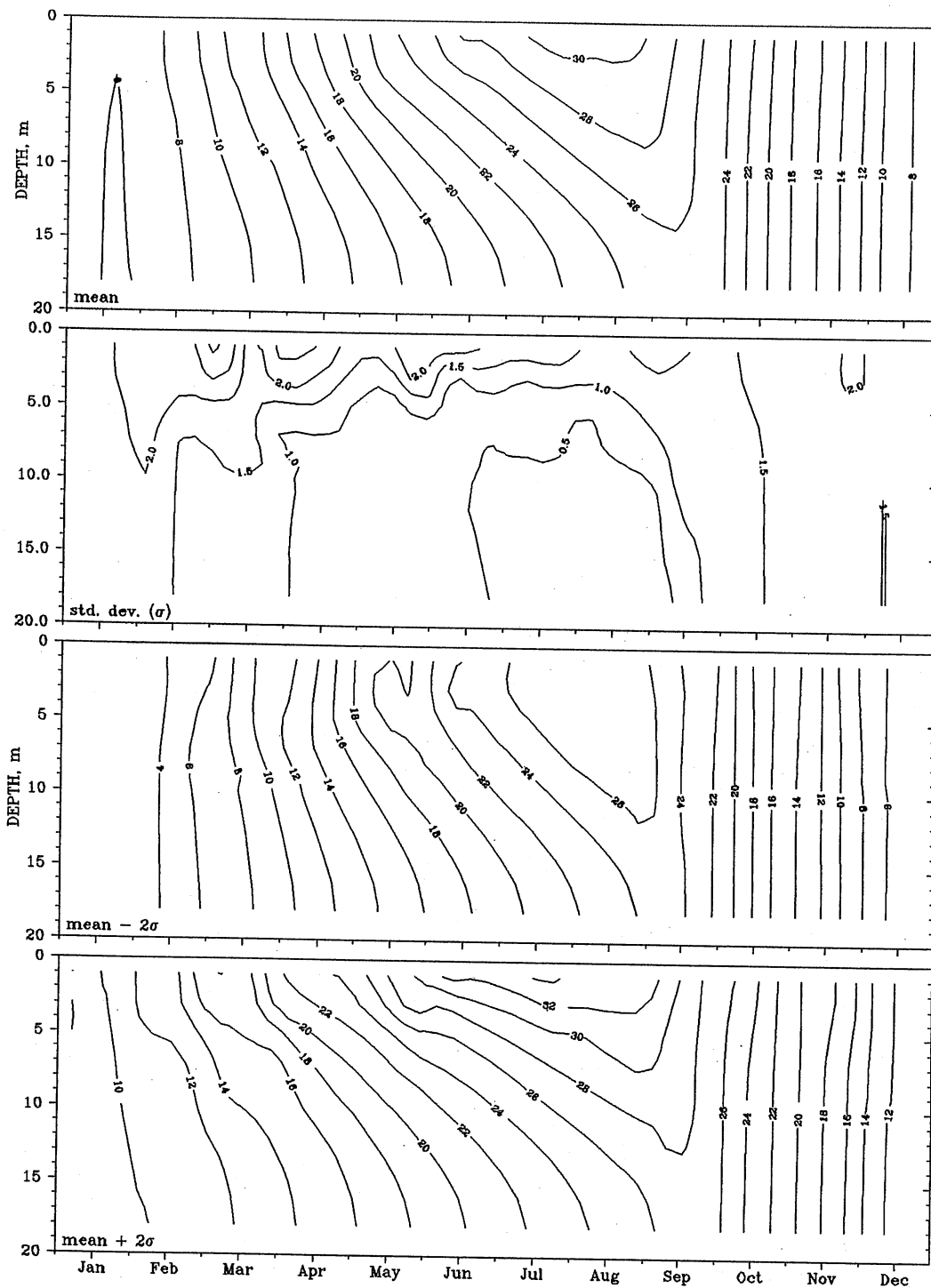


Fig. 6.11. Isotherms (°C) in Jordan Reservoir for an average year under the 2xCO₂ climate scenario (top) with isopleths of standard deviations (σ) and isotherms for extreme (mean $\pm 2\sigma$) events.

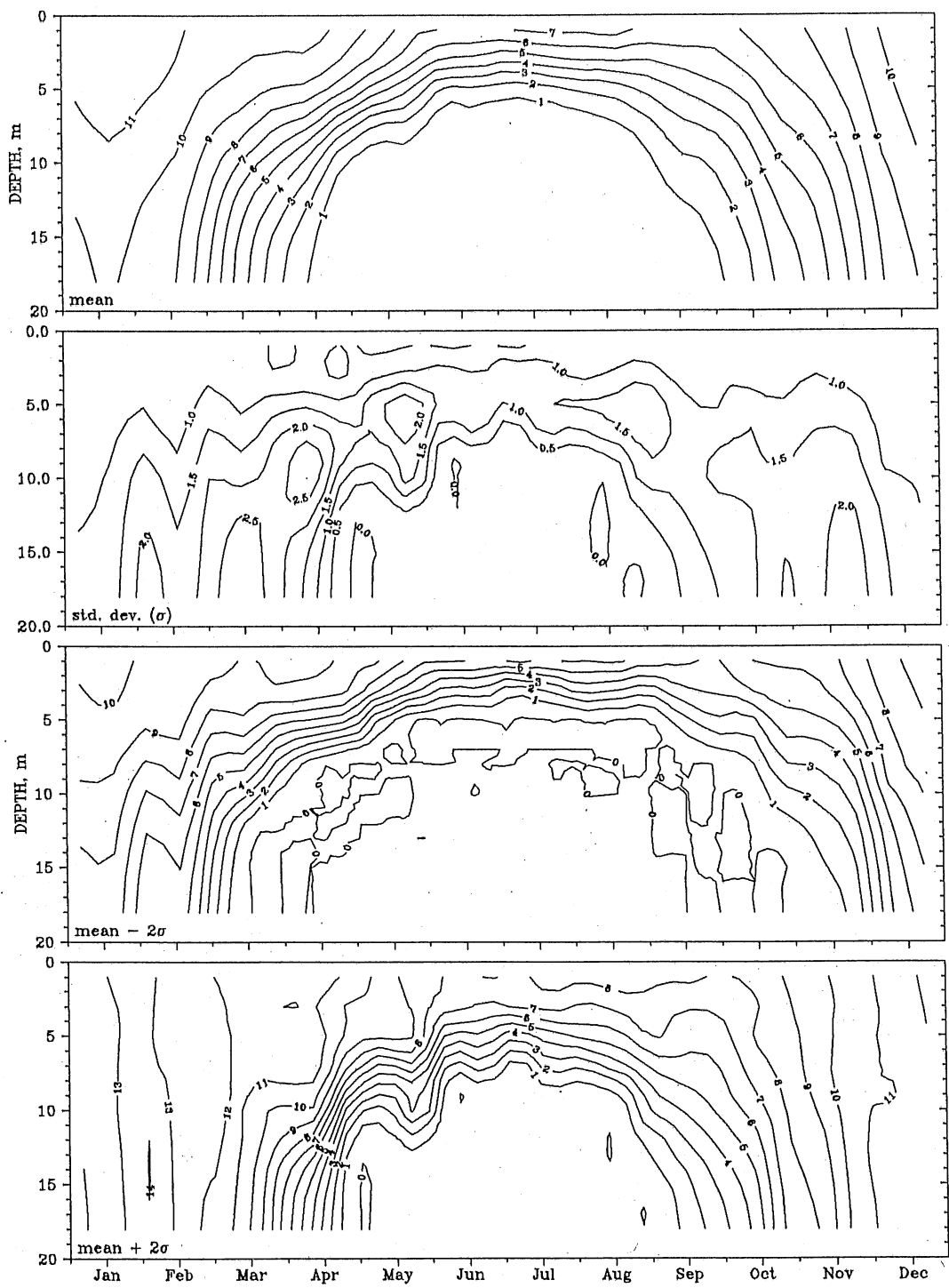


Fig. 6.12. DO isopleths (mg L⁻¹) in Jordan Reservoir for an average year under the 2xCO₂ climate scenario (top) with isopleths of standard deviations (σ) and of DO for extreme (mean \pm 2 σ) events.

For **Lake James** (Table 6.8), the averages of T_{epi} and T_{hyp} were 31.6 °C and 18.6 °C, respectively. The maximum temperature difference between the surface and bottom was 17.4 °C. The minimum bottom DO was 0 mg L⁻¹. The maximum percent of the lake volume with anoxia was less than 1%, and the percentage volumes for $DOV_{2.0}$, $DOV_{2.5}$, and $DOV_{3.0}$ were 48%, 49%, and 51%, respectively. The maximum numbers of consecutive days with bottom DO less than 0.1, 2, 2.5, and 3 mg L⁻¹ were 1, 189, 196, and 204, respectively. The average cumulative annual evaporative water loss was 952 mm yr⁻¹. Temperature and DO isopleths are given in Figs. 6.13 and 6.14, respectively.

The maximum epilimnetic and hypolimnetic temperatures under the 2xCO₂ climate scenario were 30.5 °C and 10.8 °C, respectively, in **Santeetlah Lake** (Table 6.9). The maximum temperature difference between the surface and bottom was 21.7 °C. The average minimum bottom DO was 0 mg L⁻¹. The maximum percent of the lake volume with anoxic conditions was virtually 0%, while 59% of the lake volume went below 2 mg L⁻¹ DO and 60% was below 3 mg L⁻¹. The values of $DAY_{0.1}$, $DAY_{2.0}$, $DAY_{2.5}$, and $DAY_{3.0}$ were 3, 308, 314, and 319, respectively. The average cumulative annual evaporative water loss was 1049 mm yr⁻¹. Fig. 6.15 shows isotherms for an average 2xCO₂ year. During extreme events, Santeetlah Lake will not entirely mix and very low DO conditions can exist in the bottom portion of the lake during the entire year (Fig. 6.16).

For coastal **Lake Phelps** (Table 6.10), T_{epi} and T_{hyp} were 35.1 °C and 35.0 °C, respectively. The maximum temperature difference between the surface and bottom was 0.8 °C. The minimum bottom DO was 5.4 mg L⁻¹. There was no portion of the lake volume that had DO values less than 3 mg L⁻¹ for any one day. The average cumulative annual evaporative water loss was 1439 mm yr⁻¹. Isoleths of temperature and DO are given in Figs. 6.17 and 6.18, respectively.

In **Lake Waccamaw** (Table 6.11), the maximum epilimnetic and hypolimnetic temperatures were 35.2 °C and 34.8 °C, respectively. The maximum temperature difference between the surface and bottom was 2.5 °C, indicating weak stratification. The minimum bottom DO was 3.8 mg L⁻¹. There was no portion of the lake volume with DO less than 2.5 mg L⁻¹, although, in three of the years, bottom DO went below 3 mg L⁻¹ as shown in Table 6.11. There were no days for which the bottom DO went below 2.5 mg L⁻¹, but weak stratification brought the DO below 3 mg L⁻¹ a few times for only one day. The average cumulative annual evaporative water loss was 1467 mm yr⁻¹. Isotherms and DO isopleths are shown in Figs. 6.19 and 6.20, respectively.

A summary of all the results is shown in Table 6.12. Comparing the averages for each lake to the others yields the same general conclusions about stratification and location (i.e. altitude) that were discussed in Section 6.3.

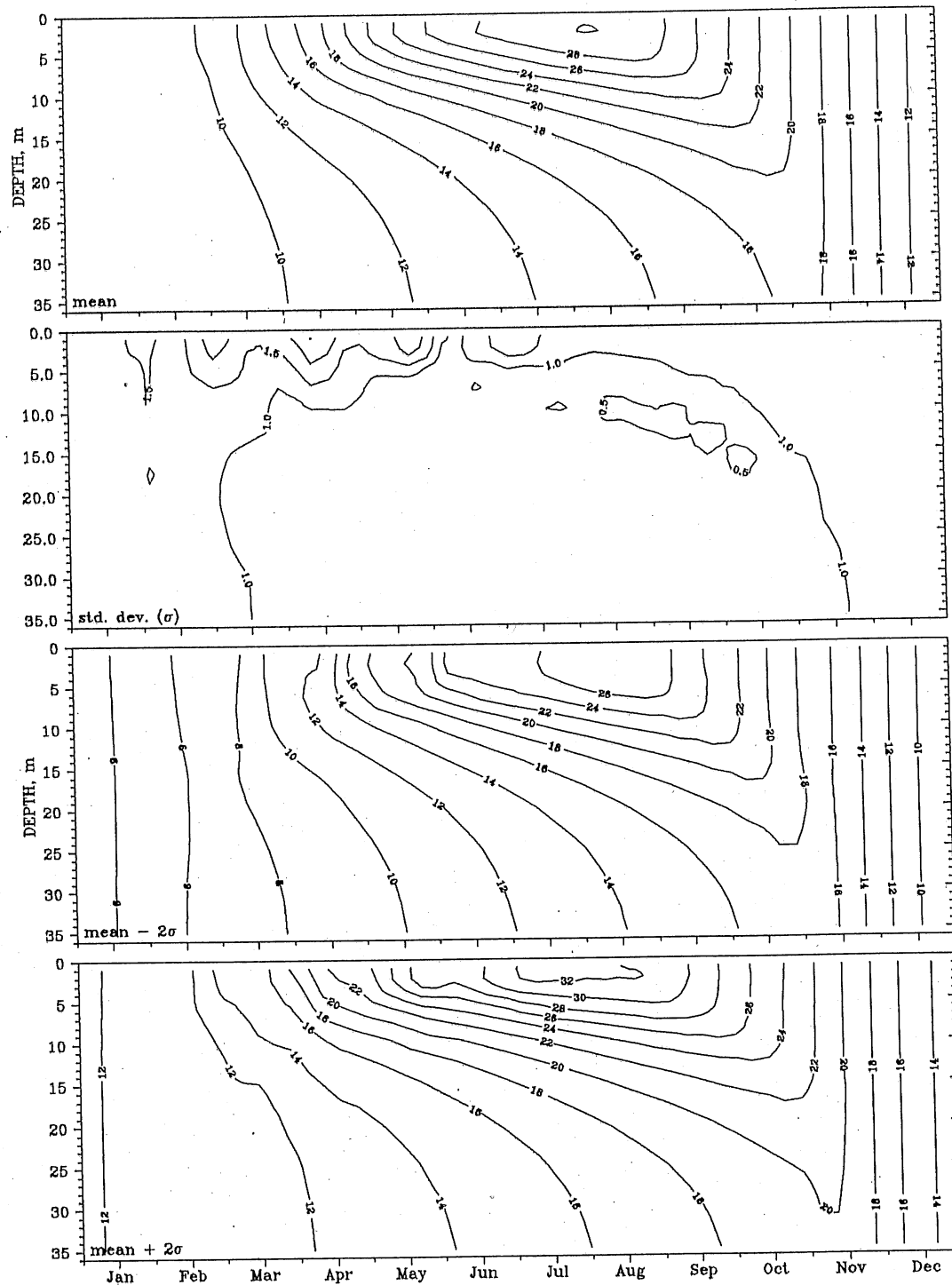


Fig. 6.13. Isotherms ($^{\circ}\text{C}$) in Lake James for an average year under the $2\times\text{CO}_2$ climate scenario (top) with isopleths of standard deviations (σ) and isotherms for extreme (mean $\pm 2\sigma$) events.

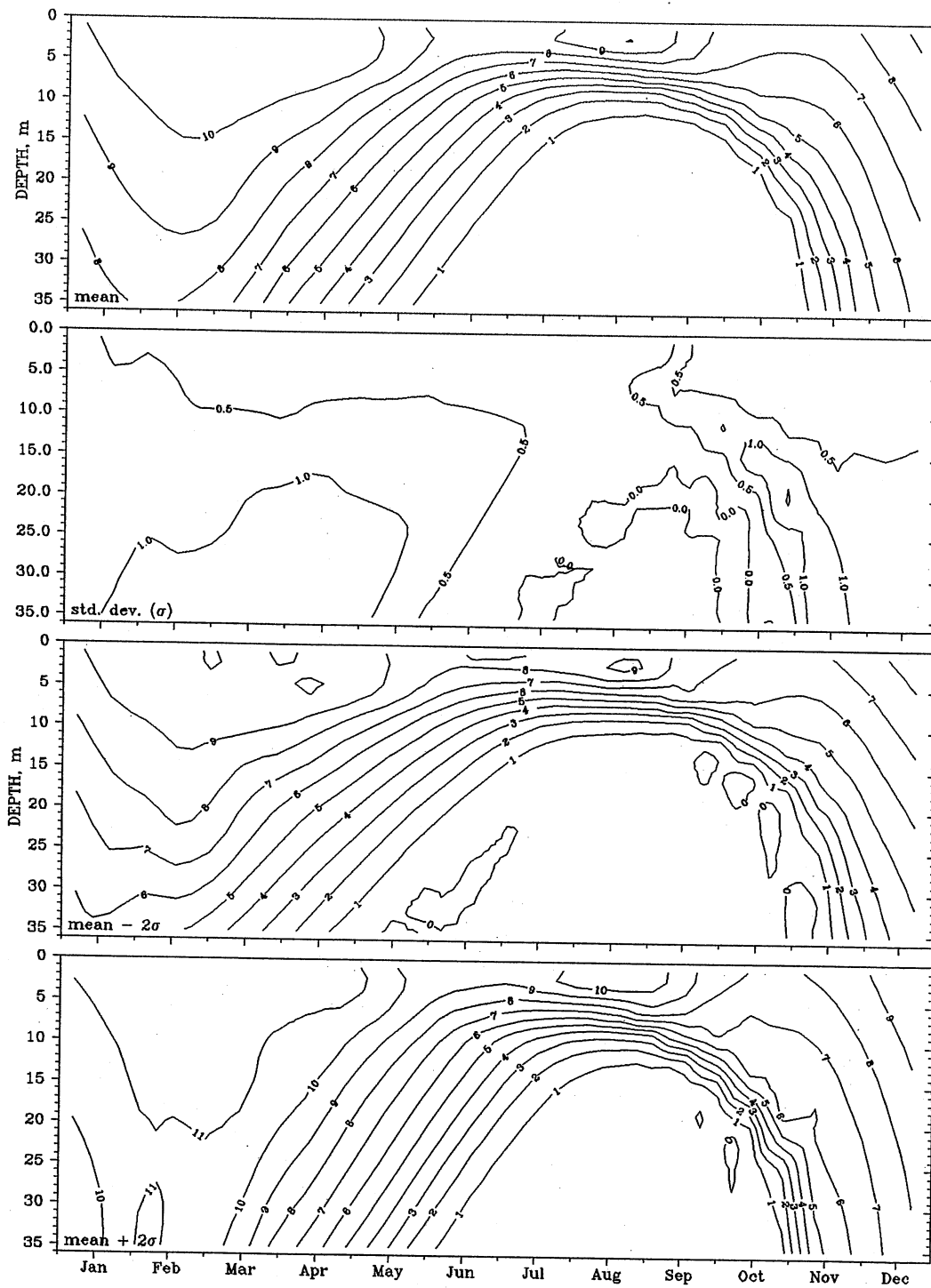


Fig. 6.14. DO isopleths (mg L^{-1}) in Lake James for an average year under the $2\times\text{CO}_2$ climate scenario (top) with isopleths of standard deviations (σ) and of DO for extreme ($\text{mean} \pm 2\sigma$) events.

Table 6.9. Selected characteristics from simulation of Santeetlah Lake under the CCC 2xCO₂ climate scenario. Each is a daily extreme value for a particular year (except EVAP, which is cumulative).

Year	T _{epi} °C	T _{hyp} °C	T _{diff} °C	DO _{hyp} mg L ⁻¹	EVAP mm
1	28.9	10.9	20.4	0.1	964
2	29.4	11.2	19.9	0.0	1061
3	30.8	10.9	21.8	0.0	1103
4	30.3	10.7	22.5	0.0	944
5	29.5	11.1	20.0	0.1	1045
6	29.2	10.0	21.3	0.0	978
7	28.2	10.7	19.7	0.0	991
8	32.7	10.5	23.8	0.0	1082
9	32.1	10.3	23.6	0.0	1113
10	30.9	10.4	22.7	0.0	1055
11	29.4	10.8	20.7	0.0	1013
12	30.6	11.7	20.7	0.0	1359
13	30.0	10.9	20.8	0.0	1044
14	30.1	11.9	19.4	0.1	1067
15	30.8	12.5	19.7	0.1	1042
16	29.9	10.8	20.9	0.0	1145
17	32.1	9.8	24.8	0.1	1130
18	31.8	9.8	24.7	0.1	1085
19	32.6	10.5	24.2	0.1	1012
average	30.5	10.8	21.7	0.04	1049
std. dev.	1.26	0.67	1.77	0.05	54

See Table 6.7 for the definition of each characteristic.

Table 6.9. (cont'd.)

Year	DOV _{0.1} %	DOV _{2.0} %	DOV _{2.5} %	DOV _{3.0} %	DAY _{0.1}	DAY _{2.0}	DAY _{2.5}	DAY _{3.0}
1	0.001	60.4	60.4	60.4	1	297	300	303
2	0.009	60.4	60.4	60.4	4	296	300	315
3	0.001	52.9	60.4	60.4	1	280	286	292
4	0.009	52.9	60.4	60.4	6	308	310	311
5	0.009	60.4	60.4	60.4	3	321	330	365
6	0.009	52.9	60.4	60.4	1	310	315	320
7	0.009	52.9	60.4	60.4	3	301	303	304
8	0.001	60.4	60.4	60.4	2	283	388	291
9	0.001	60.4	60.4	60.4	2	269	273	276
10	0.001	60.4	60.4	60.4	3	316	317	319
11	0.001	60.4	60.4	60.4	3	314	316	317
12	0.009	60.4	60.4	60.4	4	315	366	366
13	0.001	60.4	60.4	60.4	2	298	307	308
14	0	60.4	60.4	60.4	0	363	363	365
15	0.009	60.4	60.4	60.4	4	335	341	365
16	0.001	60.4	60.4	60.4	1	317	320	322
17	0.001	60.4	60.4	60.4	2	313	315	317
18	0.001	60.4	60.4	60.4	2	293	295	297
19	0.001	60.4	60.4	60.4	3	314	315	317
average	0.004	58.8	60.4	60.4	2.5	308	314	319
std. dev.	0.004	3.1	0.0	0.0	1.4	20	23	26

See Table 6.7 for the definition of each characteristic.

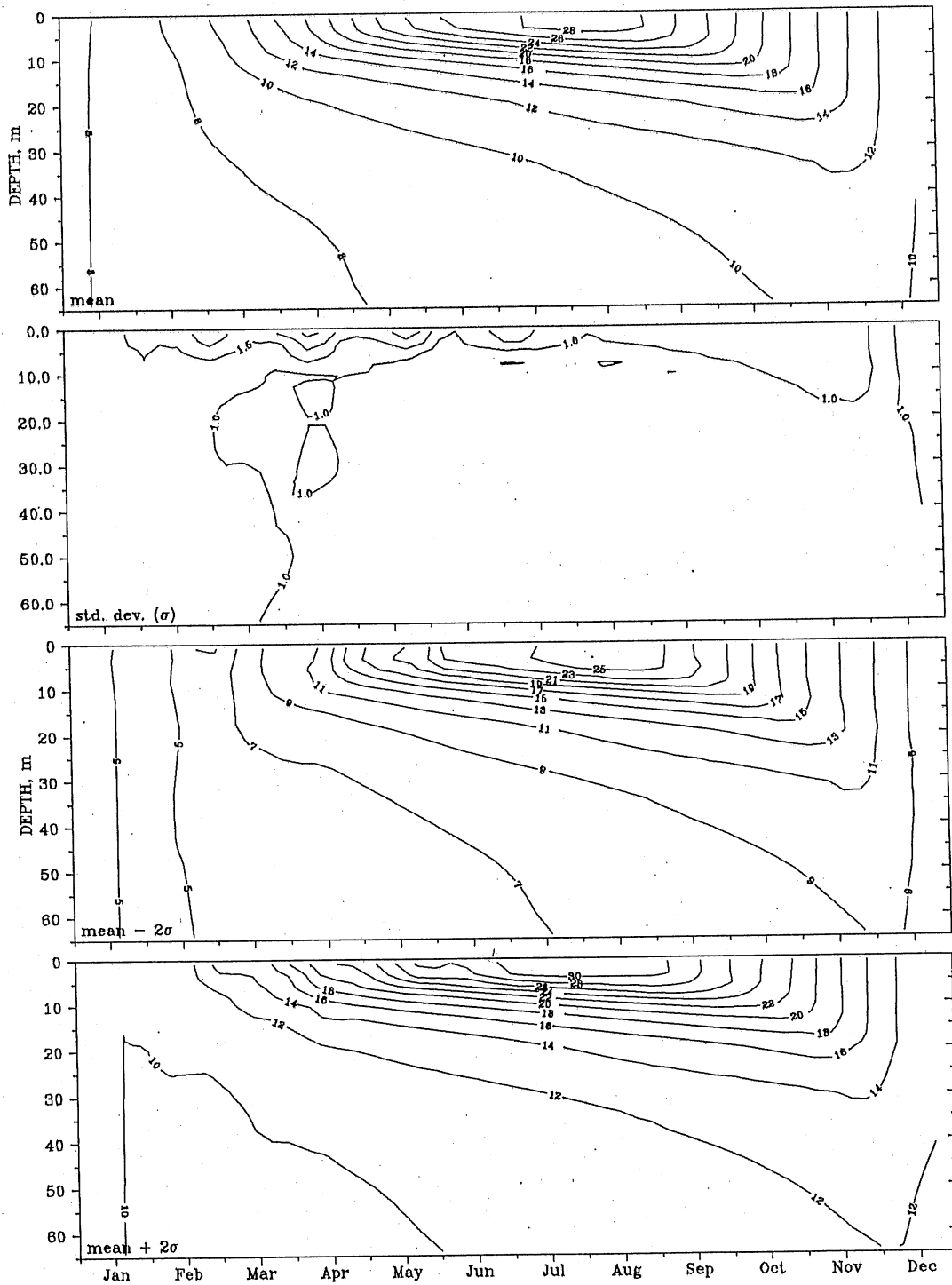


Fig. 6.15. Isotherms ($^{\circ}\text{C}$) in Santeetlah Lake for an average year under the $2\times\text{CO}_2$ climate scenario (top) with isopleths of standard deviations (σ) and isotherms for extreme (mean $\pm 2\sigma$) events.

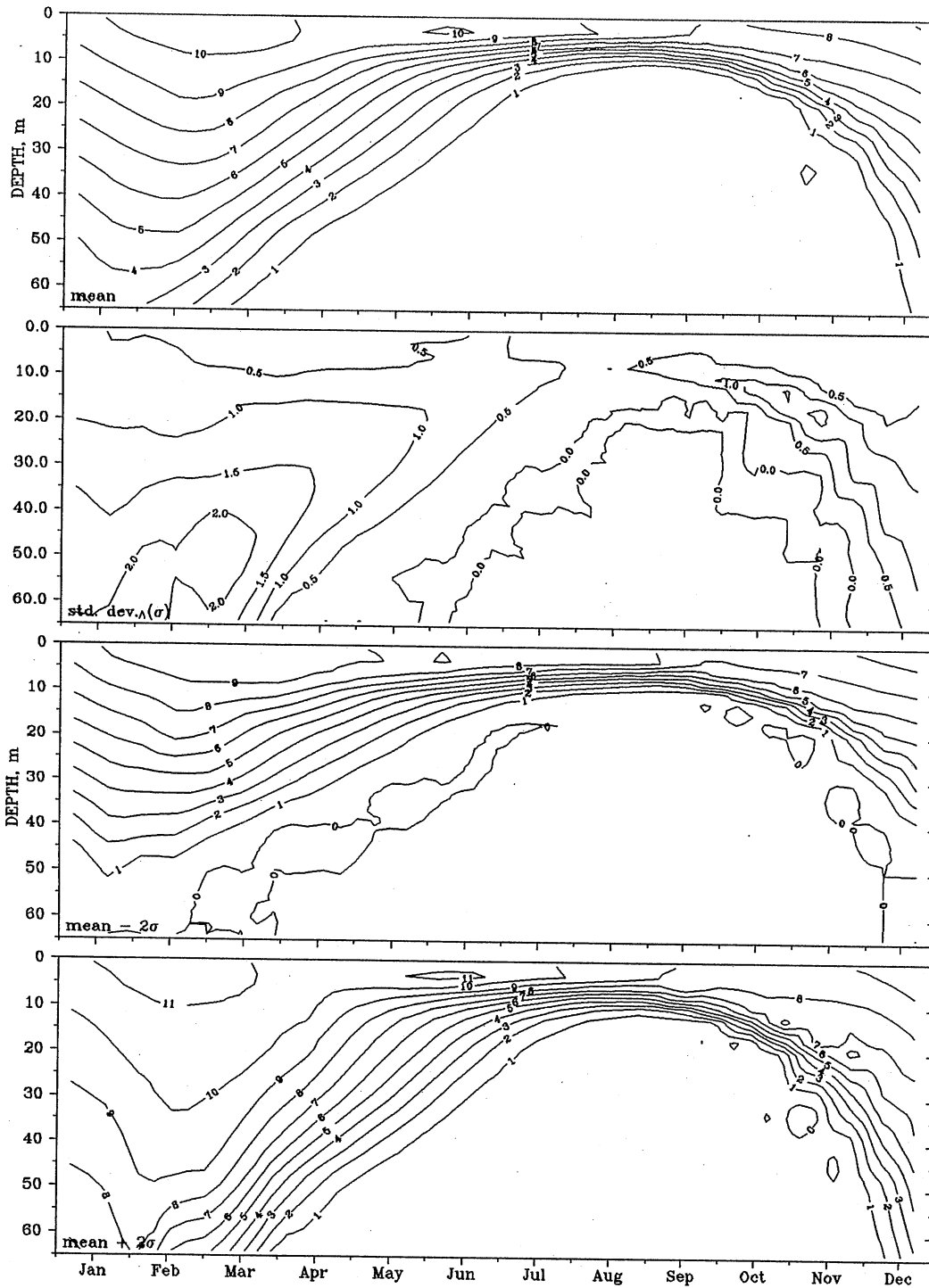


Fig. 6.16. DO isopleths (mg L^{-1}) in Santeetlah Lake for an average year under the $2\times\text{CO}_2$ climate scenario (top) with isopleths of standard deviations (σ) and of DO for extreme ($\text{mean} \pm 2\sigma$) events.

Table 6.10. Selected characteristics from simulation of Lake Phelps under the CCC 2xCO₂ climate scenario. Each is a daily extreme value for a particular year (except EVAP, which is cumulative).

Year	T _{epi} °C	T _{hyp} °C	T _{diff} °C	DO _{hyp} mg L ⁻¹	EVAP mm
1	34.6	34.6	0.7	6.0	1469
2	35.2	35.2	0.9	6.0	1430
3	35.1	35.1	0.7	5.4	1367
4	33.5	33.5	1.0	5.0	1349
5	34.4	34.4	0.8	5.0	1453
6	34.6	34.6	0.8	5.9	1480
7	34.2	34.1	1.0	5.9	1562
8	36.9	36.9	0.8	5.6	1519
9	35.1	34.9	0.6	4.7	1393
10	36.0	35.6	0.7	4.1	1401
11	34.3	34.3	0.7	5.4	1417
12	35.8	35.7	0.7	5.7	1390
13	34.4	34.3	0.5	4.9	1466
14	33.8	33.8	0.9	4.9	1402
15	35.4	35.2	0.6	5.6	1425
16	34.6	34.3	0.7	5.2	1476
17	35.8	35.8	0.5	5.7	1507
18	35.9	35.9	1.0	5.8	1418
19	36.7	36.7	0.8	5.5	1419
average	35.1	35.0	0.8	5.4	1439
std. dev.	0.91	0.90	0.15	0.50	53

See Table 6.7 for the definition of each characteristic.

Table 6.10. (cont'd.)

Year	DOV _{0.1} %	DOV _{2.0} %	DOV _{2.5} %	DOV _{3.0} %	DAY _{0.1}	DAY _{2.0}	DAY _{2.5}	DAY _{3.0}
1	0	0	0	0	0	0	0	0
2	0	0	0	0	0	0	0	0
3	0	0	0	0	0	0	0	0
4	0	0	0	0	0	0	0	0
5	0	0	0	0	0	0	0	0
6	0	0	0	0	0	0	0	0
7	0	0	0	0	0	0	0	0
8	0	0	0	0	0	0	0	0
9	0	0	0	0	0	0	0	0
10	0	0	0	0	0	0	0	0
11	0	0	0	0	0	0	0	0
12	0	0	0	0	0	0	0	0
13	0	0	0	0	0	0	0	0
14	0	0	0	0	0	0	0	0
15	0	0	0	0	0	0	0	0
16	0	0	0	0	0	0	0	0
17	0	0	0	0	0	0	0	0
18	0	0	0	0	0	0	0	0
19	0	0	0	0	0	0	0	0
average	0	0	0	0	0	0	0	0
std. dev.	0	0	0	0	0	0	0	0

See Table 6.7 for the definition of each characteristic.

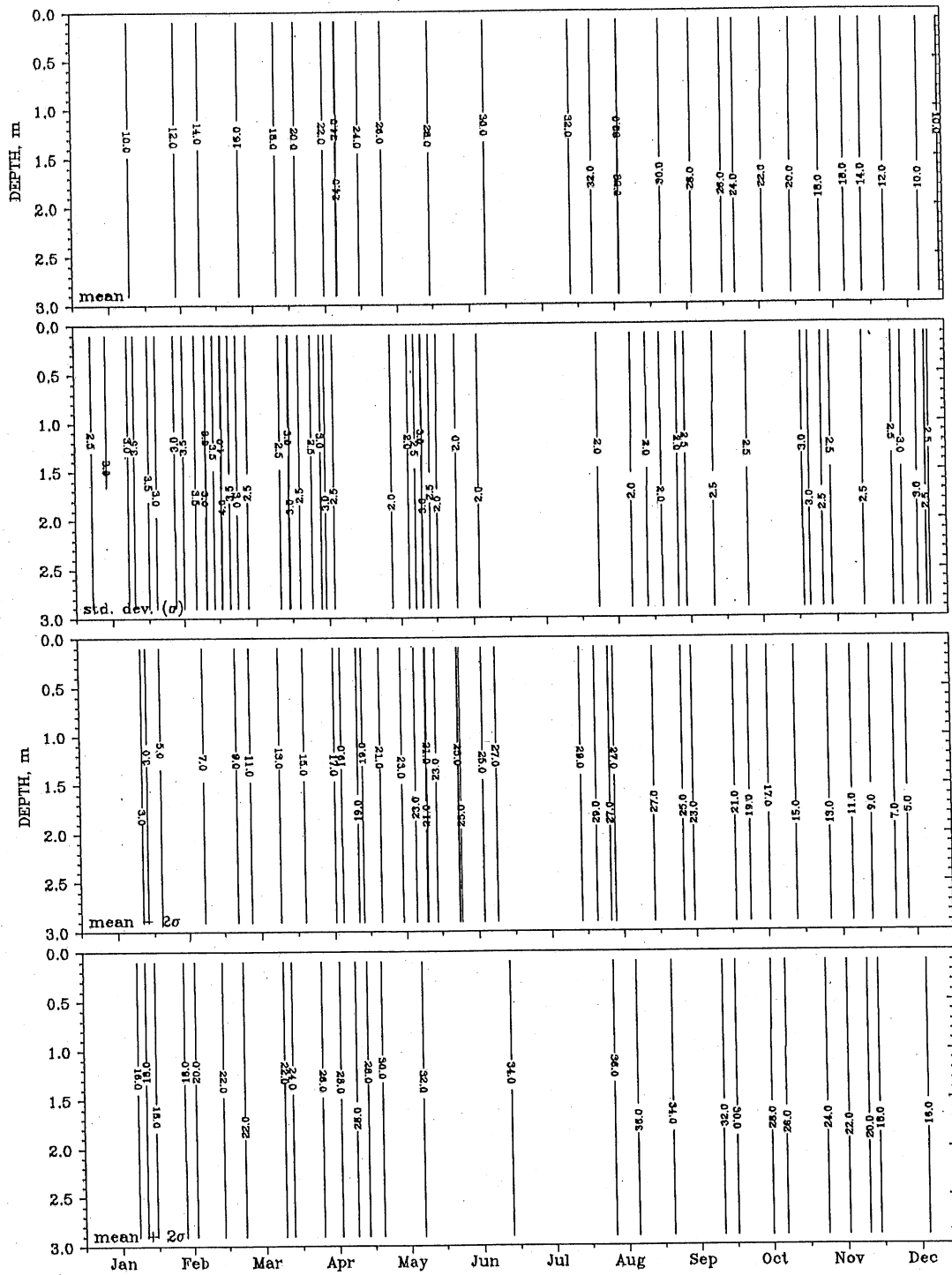


Fig. 6.17. Isotherms ($^{\circ}\text{C}$) in Lake Phelps for an average year under the $2\times\text{CO}_2$ climate scenario (top) with isopleths of standard deviations (σ) and isotherms for extreme (mean $\pm 2\sigma$) events.

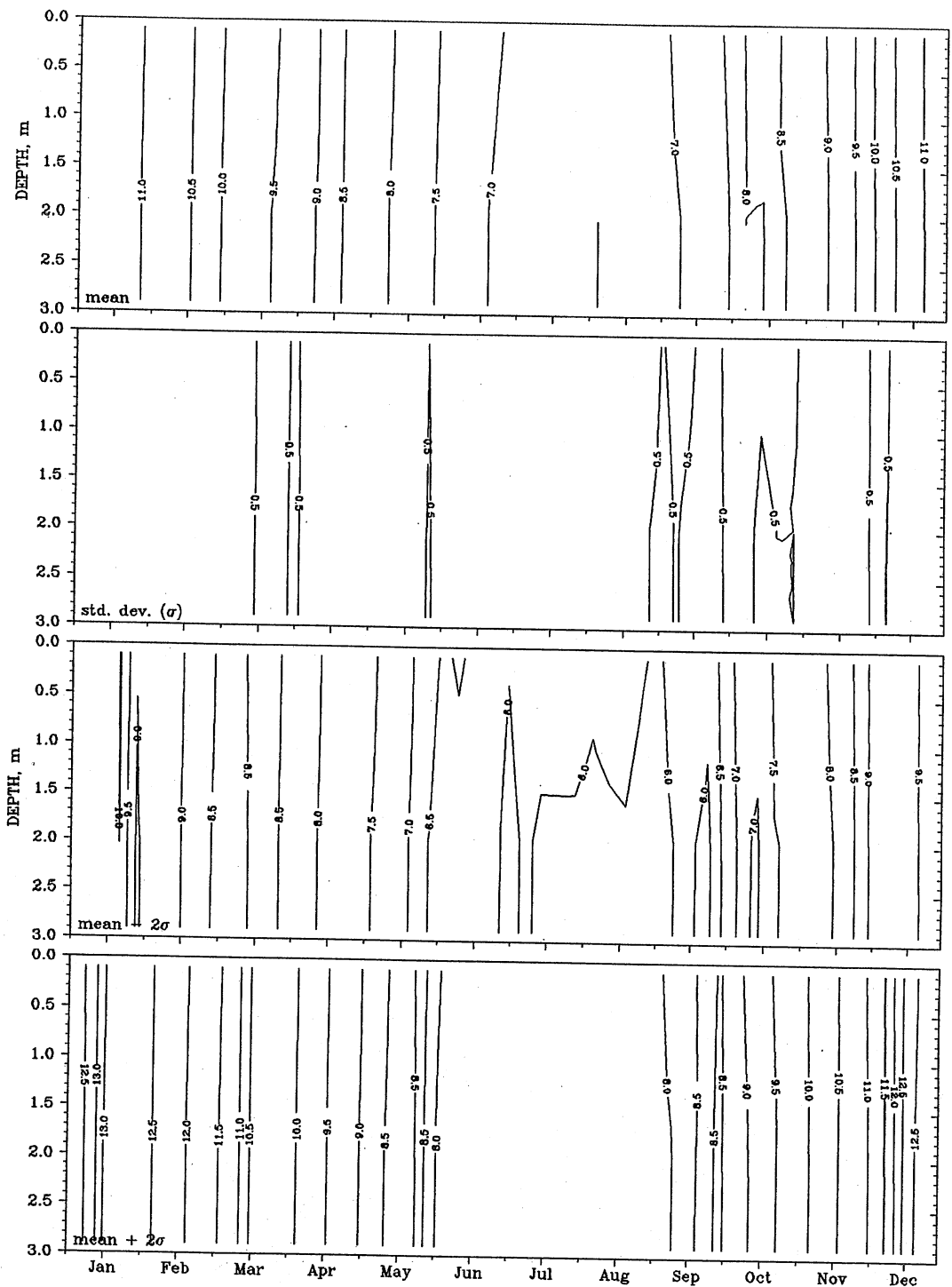


Fig. 6.18. DO isopleths (mg L⁻¹) in Lake Phelps for an average year under the 2xCO₂ climate scenario (top) with isopleths of standard deviations (σ) and of DO for extreme (mean $\pm 2\sigma$) events.

Table 6.11. Selected characteristics from simulation of Lake Waccamaw under the CCC 2xCO₂ climate scenario. Each is a daily extreme value for a particular year (except EVAP, which is cumulative).

Year	T _{epi} °C	T _{hyp} °C	T _{diff} °C	DO _{hyp} mg L ⁻¹	EVAP mm
1	34.7	34.7	2.7	4.3	1496
2	35.3	34.1	3.0	4.1	1456
3	35.2	35.1	2.6	3.5	1393
4	33.5	33.5	2.7	3.6	1374
5	34.5	34.4	3.0	3.6	1480
6	34.7	34.4	2.5	3.2	1508
7	34.3	33.9	4.6	4.3	1589
8	37.0	36.9	2.3	4.2	1548
9	35.3	34.7	1.8	4.3	1421
10	36.2	35.3	1.8	2.9	1429
11	34.4	34.4	2.7	2.6	1444
12	35.9	35.2	1.9	4.3	1418
13	34.6	34.2	1.8	3.0	1495
14	33.8	33.8	2.5	3.7	1430
15	35.5	35.1	1.8	3.8	1452
16	34.7	34.3	2.0	3.6	1504
17	35.9	35.9	2.0	4.6	1536
18	35.9	35.7	2.4	4.2	1446
19	36.8	36.5	2.7	4.0	1446
average	35.2	34.8	2.5	3.8	1467
std. dev.	0.93	0.89	0.65	0.54	53

See Table 6.7 for the definition of each characteristic.

Table 6.11. (cont'd.)

Year	DOV _{0.1} %	DOV _{2.0} %	DOV _{2.5} %	DOV _{3.0} %	DAY _{0.1}	DAY _{2.0}	DAY _{2.5}	DAY _{3.0}
1	0	0	0	0	0	0	0	0
2	0	0	0	0	0	0	0	0
3	0	0	0	0	0	0	0	0
4	0	0	0	0	0	0	0	0
5	0	0	0	0	0	0	0	0
6	0	0	0	0	0	0	0	0
7	0	0	0	0	0	0	0	0
8	0	0	0	0	0	0	0	0
9	0	0	0	0	0	0	0	0
10	0	0	0	0.6	0	0	0	1
11	0	0	0	2.1	0	0	0	1
12	0	0	0	0	0	0	0	0
13	0	0	0	0.6	0	0	0	1
14	0	0	0	0	0	0	0	0
15	0	0	0	0	0	0	0	0
16	0	0	0	0	0	0	0	0
17	0	0	0	0	0	0	0	0
18	0	0	0	0	0	0	0	0
19	0	0	0	0	0	0	0	0
average	0	0	0	0.2	0	0	0	0.2
std. dev.	0	0	0	0.5	0	0	0	0.4

See Table 6.7 for the definition of each characteristic.

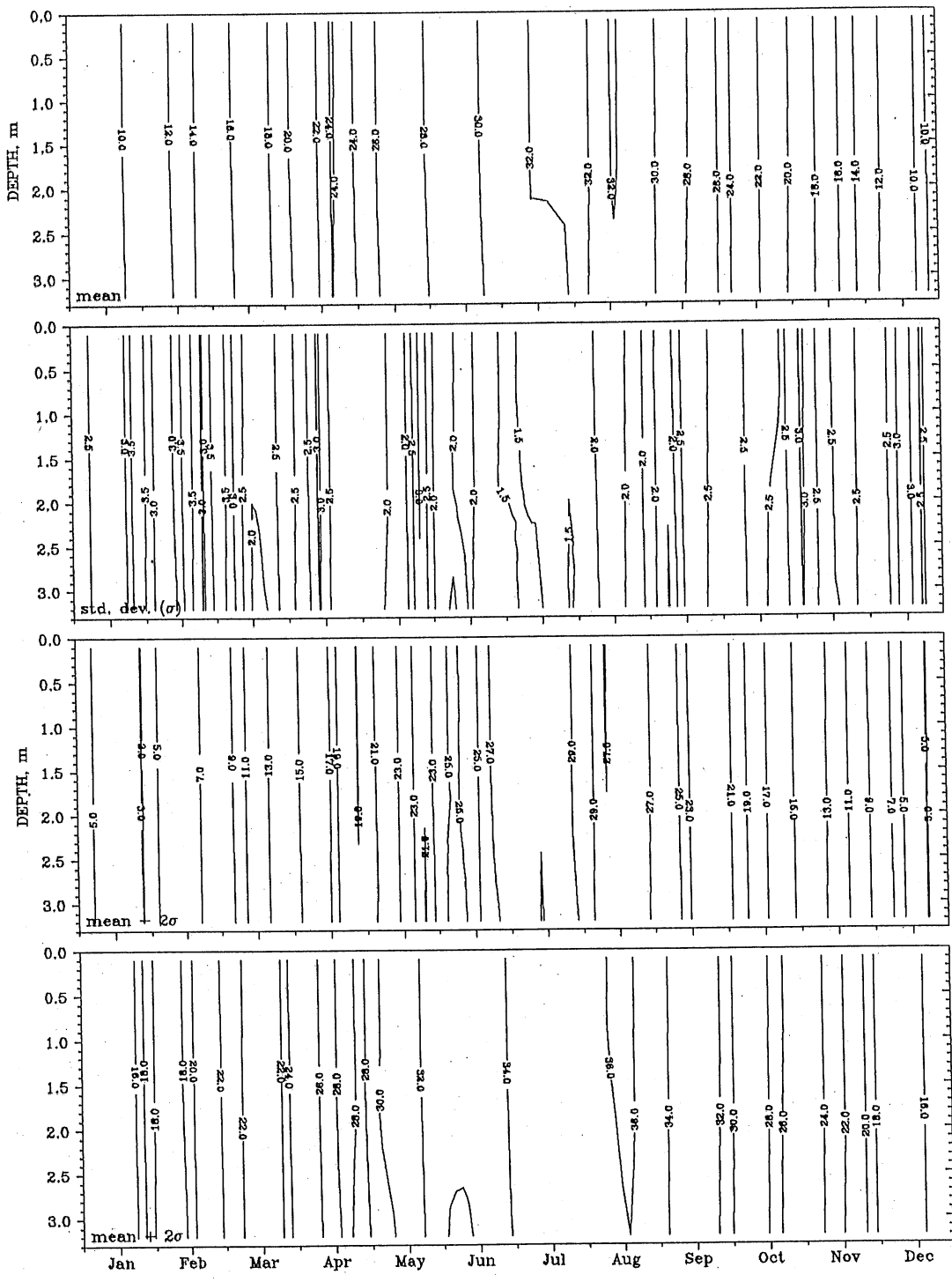


Fig. 6.19. Isotherms ($^{\circ}\text{C}$) in Lake Waccamaw for an average year under the $2\times\text{CO}_2$ climate scenario (top) with isopleths of standard deviations (σ) and isotherms for extreme (mean $\pm 2\sigma$) events.

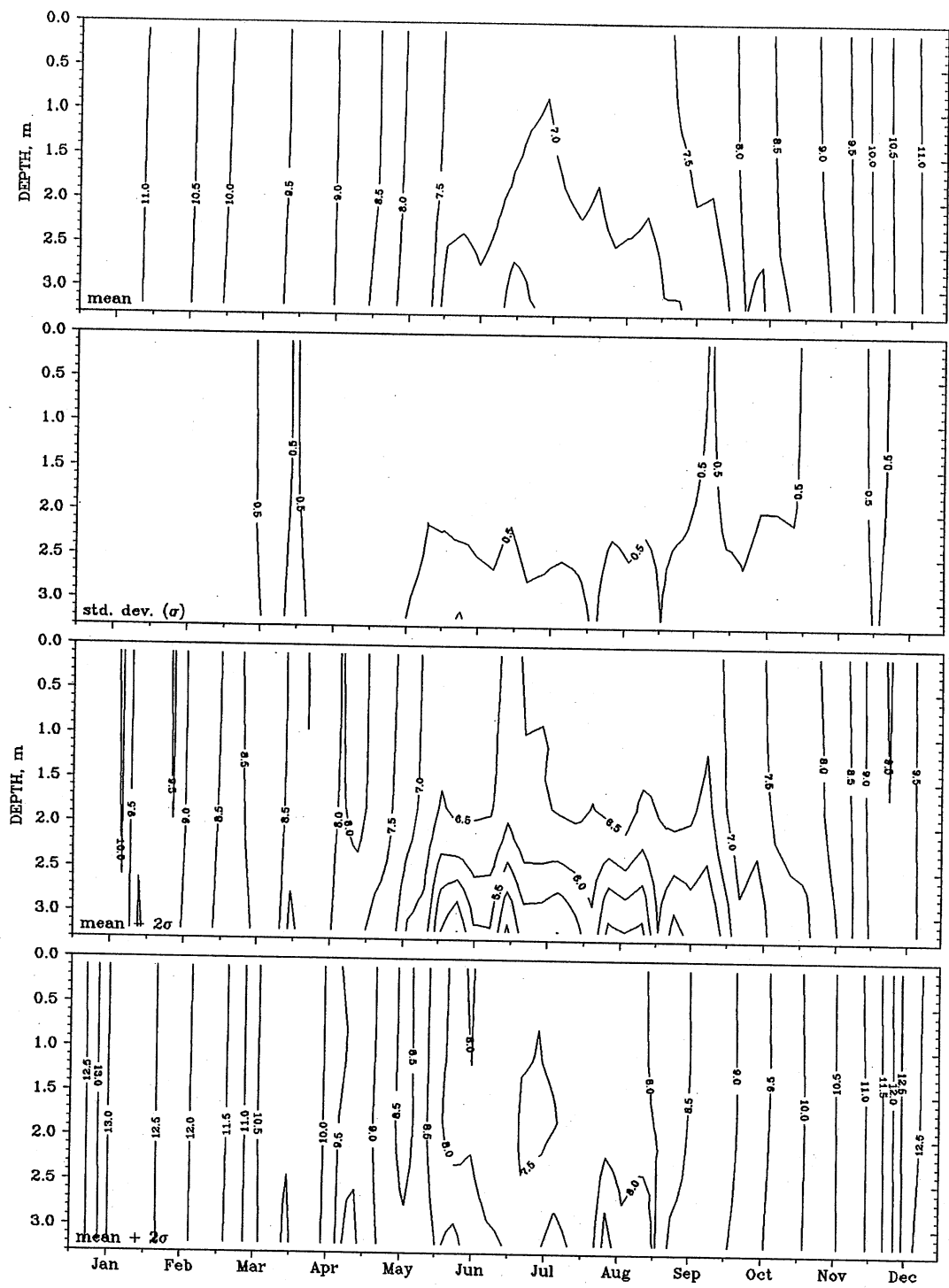


Fig. 6.20. DO isopleths (mg L^{-1}) in Lake Waccamaw for an average year under the $2\times\text{CO}_2$ climate scenario (top) with isopleths of standard deviations (σ) and of DO for extreme (mean $\pm 2\sigma$) events.

Table 6.12. Results of simulation under the 2xCO₂ climate scenario showing averages and standard deviations of selected characteristics for each lake.

Lake	T _{epi} °C	T _{hyp} °C	T _{diff} °C	DO _{hyp} mg L ⁻¹	EVAP mm	DOV _{0.1} %	DOV _{2.0} %	DOV _{2.5} %	DOV _{3.0} %	DAY _{0.1}	DAY _{2.0}	DAY _{2.5}	DAY _{3.0}
Averages													
Jordan	33.5	25.8	13.6	0.005	1381	13.8	45.7	50.4	53.1	22	182	193	205
James	31.6	18.6	17.4	0.0	952	0.3	45.7	48.7	51.4	1.4	189	196	204
Santeetlah	30.5	10.8	21.7	0.04	1049	0.004	58.8	60.4	60.4	2.5	308	314	319
Phelps	35.1	35.0	0.8	5.4	1439	0	0	0	0	0	0	0	0
Waccamaw	35.2	34.8	2.5	3.8	1467	0	0	0	0.2	0	0	0	0.2
Standard deviations													
Jordan	0.95	0.47	1.46	0.022	65	6.8	6.5	6.4	5.3	13	21	21	23
James	1.31	0.53	1.77	0.0	50	0.1	2.9	2.1	2.6	0.5	13	14	14
Santeetlah	1.26	0.67	1.77	0.05	54	0.004	3.1	0	0	1.4	20	23	26
Phelps	0.91	0.90	0.15	0.50	53	0	0	0	0	0	0	0	0
Waccamaw	0.93	0.89	0.65	0.54	53	0	0	0	0.5	0	0	0	0.4

See Table 6.7 for the definition of each characteristic.

6.5 Projected effects of climate change from 1xCO₂ to 2xCO₂ climate scenarios

Of particular interest in this study is to determine what change, if any, there is between lake characteristics simulated with the past 1xCO₂ and projected 2xCO₂ climate scenarios. A standard student's *t*-test was performed on the simulation results for each of the lakes in order to determine if there was any statistically significant change of the lake characteristics between the two climate conditions. The *t*-test was two-tailed with a level of significance of 0.05. The rejection region is $|t| > 2.101$, i.e. if the absolute value of the test statistic *t* is greater than 2.101, then the two means are not statistically the same. The results of the *t*-tests are given in Table 6.13.

The effect of projected climate change is summarized in Table 6.14. The maximum epilimnetic and hypolimnetic temperatures increased in each of the five lakes. Surface temperatures increased by 2.8-3.0 °C. Bottom temperatures increased by 1.6 to 2.0 °C in the reservoirs and 2.8 to 2.9 °C in the natural lakes. The strength of stratification, measured by the maximum temperature difference between the surface and bottom, showed little change: from 12.3 to 13.6 °C in Jordan Reservoir, from 0.6 to 0.8 °C in Lake Phelps, and from 1.9 to 2.5 °C in Lake Waccamaw. The *t*-test showed no change for either Lake James or Santeetlah Lake.

The minimum hypolimnetic DO in the three reservoirs did not change from zero (anoxia), but in the two polymictic coastal lakes, differences between the two climate scenarios were evident. The minimum hypolimnetic DO concentrations in Lake Phelps and in Lake Waccamaw decreased by 1.0 and 1.6 mg L⁻¹, respectively. The reason for this change is probably the increase in temperatures and the associated lowering of the DO saturation values in these lakes. The lowest DO values in Lake Phelps and Lake Waccamaw remained, however, above 3.5 mg L⁻¹.

The maximum percentage of anoxic lake volume $DOV_{0.1}$ and the maximum number of consecutive days at bottom anoxia $DAY_{0.1}$ changed only in Jordan Reservoir, with increases of 6% and 11 days, respectively. There were no changes in the other two reservoirs, possibly because they are deeper and smaller (Table 5.2) and tend to be more strongly stratified (Table 6.6). The two natural lakes had no anoxia in either climate scenario. The percentages $DOV_{2.0}$, $DOV_{2.5}$, and $DOV_{3.0}$ increased in the three reservoirs by 4% to 11% (overall average of 8%). The durations $DAY_{2.0}$, $DAY_{2.5}$, and $DAY_{3.0}$ increased in the reservoirs by 26 to 48 days. The greatest increases are projected for Santeetlah Lake, the smallest and deepest of the reservoirs.

In general, the lakes behave as expected with regard to dissolved oxygen. Lakes Phelps and Waccamaw are polymictic, never allowing anoxic conditions to occur near the bottom. In Jordan, James, and Santeetlah reservoirs, DO is depleted in a portion of the hypolimnion during summer stratification. While the duration of stratification does not significantly change under the projected 2xCO₂ climate (note Fig. 6.1 versus Fig. 6.11,

etc.), the increase in the duration of low hypolimnetic DO levels is substantial and can be attributed to lower DO at the onset of stratification.

Water loss by evaporation under the $2xCO_2$ climate scenario increased in each of the lakes by about 20% over the $1xCO_2$ value. The lower values for James and Santeetlah lakes reflect the fact that both are at higher elevations, and therefore cooler areas, than the other lakes.

Table 6.13. Results of student's *t*-test for the 1xCO₂ and 2xCO₂ mean values for each lake. The *t*-test was two-tailed with a level of significance of 0.05.

Lake		T _{epi}	T _{hyp}	T _{diff}	DO _{hyp}	EVAP	DOV _{0.1}	DOV _{2.0}	DOV _{2.5}	DOV _{3.0}	DAY _{0.1}	DAY _{2.0}	DAY _{2.5}	DAY _{3.0}
Jordan	(a)	9.28	13.69	2.81	0	11.16	3.26	4.38	5.85	4.97	3.35	4.39	5.78	6.40
	(b)	yes	yes	yes	no	yes	yes	yes	yes	yes	yes	yes	yes	yes
James	(a)	6.77	11.37	1.55	*	10.91	0.0	8.52	12.32	9.18	-0.62	11.58	11.15	12.05
	(b)	yes	yes	no	no	yes	no	yes	yes	yes	no	yes	yes	yes
Santeetlah	(a)	6.88	7.31	1.75	0	11.22	0.87	7.80	12.70	4.59	1.42	7.80	7.32	6.74
	(b)	yes	yes	no	no	yes	no	yes	yes	yes	no	yes	yes	yes
Phelps	(a)	10.11	9.88	4.25	-6.73	14.56	*	*	*	*	*	*	*	*
	(b)	yes	yes	yes	yes	yes	no	no	no	no	no	no	no	no
Waccamaw	(a)	9.94	9.92	3.03	-8.67	14.68	*	*	*	1.74	*	*	*	2.18
	(b)	yes	yes	yes	yes	yes	no	no	no	no	no	no	no	yes

See Table 6.7 for the definition of each characteristic.

(a) test statistic.

(b) Based on the *t*-test, is the 2xCO₂ mean different from the 1xCO₂ mean?

*Test statistic not calculated; answer in (b) based on inspection of simulation results.

Table 6.14. Projected change ($2xCO_2-1xCO_2$) in those lake characteristics found by *t*-test to be different.

Lake	T _{epi} °C	T _{hyp} °C	T _{diff} °C	DO _{hyp} mg L ⁻¹	EVAP mm	DOV _{0.1} %	DOV _{2.0} %	DOV _{2.5} %	DOV _{3.0} %	DAY _{0.1}	DAY _{2.0}	DAY _{2.5}	DAY _{3.0}
Jordan	3.0	2.0	1.3	none	230	6.1	8.5	10.9	9.3	11	26	35	42
James	2.9	1.9	none	none	165	none	8.3	8.8	7.6	none	42	44	46
Santeetlah	2.8	1.6	none	none	186	none	6.7	6.7	4.0	none	47	48	48
Phelps	3.0	2.9	0.2	-1.0	248	none	none	none	none	none	none	none	none
Waccamaw	3.0	2.8	0.6	-1.6	250	none	none	none	none	none	none	none	0.2

See Table 6.7 for the definition of each characteristic.

CHAPTER 7

IMPLICATIONS FOR FISH HABITAT AND GROWTH

Where fishes can live and thrive in a lake is determined by several factors; among the most significant are water temperature, dissolved oxygen, food, and shelter. Pending other conditions being favorable (food, etc.), fish will select temperatures near their growth optimum, i.e. a few degrees below lethal, to inhabit most of the time. They do not search out "cool" temperatures in summer like humans might, unless they are cool-water species. Each species has a temperature tolerance range (Eaton et al., 1995) and a sustained DO requirement. If water temperatures are in excess of this range, or DO concentrations are below those required, fish will not survive. In stratified lakes fish are therefore forced to find water layers where their requirements are met. In practice this can mean that fish are driven out of excessively warm surface waters into deeper cool layers of a lake where they will persist, so long as adequate DO remains in the zone of retreat. This may leave only a narrow habitat space between water layers which are too warm and those that do not provide sufficient oxygen. As climate warms the surface waters, this "temperature-oxygen vise" can pose a serious reduction in fish habitat.

To examine (briefly) the question of possible fish habitat changes in the three reservoirs and two natural lakes investigated, we shall use the water temperature isotherms and DO isopleths given in the foregoing sections. As temperature and DO criteria to define suitable fish habitat we shall apply the values previously used for cold-, cool-, and warm-water fishes (Stefan et al., 1992). The criteria are summarized in Table 7.1.

To relate these criteria to simulated lake characteristics under $1\times\text{CO}_2$ and $2\times\text{CO}_2$ climate scenarios Table 7.2 was prepared. It gives maximum temperatures in the epilimnion and the hypolimnion of each lake, minimum hypolimnetic DO, maximum length of the period for which hypolimnetic DO is less than 2.5 mg L^{-1} ($\text{DAY}_{2.5}$) and maximum fraction of lake volume (percent) for which DO is less than 2.5 mg L^{-1} ($\text{DOV}_{2.5}$).

Examining the numbers in Table 7.2 clearly shows that the situation is very different in the reservoirs compared to the shallow natural lakes. The deeper the lake, the larger the fraction of lake volume that is unavailable for fish because of anoxia. In the large and very shallow natural lakes anoxia imposes no limitation at all; in Santeetlah Lake up to half of the reservoir volume is unsuitable to fish because of insufficient oxygen.

With regard to temperatures, there are no limitations for the warm-water fish guild. Cool-water fishes will be strongly stressed in the natural lakes but find habitat in the reservoirs. Cold-water fishes would find suitable temperatures only in the hypolimnia of the two deepest reservoirs, but anoxia will prevent them from taking full advantage of these low temperatures.

Under the $2xCO_2$ climate scenario fish habitat availability would decrease. Cold-water species could not find habitat in any of the five lakes. Cool-water species would find limited habitat only in the deepest and smallest of the reservoirs (Santeetlah) and be eliminated from the other lakes. Warm-water species would be the main fishes in the reservoirs and in the two shallow natural lakes. Only the most thermally tolerant could exist.

A better interpretation of the temperature-oxygen squeeze can be obtained by overlaying isotherms and DO isopleths from Figs. 6.1 through 6.16 and determining the remaining habitat between them. In agreement with the criteria in Table 7.1 the 3.0 and 2.5 mg L⁻¹ isopleths for DO the 23.4, 30.4, and 33 °C isotherms were used for cold-water, cool-water and warm-water fishes respectively. The results of this analysis are summarized in Table 7.3. Under the $1xCO_2$ climate scenario there is only a minimal chance for cold-water fish survival and then only in the two deeper reservoirs. Cool-water fish do, however, have sufficient habitat and warm-water fish can thrive.

Under the $2xCO_2$ climate scenario cold-water fish unquestionably will be eliminated from all lakes. Cool-water fishes will not be expected to survive the warm summer temperatures in the two shallow natural lakes, but they can probably survive in the surface mixed layers of the reservoirs, where enough DO will be available. Whether they actually do survive will also depend on other factors like reduced competitive abilities against their better-adapted warm-water cohabitants.

The above interpretations are very coarse and exclude consideration of refugia where groundwater inflows may exist, competitive interactions, other habitat factors, indirect effects (e.g. on food webs), etc. The climate change effect projections give only mean conditions in large bodies of water.

Table 7.1. Thermal and dissolved oxygen habitat criteria for fish.

Fish guild	Upper temp. limit		Optimum temp.		Lower DO limit mg L ⁻¹
	mean °C	range °C	mean °C	range °C	
Cold-water	23.4	22.1-26.6	15.3	11.5-18.7	3.0
Cool-water	30.4	28.0-32.3	25.1	24-25.7	3.0
Warm-water	31.4*	28.7-33.6	29.2	27-32	2.5

*This value indicates only observations in the U.S. and is likely to be too low.

Table 7.2. Lake characteristics related to fish habitat.

Lake		Max. temp.		Min. DO	<i>DAY</i> _{2.5} *	<i>DOV</i> _{2.5} *
		epil. °C	hypol. °C	hypol. mg L ⁻¹	days	%
Jordan	(1)	30.5	23.8	0	158	39
	(2)	33.5	25.8	0	193	50
James	(1)	28.7	16.7	0	152	39
	(2)	31.6	18.6	0	196	48
Santeetlah	(1)	27.7	9.2	0	266	53
	(2)	30.5	10.8	0	314	60
Phelps	(1)	32.1	32.1	6.3	0	0
	(2)	35.1	35.0	5.4	0	0
Waccamaw	(1)	32.2	32.0	5.4	0	0
	(2)	35.2	34.8	3.8	0	0

(1) 1xCO₂ climate scenario

(2) 2xCO₂ climate scenario

*See Table 6.1 for definitions.

Table 7.3. Fish habitat limitations.

Lake		Cold-water fishes	Cool-water fishes	Warm-water fishes
Jordan	(1)	June 20-Sept 15*	-	-
	(2)	June 1-Oct 3	< 5 m layer	-
James	(1)	< 3 m layer**	-	-
	(2)	July 28-Sept 30	-	-
Santeetlah	(1)	< 3 m layer	-	-
	(2)	Aug 15-Sept 10	-	-
Phelps (temp. limitations only)	(1)	May 8-Sept 11	-	-
	(2)	April 17-Oct 8	June 28-Sept 1	-
Waccamaw (temp. limitations only)	(1)	May 7-Sept 25	-	-
	(2)	Apr 17-Oct 8	June 30-Sept 1	-

(1) 1xCO₂ climate scenario

(2) 2xCO₂ climate scenario

*Dates give period during which fishes cannot find any water layer with suitable temperatures and DO.

**Thickness of layer in entire lake, where fishes can find suitable temperatures and DO.

CHAPTER 8

SUMMARY AND CONCLUSIONS

The objective of this study was to determine the likely effects of a doubling of atmospheric carbon dioxide on water temperature and dissolved oxygen in lakes of the southeastern United States as an extension of similar research for lakes in Minnesota.

The southeastern region was defined as the four States of Virginia, North and South Carolina, and Georgia. In this region, most natural lakes are found only along the Coastal Plain, while the water bodies found in the Piedmont and Mountain Zone areas are mainly reservoirs. The natural coastal lakes, known as "Carolina Bays," are characterized by shallow depths (less than six meters), elliptical shapes, peat or sandy bottoms, and clear but colored waters. The reservoirs vary greatly in size, shape, and depth. Waters are generally clear in the Mountain Zone but are turbid in the Piedmont region.

The climate in the southeastern region is largely determined by its proximity to the ocean, latitude, and topography. Summers are hot and humid while winters are mild to moderately cold. Daily weather records for three sites in North Carolina (Asheville, Raleigh, and Wilmington) were assembled for a 19-year period (1961-1979). Projected changes under a $2\times\text{CO}_2$ climate scenario were obtained from the Canadian Climate Centre General Circulation Model (GCM) and superimposed on the historical record using a monthly timescale.

Climate change effects were projected with the aid of a deterministic, one-dimensional, year-round lake water quality model. The MINLAKE95 model was developed with the purpose of simulating water temperature and dissolved oxygen profiles in lakes on a regional basis. Its origin was an earlier version, MINLAKE, developed for individual Minnesota lakes for management decisions. In an earlier study, lakes were classified on the basis of surface area, maximum depth, and Secchi depth (trophic state). A number of additional issues arise when attempting to model reservoirs. These issues include the effects of major in- and outflows, hydraulic residence times, suspended solids concentrations, lake shape, horizontal variations in water quality, and changes in lake stage.

Regional modeling requires a classification of the lakes in a region. In addition to surface area, maximum depth, and Secchi depth, which were used for Minnesota lakes, characteristics such as hydraulic residence time, suspended solids, inflow rate and quality,

elevation of reservoir outlet, and basin shape would have to be considered for the southeastern U.S. With more than three or four independent parameters to consider, any regional classification is cumbersome and, therefore, was not attempted.

Case studies of five lakes in North Carolina, three reservoirs (Jordan, James, and Santeetlah) and two natural coastal lakes (Phelps and Waccamaw), were made. The reservoirs are deep (20 m to 65 m maximum depth) and show strong summer stratification, while the coastal lakes are shallow (3 m maximum depth) and well-mixed most of the time. All five lakes had surface areas larger than 11 km². The reservoirs had relatively long hydraulic residence times of more than 160 days. Each lake was simulated using past meteorological data and results were compared to field measurements. Field data from four to eight years were available, and the total number of measurements varied from 14 to 405 data points. A few input coefficients related to wind or sediment oxygen demand were calibrated in order to improve the results. A general cycle superimposed on mean annual chlorophyll-a concentrations was used for four of the lakes which had insufficient chlorophyll-a field measurements.

Overall standard errors of simulation were 2.0 °C for water temperature and 1.4 mg L⁻¹ for dissolved oxygen. The results for the reservoirs were encouraging, given the types of difficulties associated with modeling such water bodies. The temperatures simulated for the coastal lakes were generally higher than field measurements and poorer than would be expected for natural lakes. Attempts to find a deterministic explanation of these results were unsuccessful. Unfortunately, the data were few and were clustered in the high temperature season.

After model validation, each of the lakes was simulated in a continuous mode for a 19-year period under two climate scenarios. The first was the period 1961-1979, which was considered to be representative of past 1xCO₂ conditions. The second scenario was the climate projected by the Canadian Climate Center GCM under a doubling of atmospheric carbon dioxide (2xCO₂). Daily temperature and DO profiles representative of the pelagic portions of each lake were simulated with daily weather data as input. These profiles were then further analyzed to extract several parameters important for fish habitat, such as maximum daily surface temperature, maximum percent of lake volume with DO levels below 2.5 mg L⁻¹, and number of consecutive days with bottom DO below 2.5 mg L⁻¹. These parameters were determined for each year for each lake under each climate scenario. A standard student's *t*-test was used to identify which of the investigated lake characteristics changed significantly between the two climate scenarios.

Significant climate change effects on water temperatures and dissolved oxygen concentrations were found in each of the lakes. In general, the projections were for higher water temperatures and lower DO concentrations as the climate scenario was changed from 1xCO₂ to 2xCO₂. The two natural shallow coastal lakes responded differently from the three deeper, seasonally stratified reservoirs. Maximum daily temperatures increased by up to 3.0 °C in the surface layers and by at least 1.6 °C at the

bottom of the reservoirs. Minimum DO decreased in the two natural lakes by up to 1.6 mg L⁻¹ in response to the increased water temperatures. The well mixed nature of the shallow coastal lakes prevents any DO limitations for fish under either climate scenario. Water losses from evaporation increased by about 20% (up to 250 mm per year) in each of the five lakes.

In the reservoirs, the maximum percentage of lake volume with mean DO levels lower than those needed for fish (2 to 3 mg L⁻¹) increased to 53% under the 2xCO₂ climate scenario as compared to 45% under the 1xCO₂ scenario. The number of consecutive days for which reservoir bottom DO values were below 2.5 mg L⁻¹ increased by an average of 22% from 192 days under the 1xCO₂ scenario to 234 days under the 2xCO₂ scenario. These increases are mostly due to lower overall DO levels at the onset of stratification and longer lasting stratification.

Over the simulated 19-year period, reservoir water temperatures were most variable during the onset of spring stratification, indicating the sensitivity to the meteorological conditions which themselves are highly variable in spring. Simulated DO concentrations were most variable in the hypolimnion at the times of stratification onset in spring or turnover in fall.

Under the general climatic warming predicted under a doubling of atmospheric CO₂, cold-water fishes will not find suitable habitat in any of the five studied lakes. Cool-water fishes are not expected to survive the summer extreme temperatures in the two shallow coastal lakes but may survive in the surface mixed layers of the reservoirs. Warm-water fishes will thrive, but in the shallow lakes only the most temperature tolerant species will be able to cope with the 34 °C summer water temperatures predicted.

REFERENCES

- Bannister, T. T. 1974. "Prediction equations in terms of chlorophyll concentration, quantum yield, and upper limit of production." *Limnology and Oceanography*, 19(1):1-12.
- Boer, G. J., N. A. McFarlane, and M. Lazare. 1992. "Greenhouse gas-induced climate change simulated with the CCC second-generation general circulation model." *Journal of Climate*, 5(10):1045-1077.
- Carlson, R. E. 1977. "A trophic state index for lakes." *Limnology and Oceanography*, 22(2):361-369.
- Collins, W. D. 1925. "Temperature of water available for industrial use in the United States." *Water Supply Paper 520-F*. United States Geological Survey.
- Eaton, J. G., J. H. McCormick, B. E. Goodno, D. G. O'Brien, H. G. Stefan, M. Hondzo, and R. M. Scheller. 1995. "A field information-based system for estimating fish temperature tolerances." *Fisheries*, 20(4):10-18.
- Fang, X. and H. G. Stefan. 1994. "Modeling of dissolved oxygen stratification dynamics in Minnesota lakes under different climate scenarios." *Project Report No. 339*. St. Anthony Falls Hydraulic Lab., University of Minnesota, Minneapolis, Minnesota.
- Fang, X. and H. G. Stefan. 1996. "Dynamics of heat exchange between sediment and water in a lake." *Water Resources Research*, in print.
- Ford, D. E. 1990. "Reservoir transport processes." In K. W. Thornton, B. L. Kimmel, and F. E. Payne (eds.), *Reservoir Limnology: Ecological Perspectives*. New York: J. Wiley & Sons.
- Georgia Dept. of Natural Resources, Environmental Protection Division. 1993. "Water quality in Georgia, 1992-1993."
- Gorham, E. and F. M. Boyce. 1989. "Influence of lake surface area and depth upon thermal stratification and the depth of the summer thermocline." *J. Great Lakes Res.*, 15:233-245.

- Gu, R. and H. G. Stefan. 1990. "Year-round temperature simulation of cold climate lakes." *Cold Regions Science and Technology*, 18:147-160.
- Hannan, H. H., D. Barrows, and D. C. Whitenberg. 1980. "The trophic status of a deep-storage reservoir in central Texas." Paper No. 4-25 in H. G. Stefan (ed.), *Proceedings of the Symposium on Surface Water Impoundments*. New York: ASCE. pp. 425-434.
- Higgins J. M., W. L. Poppe, and M. L. Iwanski. 1980. "Eutrophication analysis of TVA reservoirs." Paper No. 4-23 in H. G. Stefan (ed.), *Proceedings of the Symposium on Surface Water Impoundments*. New York: ASCE. pp. 404-412.
- Hondzo, M. and H. G. Stefan. 1992. "Water temperature characteristics of lakes subjected to climate change." *Project Report No. 329*. St. Anthony Falls Hydraulic Lab., University of Minnesota, Minneapolis, Minnesota.
- Idso, S. B. and G. R. Gilbert. 1974. "On the universality of the Poole and Atkins Secchi disk-light extinction equation." *J. of Applied Ecology*, 11:399-401.
- Jones, P. D., T. M. L. Wigley, and P. B. Wright. 1986. "Global temperature variations between 1861 and 1984." *Nature*, 322(6078):430-434.
- Kimmel, B. L., O. T. Lind, and L. J. Paulson. 1990. "Reservoir primary production." In K. W. Thornton, B. L. Kimmel, and F. E. Payne (eds.), *Reservoir Limnology: Ecological Perspectives*. New York: J. Wiley & Sons.
- Kimsey, C. D. Jr., A. C. Boozer, J. N. Knox, L. E. Turner, K. K. Cain, and G. W. Long. 1982. "South Carolina clean lakes classification survey." *Technical Report No. 019-82*. South Carolina Dept. of Health and Environmental Control, Office of Environmental Quality Control.
- Koenings J. P. and J. A. Edmundson. 1991. "Secchi disk and photometer of light regimes in Alaskan lakes: Effects of yellow color and turbidity." *Limnology and Oceanography*, 36(1):91-105.
- Marshall, C. T. and R. H. Peters. 1989. "General patterns in the seasonal development of chlorophyll *a* for temperate lakes." *Limnol. Oceanogr.*, 34(5):856-867.
- McFarlane, N. A., G. J. Boer, J. P. Blanchet, and M. Lazarc. 1992. "The Canadian Climate Center Second Generation Circulation Model and its equilibrium climate." *J. Climate*, 5:1013-1044.

- Megard, R. O., W. S. Combs, P. D. Smith, A. S. Knoll. 1979. "Attenuation of light and daily integral rates of photosynthesis attained by planktonic algae." *Limnology and Oceanography*, 24(6):1038-1050.
- National Oceanic and Atmospheric Administration (NOAA). 1974. *Climate of the States*. Washington, D.C.
- North Carolina Dept. of Environment, Health, and Natural Resources, Water Quality Section. 1992. "North Carolina lake assessment report." *Report No. 92-02*.
- Poole, H. H. and W. R. G. Atkins. 1929. "Photo-electric measurement of submarine illumination through the year." *J. Mar. Biol. Assoc.*, 16:297-324.
- Reid, G. K. and R. D. Wood. 1976. *Ecology of Inland Waters and Estuaries*. New York: D. van Nostrand Co.
- Riley, M. J. and H. G. Stefan. 1987. "Dynamic lake water quality simulation model 'MINLAKE'." *Project Report No. 263*. St. Anthony Falls Hydraulic Lab., University of Minnesota, Minneapolis, Minnesota.
- Sinokrot, B. A. and H. G. Stefan. 1992. "Deterministic modeling of stream water temperatures: Development and applications to climate change effects on fish habitat." *Project Report No. 337*. St. Anthony Falls Hydraulic Lab., University of Minnesota, Minneapolis, Minnesota.
- Stecker, K. K. and M. Crocker. 1991. "South Carolina lake classification survey 1991." *Technical Report No. 006-91*. South Carolina Dept. of Health and Environmental Control, Water Quality Monitoring Section.
- Stefan, H., T. Skoglund, and R. O. Megard. 1976. "Wind control of algae growth in eutrophic lakes." *J. of Environmental Engineering Div.*, ASCE, 102(EE6):1201-1213.
- Stefan, H. G., M. Hondzo, B. Sinokrot, X. Fang, J. G. Eaton, B. E. Goodno, K. E. F. Hokanson, J. H. McCormick, D. G. O'Brien, and J. A. Wisniewski. 1992. "A methodology to estimate global climate change impacts on lake and stream environmental conditions and fishery resources with application to Minnesota" (2nd ed.). *Project Report No. 323*. St. Anthony Falls Hydraulic Lab., University of Minnesota, Minneapolis, Minnesota.
- Stefan, H. G., M. Hondzo, and X. Fang. 1993. "Lake water quality modeling for projected future climate scenarios." *J. of Environmental Quality*, 22(3):417-431.

- Stefan, H. G., M. Hondzo, X. Fang, and A. H. Rasmussen. 1994. "Year-round water temperature and dissolved oxygen simulation model for lakes with winter ice cover." *Project Report No. 355*. St. Anthony Falls Hydraulic Lab., University of Minnesota, Minneapolis, Minnesota.
- Stefan, H. G. and X. Fang. 1995. "A methodology to estimate year-round effects of climate change on water temperature, ice and dissolved oxygen characteristics of temperate zone lakes with application to Minnesota." *Project Report No. 377*. St. Anthony Falls Lab., University of Minnesota, Minneapolis, Minnesota.
- South Carolina Water Resources Commission. 1991. "Inventory of lakes in South Carolina: Ten acres or more in surface area." *Report No. 171*.
- Thomann, R. V. and J. A. Mueller. 1987. *Principles of Surface Water Quality Modeling and Control*. New York: Harper Collins.
- Thornton, K. W., B. L. Kimmel, and F. E. Payne (eds.). 1990. *Reservoir Limnology: Ecological Perspectives*. New York: J. Wiley & Sons.
- Todd, D. K. 1980. *Groundwater hydrology*, 2nd. ed. New York: J. Wiley & Sons.
- Virginia Dept. of Environmental Quality. 1994. "Virginia water quality assessment for 1994: 305(b) report to EPA and Congress." *Information Bulletin #597*.
- Yount, J. L. 1966. "South Atlantic states." In D. G. Frey (ed.), *Limnology in North America*. Madison: Univ. of Wisconsin Press. pp. 269-286.

APPENDIX

SENSITIVITY OF SIMULATION RESULTS FOR LAKES PHELPS AND WACCAMAW TO LOCAL HYDROLOGY, GEOLOGY, AND METEOROLOGY

When compared to the results of previous studies of other natural lakes (Stefan and Fang, 1995), the initial results of the temperature simulations of Lakes Phelps and Waccamaw were not as good as would be expected. Standard errors were 2.1 °C compared to about 1 °C in previous studies. Unfortunately, the data points for this study were lumped (Figs. 5.33 and 5.37) and only available for the summer months. With more and better distributed data the fit may have been better. Nevertheless, several hypotheses were examined to explain the poorer-than-expected results: (1) Inappropriate weather station location, (2) inaccurate wind coefficients, (3) groundwater inflow and outflow, (4) precipitation input, (5) thermal effects of sediments, and (6) non-representativeness of the field data. None has to date provided an adequate explanation or means to improving the performance of the modeling effort.

Weather station

Wilmington, NC, may not be representative of the weather at Lake Phelps, located approximately 210 km to the northeast. However, the next closest alternative weather station, Raleigh, NC, is located further inland in the Piedmont region and does not represent coastal weather. Simulation errors for water temperatures for Lake Waccamaw, which is located only 50 km from Wilmington, were similar to those for Lake Phelps. Hence, weather data were ruled out as a significant cause of the observed errors.

Wind effects

Since the simulated temperatures were usually higher than the field measurements, it was considered that not enough evaporative cooling was being applied by the model. In a sensitivity test, the wind coefficient (W_{coef}), used in the determination of latent heat losses, was varied from 1.0 to 2.5. The resulting reductions in the standard errors were significant (Table A.1). It seems that a value of 1.6 for W_{coef} would give better results for both water temperature and DO than a value of 1.0. However, such a large value for

W_{coef} is not physically justified, because the greater resultant cooling also brought ice formation during the winter (up to 6 cm in thickness during one simulation) which is not realistic. For these reasons, this investigation of wind effects was discontinued.

The wind sheltering coefficient (W_{str}), which is used to determine the kinetic energy of the wind imparted onto the lake, was also varied in order to see the changes in water temperature simulation results, but again without improvement (Table A.2).

Groundwater

It is known that inflow of groundwater can cool a lake in summer. However, inflow of groundwater has to be substantial, and that is why its contribution is neglected by MINLAKE95. The hydrologic setting of the two large and shallow coastal lakes is in a coastal plain. Surface inflows and outflows seem small and poorly documented. Because the lakes have small volumes relative to their areas and are embedded in sandy and/or organic materials, it seemed logical to consider a significant groundwater input component in the heat budget. As a first try, it was considered that the volume of groundwater flowing into the lake was equal to the amount lost to evaporation. According to the 1xCO₂ simulation (Chapter 6), the average annual depth of water lost to evaporation from Lake Phelps is 1191 mm yr⁻¹ (Table 6.4), which means that, at a constant flowrate, the groundwater input Q_{gw} would be $2.19 \times 10^5 \text{ m}^3 \text{ d}^{-1}$. The same method yields a value for Q_{gw} of $1.21 \times 10^5 \text{ m}^3 \text{ d}^{-1}$ for Lake Waccamaw. These volumes of groundwater input represent between 30 and 40% of the total lake volume. Using a temperature of 15 °C for the groundwater (Fig. 5.3), the thermal effect of groundwater was put into Eq. 4.2 as a heat source of magnitude

$$H_g = \frac{Q_{\text{gw}} \rho c_p (15 - T_w)}{\rho c_p V_w} \quad (\text{A.1})$$

where H_g is the groundwater heat source, ρ is the density of water, c_p is the heat capacity of water, T_w is the temperature of the receiving lake water, and V_w is the volume of the layer in which the groundwater is placed. The groundwater was placed in either the top layer or the bottom layer on a year-round basis. Neither simulation improved the lake water temperature results. Since it is conceivable that groundwater flows into the shallow coastal lakes in excess of the evaporation rates, Q_{gw} was increased by one and two orders of magnitude. The results of these simulations are given in Table A.3. Some of the attempts improved the standard errors of simulation to below 2 °C, but not significantly enough to warrant further simulations, i.e. to identify an optimum groundwater inflow at which the standard error has a minimum. Other trials were done with lower groundwater temperatures ($T_{\text{gw}}=10$ and 3 °C), but these attempts did not significantly improve the standard errors of simulation.

It appears evident that the heat exchange between these shallow lakes and the atmosphere is so strong that any input of cold groundwater is rapidly heated to near equilibrium temperatures.

Precipitation

According to the North Carolina DEHNR (1992), Lake Phelps has no known overland inflow and most of its recharge comes from precipitation with a small fraction from groundwater. With this in mind, it was considered that some lake cooling may result from precipitation instead of groundwater. Average annual precipitation is about 1270 mm yr⁻¹ (NOAA, 1974). However, given that rain is usually warmer than groundwater and that the simulation trials with groundwater effects were unsuccessful, rainfall was rejected as a likely reason that MINLAKE95 simulated Lake Phelps temperatures worse than expected.

Sediment thermal conductivity

Thermal effects of the sediments underlying a shallow lake can be significant (Fang and Stefan, 1996). Therefore conductivities of various geologic materials were examined (Table A.4) and used in the simulations. The standard errors did not significantly change from the original simulation results.

Field data

It was also considered that the "instantaneous" single station field measurements may not be representative of the entire lake or of the average daily values. The goodness of fit is based on only a small number of points (19 for Phelps and 14 for Waccamaw); a single day's measurements which may be inaccurate or not representative can consequently easily skew the results. Nevertheless, the model almost consistently simulated temperatures which were higher than the field data, and, hence, the probability that many of the field data are problematic is unlikely.

Table A.1. Standard errors (S.E.) of water temperature and DO simulations with varying values of wind coefficient (W_{coef}).

Lake Phelps						
$W_{\text{coef}} (-)$	1.0*	1.6	1.7	2.0	2.1	2.5
S.E. T (°C)	2.28	1.59	1.56	1.59	1.64	1.91
S.E. DO (mg L ⁻¹)	1.49	1.45	1.44	1.44	1.44	1.44
Lake Waccamaw						
$W_{\text{coef}} (-)$	1.0*	1.5	1.6	1.7		
S.E. T (°C)	2.01	1.52	1.47	1.56		
S.E. DO (mg L ⁻¹)	0.57	0.69	0.71	0.73		

*Initial values which were also used in the final simulations reported in Chapter 5.

Table A.2. Standard errors (S.E.) of water temperature and DO simulations with varying values of wind sheltering coefficient (W_{str}).

Lake Phelps				
$W_{\text{str}} (-)$	1.0*	1.05	1.20	1.30
S.E. T (°C)	2.28	2.28	2.28	2.28
S.E. DO (mg L ⁻¹)	1.49	1.49	1.49	1.49
Lake Waccamaw				
$W_{\text{str}} (-)$	1.0*	1.05	1.20	1.30
S.E. T (°C)	2.01	2.01	2.01	2.01
S.E. DO (mg L ⁻¹)	0.57	0.57	0.57	0.57

*Initial values which were also used in the final simulations reported in Chapter 5.

Table A.3. Standard errors (S.E.) of water temperature and DO simulations with varying inputs of groundwater. $Q_{gw}=0$ represents the current MINLAKE95 method.

Lake Phelps							
Q_{gw} ($m^3 d^{-1}$)	0	2.19×10^5		2.19×10^6		2.19×10^7	
Layer*	-	surface	bottom	surface	bottom	surface	bottom
S.E. T ($^{\circ}C$)	2.28	2.24	2.25	1.96	2.00	2.95	1.99
S.E. DO ($mg L^{-1}$)	1.49	1.49	1.49	1.47	1.48	1.48	1.44

Lake Waccamaw							
Q_{gw} ($m^3 d^{-1}$)	0	1.21×10^5		1.21×10^6		1.21×10^7	
Layer	-	surface	bottom	surface	bottom	surface	bottom
S.E. T ($^{\circ}C$)	2.01	1.97	1.98	1.69	1.64	2.72	3.30
S.E. DO ($mg L^{-1}$)	0.57	0.58	0.58	0.61	0.59	1.05	0.57

*This is the layer in which the groundwater was placed.

Table A.4. Thermal diffusivities of various materials.

Material	Thermal diffusivity $m^2 d^{-1}$
Water	0.013
Clay	0.086
Sandstone	0.103
Rum River sediment	0.045
Previously used value for Minnesota lakes	0.040

